Deciphering the Interplay Between Lipid Metabolism and ExoU Activity In *Pseudomonas Aeruginosa*-Induced Host Cell Death

Adam Mahdi

Thesis Submitted to the University of Ottawa
In Partial Fulfillment of Requirements
For the M.Sc degree in Biochemistry

Department of Biochemistry, Microbiology and Immunology
Faculty of Medicine
University of Ottawa

ABSTRACT

ExoU is a phospholipase A_2 (PLA_2)-like enzyme, expressed by the gram-negative bacterium *Pseudomonas aeruginosa* (*P. aeruginosa*). ExoU is associated with high mortality rates in patients because it induces high levels of cytotoxicity in host cells. Yet, the precise lipidomic changes it mediates in the host are unknown. To address this, I investigated the impact of ExoU on the viability of human THP-1 macrophages and NuLi epithelial cells. I found that exposure to *P. aeruginosa* expressing ExoU significantly reduces cell viability in THP-1 and NuLi cells compared to ExoU mutant strains. I validated these findings across various time points and multiplicities of infection and showed that ExoU-expressing *P. aeruginosa* induces higher levels of cell death. I then assessed the impact of inhibiting ExoU intracellular translocation to the inner leaflet of the plasma membrane by treating THP-1 cells with a late endosome inhibitor and showed that the treatment led to no change in cell viability. To determine the type of cell death induced by ExoU, I tested various pharmacological inhibitors to inhibit apoptosis, necroptosis, and ferroptosis. I demonstrated that while inhibiting apoptosis and necroptosis resulted in no change in viability, inhibiting ferroptosis at early time points transiently increased viability. To validate the role of ferroptosis, I treated cells with an inducer of ferroptosis; however, found no effect of the treatment on cell viability. Lastly, to elucidate the mechanism of ExoU's activity, I performed a lipidomic assessment of glycerophosphocholines (GPCs) in THP-1 cells using high-performance liquid chromatography-electrospray ionization tandem mass spectrometry (LC-ESI MS/MS). I found that exposure to *P. aeruginosa*-expressing ExoU increases the levels of lysophosphatidylcholines (LPCs), providing direct evidence of host cell membrane hydrolysis. Taken together, this thesis confirms ExoU's PLA2 activity is associated with enhanced cytotoxicity.

ACKNOWLEDGMENTS

Dear reader, thank you for picking up this thesis, whether by curiosity, obligation, or accident. As I procrastinate for the very last time on this document, I find myself hoping that some fragment of the knowledge will be useful to you. With this, I pass the torch on to the next brave, not-yet-capable scientist-in-training. I would love to say I followed a meticulous plan or a straight path, but truthfully, most of what I set out to do didn't quite happen that way. There were moments I wasn't sure I'd ever reach this page, let alone know what to write. I rehearsed countless ways I'd express my feelings and reflect on the journey, and now, having arrived, I've forgotten nearly all of them.

This work is a product of many emotions; excitement, frustration, joy, boredom, pride... All of them came and went, sometimes unexpectedly. But somehow, I find myself back at the beginning; curious, hopeful, and just a little bit wiser. I did not plan for this path, but here I am walking it. To my advisors and mentors: thank you for your guidance, your patience, and for believing in me when I wasn't so sure myself. To my colleagues and labmates: your support, humor, and shared complaints made the tough days easier and the good days memorable. To my family and friends: thank you for your endless encouragement, your reminders to sleep, and your willingness to listen to rants you didn't sign up for. This thesis doesn't mark an end, but a step forward. Someone once told me, "If you want to be a whale, go to the sea." That idea stayed with me, a quiet push to keep moving forward, and to keep looking toward what's next. To the institutions, labs, and coffee machines that fueled this journey thank you for providing the space and sustenance to think, create, and push forward. "When life gives you lemons, make lemonade." – Elbert Hubbard

And if that doesn't work… just add more sugar. It usually does the trick.

TABLE OF CONTENTS

ABSTRACT ..... **ii**
ACKNOWLEDGMENTS ..... **iii**
TABLE OF CONTENTS ..... **iv**
LIST OF FIGURES ..... **vi**
ABBREVIATIONS ..... **vii**
LIST OF TABLES ..... **xiv**
1 INTRODUCTION **1**
1.1 *Pseudomonas aeruginosa* (*P. aeruginosa*) Pathogenesis 1
1.1.1 Clinical manifestations of *P. aeruginosa* infection and its prevalence in hospitals 1
1.1.2 Role of T3SS in *P. aeruginosa* virulence 2
1.1.3 T3SS effector proteins and ExoU 3
1.1.4 The ExoU translocation pathway following injection into host cells 9
1.1.5 ExoU co-factors and co-activators lead to enhanced activity 9
1.1.6 ExoU's PLA_2 activity 10
1.2 Cell death pathways 12
1.2.1 Apoptosis, general overview of mechanism 12
1.2.2 Necroptosis, general overview of mechanism 13
1.2.3 Ferroptosis, general overview of mechanism 14
1.2.4 Necrosis, general overview 17
1.2.5 Effect of lysophospholipids and fatty acids on membrane integrity and necrosis 18
1.2.6 Overview of Phosphatidylinositol 4,5-bisphosphate (PI(4,5)P2) 20
1.3 Innate immunity 20
1.3.1 Macrophage and epithelial cells in the innate immune system 20
1.3.2 Role of immune mechanisms in response to bacterial infection 21
1.3.3 IL-1ß and immune response to bacterial infection 22
1.4 Phospholipid metabolism 23
1.4.1 Glycerophosphocholine (GPC) synthesis pathways 23
1.4.2 Phospholipid remodeling (Lands cycle) 25
1.4.3 Phospholipid oxidation and lipid peroxidation pathways 27
1.5 The role of lipids' in inflammasome activation 28
1.5.1 Effect of phospholipid saturation and oxidation on TLR4 activation 28
1.5.2 Lipids in non-canonical inflammasome activation and the release of IL-1ß 31

1.6 Hypothesis and Objective 31
2 MATERIALS AND METHODS 32
2.1 Cell culture 32
2.2 Bacterial culture and infection 33
2.3 Cell viability assays 34
2.4 IL-1β ELISA 34
2.5 Cell inhibitor treatment 35
2.6 CFU counting 35
2.7 Lipid extraction and collection 35
2.8 LC-ESI-MS/MS 37
2.9 Statistical Analysis 41
3 RESULTS 43
3.1 Expression of ExoU enhances *P. aeruginosa* cytotoxicity in human THP-1 macrophages and NuLi epithelial cells 43
3.2 Quercetin treatment does not increase THP-1 macrophage viability 44
3.3 Pan-caspase inhibition does not enhance THP-1 macrophage viability following PA14 WT infection 48
3.4 Inhibition of necroptosis does not enhance THP-1 macrophage viability following PA14 WT infection 48
3.5 Ferrostatin-1 enhances THP-1 macrophage viability following one h but not three h of PA14 WT infection 50
3.6 ExoU is required for *P. aeruginosa*-induced host cell ferroptosis 50
3.7 Inhibiting ExoU-induced ferroptosis enhances inflammasome-linked IL-1β release 51
3.8 ExoU alters the THP-1 macrophage lipidome. 51
4 DISCUSSION 54
4.1 ExoU contributes to *P. aeruginosa* virulence 63
4.2 Mechanism of ExoU-induced cell death may differ in macrophages 64
4.3 Ferroptosis is induced in ExoU-infected cells 65
4.4 ExoU increases levels of IL-1ß secretion 69
4.5 ExoU alters macrophage lipidome 70
5 CONCLUSION 73
6 REFERENCES 74

LIST OF FIGURES

Figure 1: ExoU-induced necrosis. **4**

Figure 2: Crystal structure of P. aeruginosa's effector protein ExoU and its chaperone SpcU. **7**

Figure 3: PLA_2 activity on a phospholipid. **8**

Figure 4: Lipid peroxidation through Fenton chemistry. **16**

Figure 5: General overview of cell death pathways. **19**

Figure 6. Canonical and non-canonical inflammasome activation pathway. **24**

Figure 7: Phosphatidylcholine synthesis pathway. **26**

Figure 8. Phospholipid remodeling and oxidation. **29**

Figure 9: Loss of ExoU function increases THP-1 survival when exposed to *P. aeruginosa*. **45**

Figure 10: Loss of ExoU function increases NuLi survival when exposed to *P. aeruginosa*. **46**

Figure 11: Ectopic expression of ExoU in the P. aeruginosa strain decreases THP-1 viability than the non-expressing *P. aeruginosa* strain. **47**

Figure 12: Quercetin treatment followed by exposure to *P. aeruginosa* does not reduce viability **49**

Figure 13: Inhibiting various cell death mechanisms only increases viability when inhibiting ferroptosis at one h in THP-1 cells following exposure to *P. aeruginosa*. **52**

Figure 14: Inhibiting ferroptosis increases IL-1ß secretion only after long exposure to *P. aeruginosa*. **53**

Figure 15: GPC structural variation. **55**

Figure 16: GPC alteration in THP-1 showing the effect of ExoU **56**

Figure 17: PA14 WT increases levels of lyso-phosphocholines and other GPCs in THP-1 cells. **58**

Figure 18: PA14 WT and PA14 *exoU::tn* increases levels of various GPCs in THP-1 cells. **61**

Figure 19: Unaltered GPC species after PA14 WT and PA14 *exoU::tn* infection in THP-1 cells. **62**

ABBREVIATIONS

2-ME	2-Mercaptoethanol
4-HNE	4-hydroxynonenal
AA	Arachidonic acid
AcMeOH	Acidified methanol
ACSL	long-chain acyl-CoA synthetases (ACSL)
ACSL4	acyl-CoA synthetase long-chain family member 4
ADP	Adenosine diphosphate
ALOX5	5–lipoxygenase
Apaf-1	apoptotic protease activating factor-1
ATP	adenosine triphosphate
BALF	bronchoalveolar fluids
BEBM	Bronchial Epithelial Cell Basal Medium
BEGM	Bronchial Epithelial Cell Growth Medium
BPE	Bovine Pituitary Extract
BSA	Bovine Serum Albumin
BWE	burn wound exudates
CDP	cytidine diphosphate
CEPT	CDP-choline:1,2-diacylglycerol choline/ethanolamine phosphotransferase (CEPT)
CFU	Colony Forming Units
CHT1	choline transporter
CK	Choline kinase

CMP	Cytidine monophosphate
CoA	Coenzyme A
CoQ	Coenzyme Q
COV	Compensation voltage
COX-2	Cyclooxygenase 2
cPLA2	cytosolic phospholipase A2
CPT	CDP-choline:1,2-diacylglycerol cholinephosphotransferase
CT	CTP:phosphocholine cytidylyltransferase
CTP	cytidine triphosphate
CTRL	control
CuOOH	Cumene hydroperoxide
CYP450	Cytochrome P450
Cys	cystine
DAMPs	Damage-associated molecular pattern molecules
DD	Death domain
DISC	death-inducing signaling complex
DMSO	Dimethyl Sulfoxide
DMT1	divalent metal transporter-1
DR	Death receptor
DR2	death receptor 2
DR4	death receptor 4
EEA1	Early endosome antigen 1
ELISA	Enzyme-Linked Immunosorbent Assay

EPT	CDP-ethanolamine:1,2-ethanolaminephosphotransferase
ER	Endoplasmic reticulum
ESI	Electrospray Ionization
ET	CTP:phosphoethanolamine cytidylyltransferase
exoU::tn	ExoU transposon
FA	Fatty Acid
FADD	Fas-associated protein with death domain
FAK	focal adhesion kinase
FasL	Fas ligand
FasR	Fas receptor
FBS	Fetal Bovine Serum
Fer-1	Ferrostatin-1
FSP1	Ferroptosis suppressor protein 1
GalCer	Galactosyl ceramide
GlcCer	Glucosyl ceramide
Glu	glutamate
GM3	Ganglioside
GPC	Glycerophosphocholine
GPE	Glycerophosphoethanolamine
GPL	Glycerophospholipid
GPS	glycerophosphoserine
GPX4	glutathione peroxidase 4
GSH	glutathione

GSSG	Glutathione disulfide
hEGF	Human Epidermal Growth Factor
HETE	hydroxyeicosatetraenoic acids
HPLC	High-performance Liquid Chromatography
iFSP-1	Inhibitor of ferroptosis suppressor protein 1
IL-	Interleukin
$iPLA_2$	Calcium independent phospholipase A_2
LB	Lysogeny Broth
LBP	LPS-binding protein
LPC	lysophosphatidylcholine
LPCAT1	lysophosphatidylcholine acyltransferase 1
LPCAT3	lysophophatidylcholine acyltransferase 3
LPS	Lipopolysaccharide
LTB4	Leukotriene B4
lysoPL	lysophospholipid
lysoPLAT	lysophospholipid acyltransferase
m/z	Mass to charge ratio
MAFP	methyl arachidonyl fluorophosphonate
MDA	malondialdehyde
Mito-MAM	mitochondrial membrane-associated ER membranes (mito-MAM)
MLD	membrane localization domain
MLKL	Mixed lineage kinase domain-like pseudokinase
MOI	Multiplicity Of Infection

MRM	multiple reaction monitoring
MS	Mass Spectrometry
MS/MS	Tandem mass spectrometry
MUFA	Monounsaturated Fatty Acid
nLC-ESI-	nanobore high performance liquid chromatography-electrospray
DMS-	ionization, differential mobility spectrometry, tandem mass
MS/MS	spectrometry
NR	Neutral Red
OD	Optical Density
OD_{600}	Optical Density at 600 nm
oxPL	Oxidized Phospholipids
P. aeruginosa	*Pseudomonas aeruginosa*
PARP-1	poly (ADP-ribose) polymerase-1
PBS	Phosphate Buffered Saline
PC	phosphocholine
PC-O	Ether linked PC
PC-P	plasmalogen PC
PEMT	phosphatidylethanolamine N-methyltransferase
PGE2	Prostaglandin E2
PHF	Primary Human Fibroblasts
PL	phospholipid
PLA_2	Phospholipase A_2
PMA	phorbol 12-myristate 13-acetate

PRR	pattern-recognition receptors
PRRs	pathogen recognition receptors
PUFA	Poly Unsaturated Fatty Acid
$PUFA_2$	diacyl PUFA
Quer	Quercetin
R8	RPMI 1640 supplemented with 8% fetal bovine serum
RIPK1/ RIPK3	Receptor-interacting serine-threonine protein kinase 1/3
ROS	Reactive oxygen species
RPMI	Roswell Park Memorial Institute (RPMI) medium
RTA	Radical trapping agent
SFA	Saturated Fatty Acid
SM	Sphingomyelin
SPH	Sphingolipid
Steap3	six-transmembrane epithelial antigen of the prostate 3
T3SS	Type III secretion system
TLR4	toll-like receptor 4
TNF	tumor necrosis factor
TNFR1	TNF receptor 1
TRADD	TNFR1-associated death domain protein
TRAIL	TNF-related apoptosis-inducing ligand
TrxR1	thioredoxin reductase 1
Ub	Ubiquitin

VAP	ventilator-associated pneumonia
WT	Wild type
ZBP1	Z-DNA binding protein
zVAD	Z-VAD-FMK

LIST OF TABLES

Table 1: Inhibitors and inducers used in cell treatment experiments..... 36
Table 2: Mass spectrometry experimental controls..... 39
Table 3: Mass spectrometry lipid internal standards..... 40
Table 4: Spike in LC/MS standards..... 42

1 INTRODUCTION

1.1 *Pseudomonas aeruginosa* (*P. aeruginosa*) Pathogenesis

1.1.1 Clinical manifestations of *P. aeruginosa* infection and its prevalence in hospitals

Pseudomonas aeruginosa is an opportunistic gram-negative bacterium that is implicated in 10% of all hospital-acquired bacterial infections, and is a major cause of lung damage in cystic fibrosis (CF) patients [1,2]. Bacterial infections lead to significant airway inflammation, along with recurrent acute and chronic opportunistic infections, which result in airway damage that can lead to end-stage lung disease[3]. The incidence of *P. aeruginosa* bacteremia increases with age, where males between the ages of 60 and above are more commonly infected than females of the same age group [4]. *P. aeruginosa* is the most common cause of ventilator-associated pneumonia (VAP) and infects burn wound exudates (BWE), leading to severe infection and delayed recovery in burn patients[5,6]. *P. aeruginosa* is the most common infection in cystic fibrosis (CF), impacting three-quarters of adult patients with the condition[7]. Unique *P. aeruginosa* strains that infect CF patients can be obtained from the environment. However, CF patients also acquire shared (clonal) strains of *P. aeruginosa*, which are often antibiotic-resistant and transmitted between individuals with CF[8]. Patients with clonal strains of *P. aeruginosa* are associated with worse prognosis and faster lung function decline than environmental strains[8]. Patients with hospital-acquired *P. aeruginosa* infections have more severe infections and a higher all-cause mortality rate[4,9]. A growing number of *P. aeruginosa* strains are developing resistance to antibiotics, resulting in increased mortality rates[10,11].

The capacity of *P. aeruginosa* strains to induce severe infections in patients is linked to their virulence factors, whereas *P. aeruginosa* strains that possess certain virulence factors, such as a

Type 3 secretion system (T3SS), are associated with worse patient outcomes[12]. The increased resistance in *P. aeruginosa* may be attributed to the enhanced persistence of *P. aeruginosa* strains in patients, depending on their virulence factors, such as the Type 3 secretion system (T3SS) and particularly the most toxic Type 3 effector protein, ExoU[13–15], particularly during the acute infection phase[16].

1.1.2 Role of T3SS in *P. aeruginosa* virulence

Bacteria, including *P. aeruginosa*, defend themselves and thrive within a host by employing various strategies to evade clearance; the most significant of these involves the expression of virulence factors that are secreted into the extracellular space or injected into the host cytoplasm through different secretion systems[17,18]. The T3SS is used by many bacteria including *Yersinia, Pseudomonas aeruginosa, Shigella flexneri, Salmonella typhimurium, enteropathogenic Escherichia coli,* and *Chlamydia* [19]. T3SS expression is regulated by multiple genes, including EsA and MvaT/MvaU, and is influenced by temperature, with T3SS activation increasing at higher temperatures nearing 30°C [20–22].

The structure of the T3SS has many conserved proteins that form a membrane-spanning syringe-like structure[23,24]. The base of the T3SS consists of a stack of proteins called the basal plate, which is composed of outer and inner membrane-anchored layers that position the T3SS on the bacterial membrane, followed by a helical needle-like structure[25–27]. The T3SS secretes pathogenic effector proteins, requiring a chaperone interaction on the chaperone-binding domain[28]. The needle tip of the T3SS is composed of three proteins: PopB, PopD, and PcrV, which interact with the host membrane to form a small pore, measuring 1 to 4 nm, that allows effector proteins to enter the host cytoplasm[29]. PopB and PopD can also act as effector proteins where they have been shown to induce histone modifications and affect the host epigenome[30].

The pore formed by the T3SS has the ability to induce host cell death caused by the increase in osmotic pressure leading to osmotic shock[31]. Therefore, the T3SS has been reported to be a major virulence determinant because of its ability to translocate effector proteins leading to cytotoxicity (**Figure 1A**)[32].

1.1.3 T3SS effector proteins and ExoU

The T3SS is able to detect host-cell contact and form a pore that releases effector proteins directly into the cytoplasm of the host[18,33,34]. There are four known effector proteins associated with the T3SS: ExoT, ExoY, ExoS, and ExoU[35]. ExoS is a T3SS effector protein with bifunctional activity, including GTPase-activating protein (GAP) activity and ADP-ribosyltransferase activity. These functions alter the host intermediate filament vimentin, causing disruption in the cytoskeleton, cell rounding, and inhibition of DNA synthesis, ultimately leading to apoptosis and cell death [36,37]. ExoT is quite similar to ExoS, sharing a 76% amino acid identity and exhibiting the same functional activity; however, ExoT seems to have lower cytotoxicity since it ribosylates fewer host proteins, demonstrating specificity for CRK proteins and only 0.2% of ExoS's ADP-ribosyltransferase activity[38–41]. ExoY is another T3SS effector protein with a unique activity, including nucleotidyl cyclase activity that increases the levels of cAMP, cGMP, and cUMP[42]. The ExoY protein leads to disruption in intercellular interactions by binding to F-actin and remodeling the cytoskeleton independent of its enzymatic activity [43,44]. ExoY is activated upon binding to F-actin, which triggers its nucleotidyl cyclase activity and disrupts host cell tau phosphorylation, resulting in microtubule breakdown[44]. ExoU, the focus of this thesis, is a 74-kDa (687 amino acids) effector protein expressed by *P. aeruginosa* and secreted via the T3SS (**Figure 1A**)[45,46].

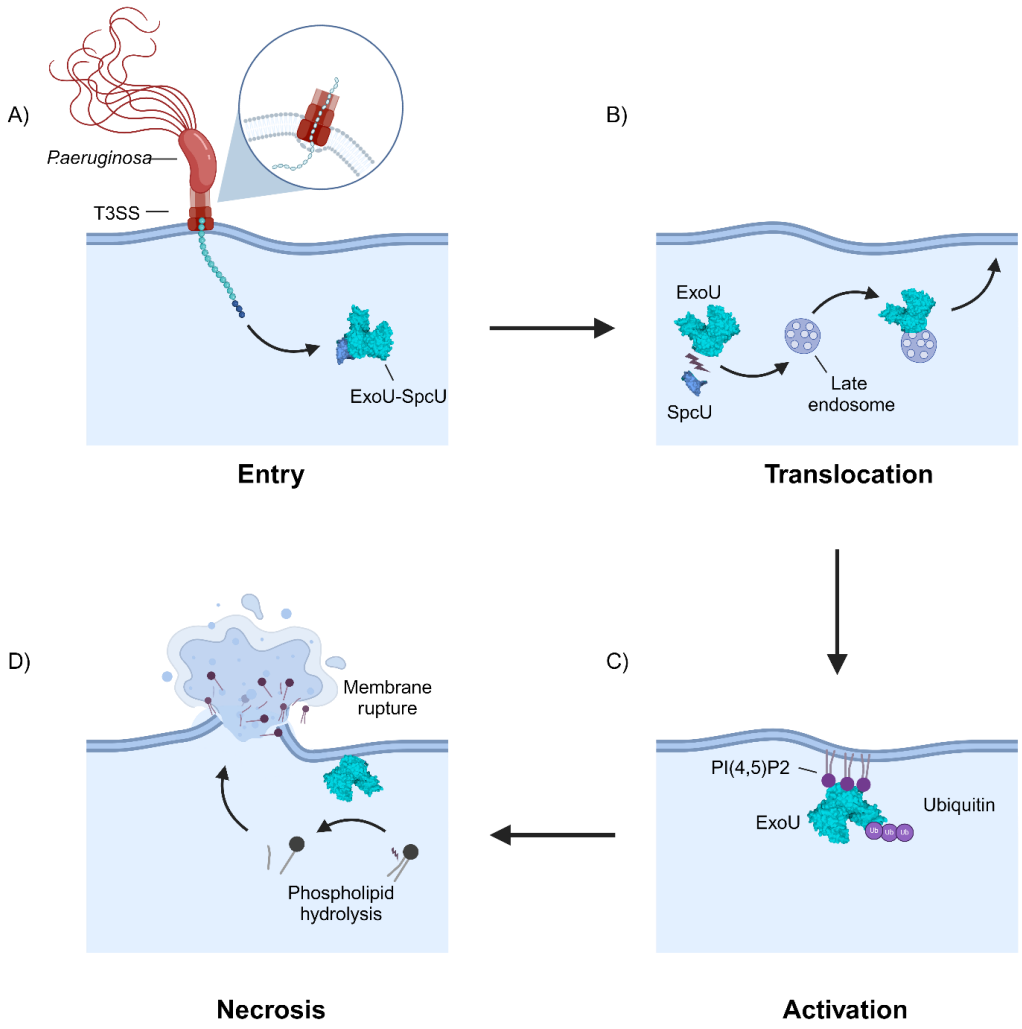

Figure 1: ExoU-induced necrosis.

A) Linear injection of ExoU-SpcU complex into the host cytoplasm through the T3SS of *P. aeruginosa.* B) Dissociation of ExoU from SpcU followed by translocation on the late endosome to the inner leaflet of the plasma membrane. C) Localization of ExoU on the inner leaflet of the plasma membrane through the association with PI(4,5)P2, and co-activation through the binding to ubiquitin. D) Hydrolysis of plasma membrane phospholipids leading to membrane rupture and necrosis.

ExoU possesses Phospholipase A_2 (PLA_2)-like activity that hydrolyzes phospholipids to produce lysophospholipids and fatty acids, leading to a rapid cell lysis [47–49]. ExoU is mutually exclusive with ExoS, as strains that express ExoU primarily do not express ExoS [35].

The T3SS effector proteins are not expressed in all *P. aeruginosa* strains, contributing to the difference in *P. aeruginosa* strain virulence. ExoS is prevalent in 58 to 72% of isolates, ExoU shows prevalence in 25 to 50%, ExoT in 90 to 100%, and ExoY in 80 to 100% of isolates, depending on the study[33]. The variability in the reported prevalence of these effector proteins between studies can be attributed to the source of isolates collected and the severity of the disease that the patients are showing. While the ExoU protein seems to be the least prevalent among the T3SS effector proteins, studies examining rates of severe infections in hospital isolates show higher numbers of ExoU-expressing strains in patients with severe infections compared to those with mild or moderate infections[35,50]. In line with these clinical findings, among the four identified effector proteins (ExoU, ExoS, ExoT, and ExoY), ExoU is linked to the greatest impact on virulence in mice[51].

The secretion of ExoU through the T3SS into host cells relies on its binding with the chaperone SpcU [52]. SpcU is a 14kDa chaperone protein that guides ExoU into the T3SS and is necessary to prevent ExoU from folding and activating in the cytoplasm of *P. aeruginosa*[52]. The ExoU-SpcU complex shows higher stability in the overall ExoU structure but lower stability in the ExoU catalytic domain[53]. SpcU binding to ExoU inactivates its catalytic activity, rendering it inert before secretion[53,54]. The ExoU-SpcU complex is secreted linearly and injected into host cells, then dissociates within the host, rendering ExoU catalytically active after injection[55].

Four domains mediate ExoU function (**Figure 2A**). The first ExoU domain spans residues 55 to 101 and is the aforementioned chaperone binding domain that binds to SpcU (**Figure 2D**)[52,53].

The second domain is the PLA_2-like catalytic domain spanning residues 102 to 471 (**Figure 2A**)[53]. The catalytic domain of ExoU possesses an oxyanion hole that stabilizes the negative charge (Gly 111, Gly 112, Gly 113), a hydrolase motif with a catalytic serine (Ser 142), and a catalytic aspartate motif (Asp 344) (**Figure 2C**). These three conserved motifs align with mammalian cytosolic phospholipase A_2 ($cPLA_2$) and Calcium-independent phospholipase A2 (iPLA2), which suggests ExoU has similar activity[48,56]. ExoU also possesses a site in its phospholipase domain that is a possible target for ubiquitination (Lys178), suggesting a potential contribution of ubiquitin to ExoU activity (**Figure 2B**)[53,54]. The C-terminus containing the third ExoU domain acts as its membrane localization domain (MLD), spanning residues 503 to 687, which creates a hydrophobic region along with a slightly polar group of residues (679 to 683) that may enable ExoU to interact with negatively charged phospholipids (**Figure 2A**)[53,54]. The fourth domain of ExoU has little known contribution to ExoU function but has been shown to interact with SpcU[53].

Consistent with sequence alignment of ExoU with mammalian $iPLA_2$ and $cPLA_2$[48,53,54], ExoU has been shown to possess a phospholipase exo-enzyme activity with the capacity to metabolize host neutral lipids and phospholipids [48]. Methoxy arachidonyl fluorophosphonate (MAFP), a phospholipase A2 inhibitor, has been shown to inhibit ExoU-induced cytotoxicity[48]. PLA_2 enzymes cleave lipids at the *sn-2* position by hydrolyzing the ester bond, producing a free fatty acid and a lysophospholipid (**Figure 3**)[57]. Mammalian $cPLA_2$ has the ability to hydrolyze phospholipids with a substrate preference for arachidonic acid at the *sn*-2 position whereas mammalian $iPLA_2$ has a broader substrate specificity [58]. The ability of ExoU to metabolize phospholipids in a similar manner to $cPLA_2$ and $iPLA_2$ suggests that PLA_2-metabolism of substrate and/or accumulation of lysophospholipid products are possible contributors to ExoU-mediated cytotoxicity [59].

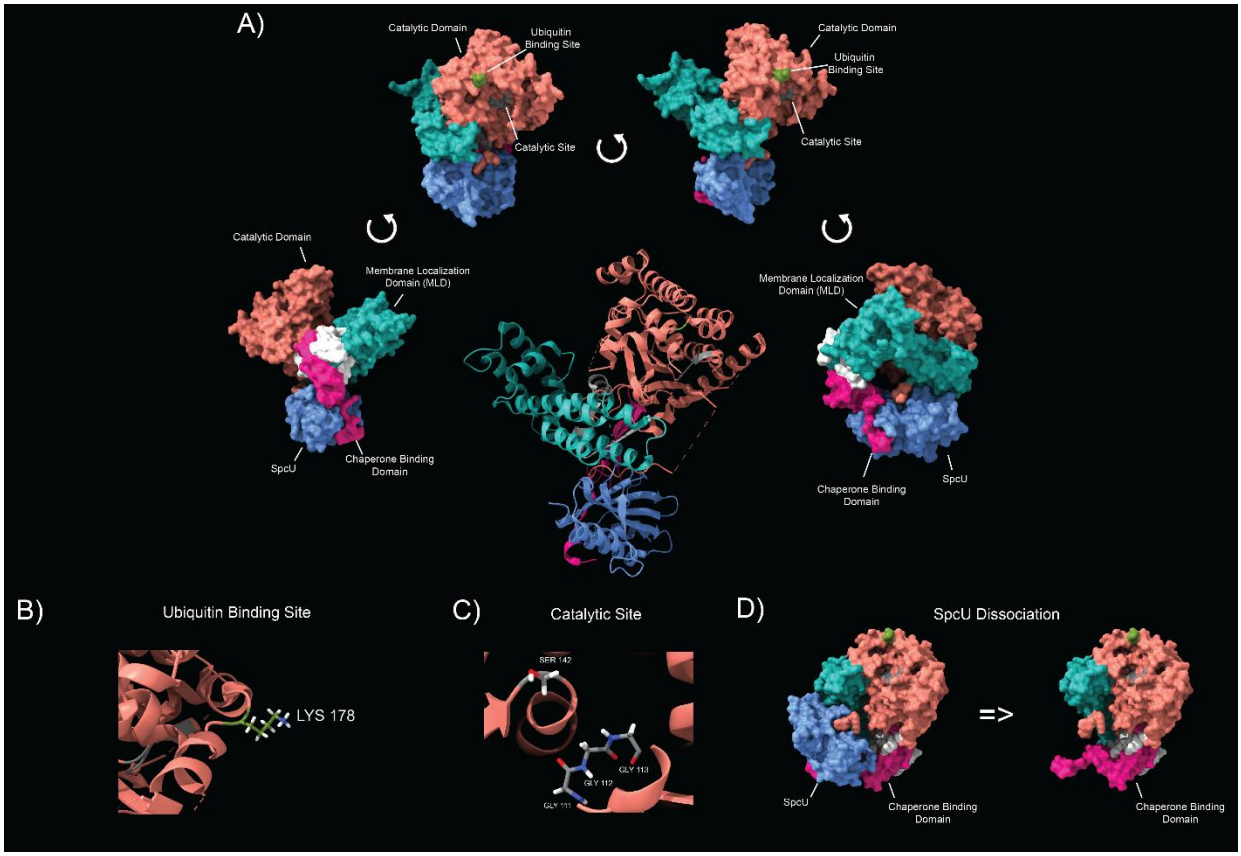

Figure 2: Crystal structure of P. aeruginosa's effector protein ExoU and its chaperone SpcU.

A) Schematic representation of ExoU's crystal structure (3TU3) [60,61] and its most important domains. The three main ExoU domains that contribute to its activity includes the catalytic domain spanning residues 102-471 (in salmon) which harbors the PLA_2-like catalytic site (in grey) and the ubiquitin binding site (in olive). The membrane localization domain (MLD) spanning residues 503-687 (in light blue) contributing to ExoU's access to the in inner leaflet of the plasma membrane lipids. The chaperone binding domain spanning residues 55-101 (in deep pink) allowing for association with the SpcU chaperone (in cornflower blue). B) The ubiquitin binding site characterized by the lysine residue (Lys 178) binds to ubiquitin or ubiquitinated species and acts a co-factor for the ExoU protein. C) ExoU catalytic site includes a catalytic triad involving three glycines (Gly 111, 112, and 113) forming an oxyanion hole. A hydrolase motif that includes serine (Ser 142), and a catalytic aspartate (Asp 344 not shown). The catalytic aspartate is located on a flexible region that is not captured in the crystal structure. D) SpcU dissociation from ExoU's chaperone binding domain following entry into host cytosol. ChimeraX was used for structural visualization of the ExoU protein crystal structure. Molecular graphics and analyses performed with UCSF ChimeraX, developed by the Resource for Biocomputing, Visualization, and Informatics at the University of California, San Francisco, with support from National Institutes of Health R01-GM129325 and the Office of Cyber Infrastructure and Computational Biology, National Institute of Allergy and Infectious Diseases.

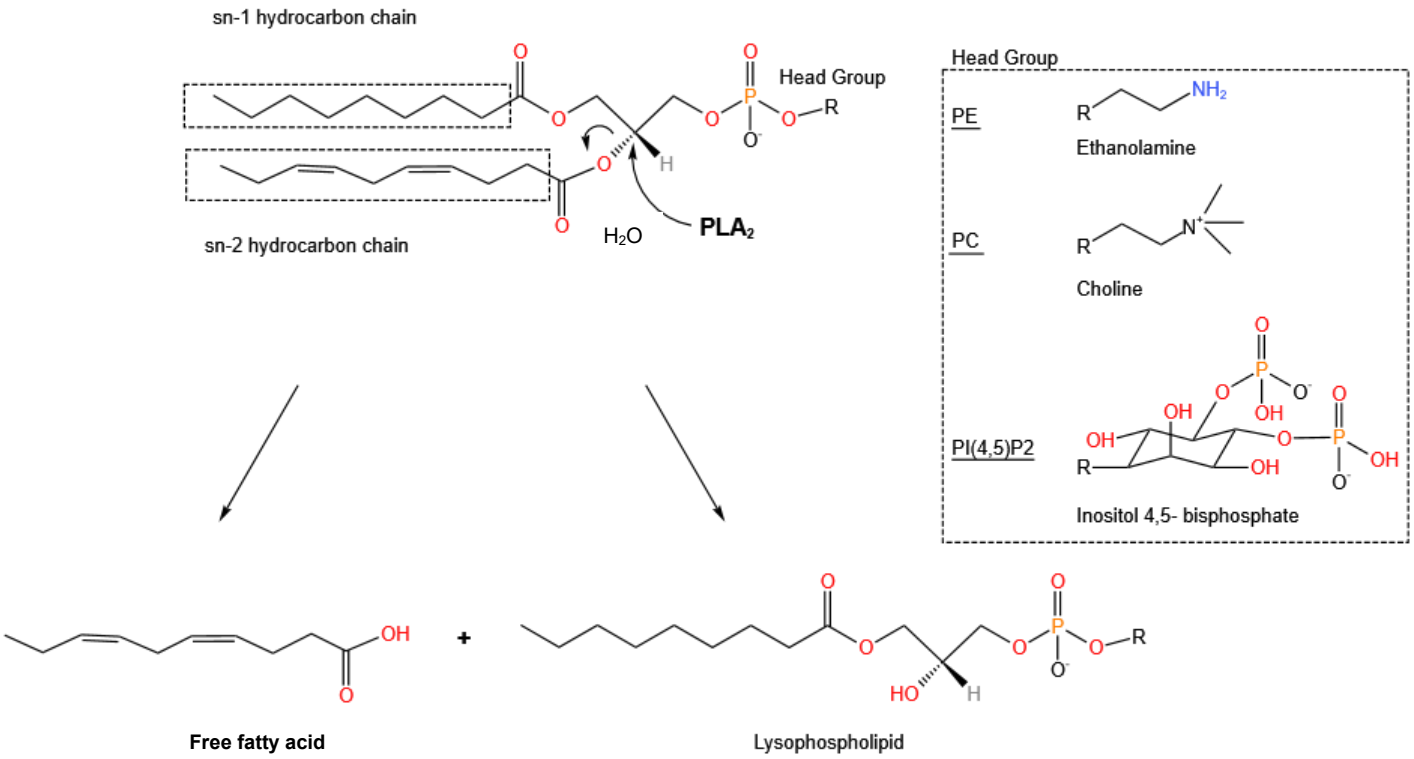

Figure 3: PLA_2 activity on a phospholipid.

A PLA_2 catalyzed reaction utilizes a phospholipid substrate with an ester-bound hydrocarbon (fatty acyl chain) at the *SN-2* position. Various phospholipid classes could be catalyzed by a PLA_2, including phosphatidylethanolamines (PE) with an ethanolamine headgroup, phosphatidylcholines with a choline headgroup, and phosphatidylinositol (PI) such as phosphatidylinositol 4,5 bisphosphate (PI(4,5)P2) with an inositol 4,5 bisphosphate headgroup. A PLA_2 enzyme stabilizes the phospholipid and forms a hydroxide ion (OH^-) generated from H_2O, which acts as a nucleophile, attacking the carbonyl group of the ester bond at the *sn-2* position. This creates an unstable intermediate that leads to the cleavage of the *sn-2* ester bond. The products of this reaction are a free fatty acid and a lysophospholipid.

1.1.4 The ExoU translocation pathway following injection into host cells

After the ExoU-SpcU complex dissociates, the ExoU protein is in the cytosol of the host cell [52]. Although not much is known about the early stages of ExoU translocation after injection, some evidence has shown partial colocalization of ExoU with early endosome antigen 1 (EEA1), a marker of the early endosomes[54]. Following its initial translocation, ExoU colocalizes with DNAJC5, a cytoplasmic protein located on the surface of late endosomes, and is required not only for transporting misfolded proteins but also for endosomal fusion to the plasma membrane and excretion of its contents[62]. ExoU is thought to hijack this anterograde vesicular trafficking and secretion pathway by localizing to the external side of DNAJC5+ late endosomes (**Figure 1B**)[63]. However, DNAJC5 only contributes to ExoU trafficking and does not contribute directly to its activity, nor is it required for ExoU docking onto the membrane[63]. Finally, ExoU binds to the inner leaflet of the plasma membrane, where it is thought to induce its cytotoxic activity (**Figure 1B**) [55]. Although little is known about other sites that ExoU might bind to other the plasma membrane, ExoU has been shown to affect the formation of lipid bodies in epithelial cells, which might suggest other localization sites that have not been well studied [64].

1.1.5 ExoU co-factors and co-activators lead to enhanced activity

Despite the catalytical activity enhanced by dissociation from SpcU, ExoU activity remains limited until improved by various host cofactors[65]. Ubiquitin (Ub) is a 76-amino acid protein that binds to proteins, signaling them for degradation. This leads to many downstream effects involving cell-cycle progression, signal transduction, transcriptomic regulation, and endocytosis [66,67]. Interestingly, ubiquitin, particularly polyubiquitin, is a cofactor for ExoU, which has been shown to enhance enzymatic activity *in vitro* [68]. Previous structural studies of the ExoU protein have suggested a possible ubiquitination site (Lys 178) on the catalytic site of ExoU (**Figure 2B**)[54]. The ubiquitination of ExoU is thought to target it to endosomal compartments, facilitating

its trafficking[54]. The ubiquitination of ExoU stabilizes the ExoU protein in its active conformation, highlighting the importance of Ub in ExoU activity (**Figure 1C**) [55]. The reliance on Ub for active ExoU activity is likely essential in preventing ExoU from impacting *P. aeruginosa* after it is expressed, as bacteria do not utilize Ub [69]. Previous experiments that co-expressed ExoU and Ub in *E. Coli* showed permeabilization of the bacterial membrane caused by ubiquitinated ExoU [68].

After ExoU is trafficked to the cell periphery on the late endosome, it utilizes its MLD to localize on the plasma membrane (**Figure 2A**)[53]. PI(4,5)P2 is an important phospholipid existing in the inner leaflet of the plasma membrane with many cell functions, including enzyme activation, membrane anchoring, and membrane trafficking[70]. As ExoU is trafficked on the late endosome, once the vesicle merges with the plasma membrane, ExoU is bound to PI(4,5)P2[63,71]. ExoU activity is enhanced by binding to phosphatidylinositol 4,5-bisphosphate (PI(4,5)P2), as PI(4,5)P2 causes a conformational change in ExoU in the presence of ubiquitin, thereby increasing ExoU activity (**Figure 1C**)[71,72]. PI(4,5)P2 has been shown to cause ExoU to form complexes or oligomers by binding to its MLD, which enhances its activity [73]. Complete ExoU activity relies on the binding to both Ub and PI(4,5)P2 [71].

1.1.6 ExoU's PLA_2 activity

ExoU has been reported to induce cytotoxicity in many host cells [51]; however, the exact mechanism and mediators that lead to cell death have not been completely identified. ExoU is active in mammalian PLA_2 activity assays, suggesting that ExoU can release similar substrates to PLA_2 [74]. As discussed above, PLA_2 hydrolyses the ester bond at the *sn-2* position of phospholipids, releasing a lysophospholipid and a fatty acid (**Figure 1D**)[75]. Among the most common fatty acids that are known to be implicated in inflammation and cell death is

arachidonic acid (AA), which is known to be released by PLA2 enzymes, leading to the induction of apoptosis and pro-inflammatory downstream events [76,77]. Arachidonic acid can be found as part of phospholipids in the plasma membrane[78]. Arachidonic acid leads to the formation of eicosanoids, which are important inflammatory mediators[79,80]. Arachidonic acid is oxidized at different sites to produce various eicosanoids, which are lipid mediators that play a role in cell signaling and inflammation [81]. COX-2 oxygenates arachidonic acid to form PGE2 and ALOX5 to form LTB4. Both lipid mediators are implicated in inflammatory pathways and disease [82,83]. ExoU-infected cells show an increase in AA release, which can be inhibited using a PLA_2 inhibitor (MAFP), indicating that the phospholipase A2 activity of ExoU could be pro-inflammatory [64,84,85]. ExoU-infected cells also exhibited elevated levels of PGE2 and LTB4 in mice's bronchoalveolar fluids (BALFs), suggesting that ExoU-cleaved AA is oxidized and converted into pro-inflammatory lipid mediators[84,86].

ExoU is thought to be able to hydrolyze a wide range of lipids, including phospholipids as well as neutral lipids[48] although few detailed lipidomic assessments of substrates have been performed [48,86]. ExoU substrates included phosphatidylcholines (PC), phosphatidylethanolamines (PE), phosphatidic acid (PA), lyso-PCs, and neutral lipids which could include triacylglycerols and diacylglycerols [48,49,86–88]. Although ExoU activity appears to have a broad range of substrates, ExoU shows a high affinity for PI(4,5)P2, which was discussed before as being important for localization (**Figure 1C**) [89]. However, ExoU is not only limited to binding to PI(4,5)P2 but also has been shown to cleave it, leading to a decrease in viability in infected cells in a dose-dependent manner [89]. The wide range of ExoU products could lead to different mechanisms of cell death that might be induced, and determining these ExoU substrates and

products could provide crucial information in determining the type of cell death induced by ExoU, which is the focus of this thesis.

1.2 Cell death pathways

1.2.1 Apoptosis, general overview of mechanism

Apoptosis is a form of regulated cell death that is required for homeostasis [90], generally characterized by cell shrinkage, chromatin condensation, and bleb formation [91,92]. Apoptosis is not an inflammatory form of cell death and is thought to have some anti-inflammatory effect, caused by the release of anti-inflammatory cytokines such as IL-10 and TGF-ß by specific apoptotic cells [93,94]. Two main known pathways initiate apoptosis, the intrinsic and extrinsic pathways that depend on the type of stimulus in the environment: binding to a death receptor (DR) leads to the activation of the extrinsic apoptosis pathways or an intracellular stimulus leading to the activation of the intrinsic apoptosis pathways [95–97].

The extrinsic apoptosis pathway is triggered by various extracellular ligands, such as tumor necrosis factor (TNF), Fas ligand (Fas-L), and TNF-related apoptosis-inducing ligand (TRAIL) binding to their DR: TNF receptor 1(TNFR1), Fas receptor (FasR) and TRAIL receptors death receptor 4 (DR4), and death receptor 2 (DR2) respectively [98,99]. Once the death ligand binds to its DR, the death-inducing signaling complex (DISC) is formed, which could consist of a Fas-associated protein with death domain (FADD), TNFR1-associated death domain (TRADD),procaspase-8, Receptor-interacting protein kinase 1 (RIPK1) and other proteins (**Figure 5A**) [99–101]. Caspases are endoproteases that play a significant role in the apoptosis pathway, and they are divided into initiator (caspase-2, -8, -9, and -10) or executioner caspases (caspase-3, -6, and -7) depending on their role in the cell death pathway [92,102,103]. The formation

of DISC results in the cleavage of procaspase-8 into caspase-8, which activates caspase-3 and caspase-7, initiating the execution pathway(**Figure 5A**) [104,105].

The intrinsic apoptosis pathway is often referred to as the mitochondrial-mediated apoptotic pathway because of the involvement of the mitochondria in its mechanism and regulation by the Bcl-2 family of proteins [106]. The intrinsic apoptosis pathway can be triggered by DNA damage, ER stress, and oxidative stress [107–109]. Two pro-apoptotic Bcl-2 family proteins, bax and bak, are activated upon apoptotic stimulus and oligomerize at the mitochondrial outer membrane, leading to mitochondrial permeabilization (**Figure 5A**) [110,111]. Once the mitochondrial membrane is compromised, cytochrome c, along with other pro-apoptotic toxic proteins, are released into the cell (**Figure 5A**) [112]. Cytochrome c binds and activates apoptotic protease activating factor-1 (Apaf-1) and pro-caspase-9, forming the apoptosome and leading to the cleavage and activation of caspase-9 (**Figure 5A**) [113,114].

The extrinsic and intrinsic apoptosis pathways can influence one another and share some parts of their pathways [115]. The two pathways converge at the last phase of the apoptosis pathway, the execution phase, driven by the executioner caspases [103]. The executioner caspases, particularly caspase-3, cleave cytokeratins, poly (ADP-ribose) polymerase-1 (PARP-1), fodrin, and the nuclear protein NuMA, leading to the DNA damage and membrane blebbing associated with apoptosis (**Figure 5A**) [116–119]. One of the most important markers of apoptotic cells is the externalization of phosphatidylserine (PS), which is detected with reagents like Annexin V [120].

1.2.2 Necroptosis, general overview of mechanism

Necroptosis has been characterized as a regulated form of cell death that could be triggered by extracellular or intracellular stimuli [121,122]. The necroptosis pathway can be initiated by FAS

and TNFR1, similar to apoptosis, but also by pathogen recognition receptors (PRRs) such as toll-like receptor 4 (TLR4), and Z-DNA binding protein (ZBP1) [123–125]. Once the necroptosis-associated receptors are activated, receptor-interacting serine-threonine protein kinase 1 (RIPK1) is recruited, leading to the activation of receptor-interacting serine-threonine protein kinase 3 (RIPK3) (**Figure 5B**)[126]. Once RIPK3 is activated, it phosphorylates the mixed lineage kinase domain-like pseudokinase (MLKL) protein (**Figure 5B**)[127]. Phosphorylated MLKL can form oligomers forming the necrosome, which travels and binds to phosphatidylinositol phosphate species, leading to membrane disruption and permeabilization (**Figure 5B**) [128,129]. Necroptosis is characterized by swelling and plasma membrane rupture [130].

1.2.3 Ferroptosis, general overview of mechanism

Ferroptosis is a regulated form of cell death that depends on iron and relies on lipid peroxidation as a mediator[131]. Similar to necroptosis and pyroptosis, ferroptosis is an inflammatory cell death that leads to the release of pro-inflammatory damage-associated molecular pattern molecules (DAMPs) such as HMGB1, KRAS, as well as pro-inflammatory lipid mediators AA, LTB4, and others [132–134]. The ferroptosis mechanism is initiated by an accumulation of iron [135]. The transferrin receptor binds and transports transferrin, carrying two ferric iron ions, through endocytosis into the cell cytoplasm (**Figure 5C**) [136]. Under acidic conditions, ferric iron (Fe^{3+}) is released and reduced by the ferrireductase six-transmembrane epithelial antigen of the prostate 3 (Steap3) into ferrous iron (Fe^{2+}) [137]. After ferric iron is reduced to ferrous iron, the divalent metal transporter-1 (DMT1) can transport the ferrous iron into the cytoplasm, becoming a part of the labile iron pool or associating and stored on ferritin [138,139]. Macrophages can uptake higher levels of iron through their CD163 hemoglobin receptor, which could lead to higher oxidation levels compared to other cell types [140,141]. The unbound

labile pool of iron is reactive and can catalyze the oxidation of lipids by driving Fenton reactions, leading to the formation of lipid peroxyl radicals generating lipid peroxides (**Figure 5C**) [142,143]. The formation of lipid peroxides does not rely on enzymes to catalyze their propagation, as they can undergo autoxidation and generate lipid hydroperoxides independently (**Figure 4**) [144]. The role of enzymatically driven lipid peroxidation, particularly involving LOXs, has been introduced as a contributing factor in ferroptosis; however, Fenton reactions are considered the primary drivers of ferroptotic cell death[144–146]. This may indicate that lipid peroxides produced from enzymatically driven reactions could play a role in the initiation process instead of propagation. The increase in lipid peroxidation can be seen as an increase in many inflammatory lipids such as isoprostanes, prostaglandins, and leukotrienes [147,148]. Lipid peroxides also can affect the plasma membrane structure and fluidity, membrane permeability, and eventually rupture (**Figure 5C**) [149–152]. Peroxides can be further degraded into secondary toxic products, including lipid aldehydes such as malondialdehyde (MDA) and 4-hydroxynonenal (4-HNE), leading to cell death [153,154].

Cells rely on many oxidation suppression defense mechanisms to prevent oxidative damage and peroxidation. The most important ferroptosis suppression mechanism revolves around glutathione peroxidase 4 (GPX4) to form the GPX4-GSH-cysteine axis [155]. Glutathione is a crucial antioxidant that a cell utilizes to reduce lipid peroxidation [156,157]. GSH reduces lipid peroxide radicals into lipid hydroxides and is converted to glutathione disulfide (GSSG) using GPX4 [158,159]. This protects the cells from membrane damage by converting lipid peroxides, which damage membrane structure, to lipid hydroxides [143]. To regenerate the pool of glutathione in the cell, the cystine (Cys) and glutamate (Glu) antiporter system Xc- transports Cys into the cell and exports Glu into the extracellular environment [160,161].

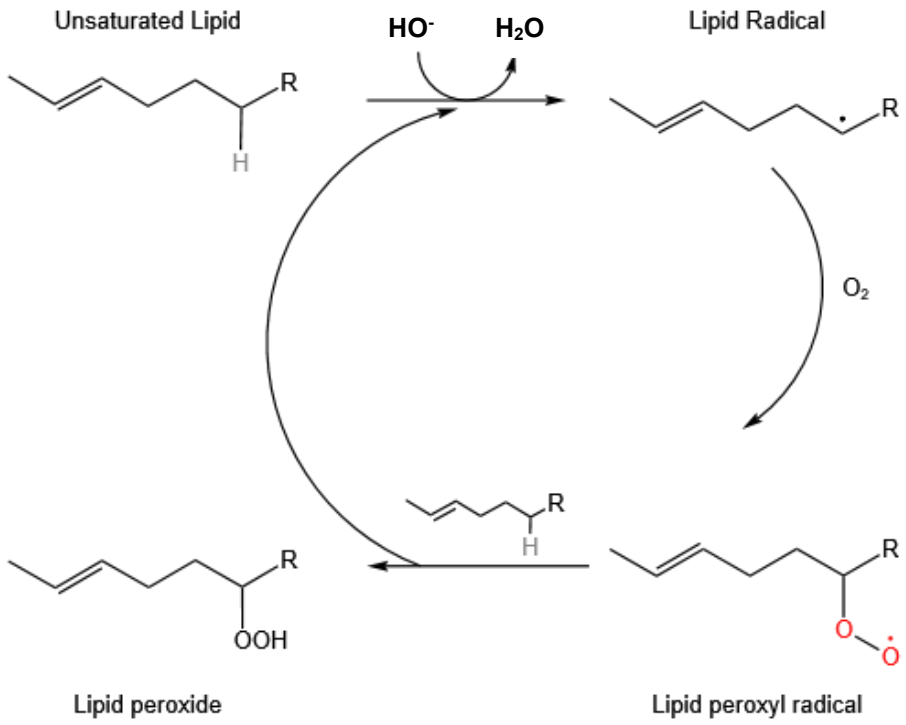

Figure 4: Lipid peroxidation through Fenton chemistry.

The generation of lipid peroxides is initiated by forming a hydroxyl radical OH^- typically catalyzed by labile iron in the intracellular environment or from a lipid radical species. The hydroxyl radical removes hydrogen from the lipid and generates a lipid radical (RO^-). The lipid radical reacts with oxygen and forms a lipid peroxyl radical (LOO·). The peroxyl radical formation allows the cycle to propagate when the lipid peroxyl radical stabilizes by removing hydrogen from a neighboring fatty acid, forming a lipid peroxide (LOOH).

Cystine is subsequently reduced to cysteine by thioredoxin reductase 1 (TrxR1), resulting in the production of additional GSH[162].

Other ferroptosis supressing axis have been identified, such as the ferroptosis suppressor protein 1 (FSP1) dependent mechanism. FSP1 acts as a NADH-dependent CoQ oxidoreductase which reduces CoQ allowing it to function as a radical-trapping antioxidant [163,164]. CoQ reduces the levels of peroxidation in a cell, which inhibits ferroptosis induction [164]. Many other mechanisms are deployed by cells to reduce oxidation, relying on a multitude of enzymes that can inhibit or induce ferroptosis in cells[165]. Disruption in lipid metabolism might lead to ferroptosis and possibly is utilized by pathogens such as bacteria to induce cell death[48,86].

1.2.4 Necrosis, general overview

Necrosis is an unregulated form of cell death characterized by cell swelling, plasma membrane rupture, and organelle breakdown, including releasing intracellular contents (**Figure 5D**)[166,167]. The release of cellular contents is often inflammatory because the intracellular content can be recognized as DAMPs, which are sensed by neighboring cells, leading to an inflammatory response[168]. Necrosis does not have a defining mechanism that induces necrotic cell death, but rather a multitude of factors that lead to the mentioned characteristics of necrosis are used to differentiate necrosis from other cell death mechanisms. Necrosis can be triggered by many stressors, including an increase in ROS, low adenosine triphosphate (ATP) levels, calcium levels, the influx of water, and disruption of the cell's cytoskeleton, all of which lead to plasma membrane disruption and rupture (**Figure 5D**) [89,169–172].

1.2.5 Effect of lysophospholipids and fatty acids on membrane integrity and necrosis

Phospholipids are the most abundant class of lipids on the plasma membrane and the major structural component of eukaryotic cells, which makes their structure and composition crucial for cell survival [173]. Plasma membrane lipid asymmetry and distribution is tightly regulated and dynamically remodeled by enzymes such as flippases, floppases, scramblases, and PLA_2 isoforms [174,175]. Phospholipid composition and structure control membrane curvature as phospholipid headgroups can undergo electrostatic repulsion depending on their charge, and the fatty acid chain length and components affect membrane thickness and contribute to curvature by changing the molecular area of the lipid [174,176,177]. Other factors such as the oxidation of the fatty acyl chain can play a role in membrane structure [178]. PLA_2 enzymes act on phospholipid structure by cleaving the ester bond at the *sn-2* of a phospholipid, releasing a lysophospholipid and a fatty acid (**Figure 3**)[179]. Free fatty acids also play a role in membrane structure, as they appear to affect protein activity at the membrane [180]. Fatty acid chain length also appears to play a role in membrane permeability [181]. Furthermore, an increase in lysophospholipids concentration in a membrane has been shown to decrease the stability of a membrane acting as a detergent, making the plasma membrane more vulnerable to permeabilization as well as higher sensitivity to increases in temperature [182,183].

Moreover, lysophospholipid chain lengths appear to play a role in their ability to disrupt membrane structure, whereas longer chain length lysophospholipids appear to have a higher ability to move from the aqueous phase to the lipid membrane and act as a detergent which could lead to more membrane permeabilization [184,185].

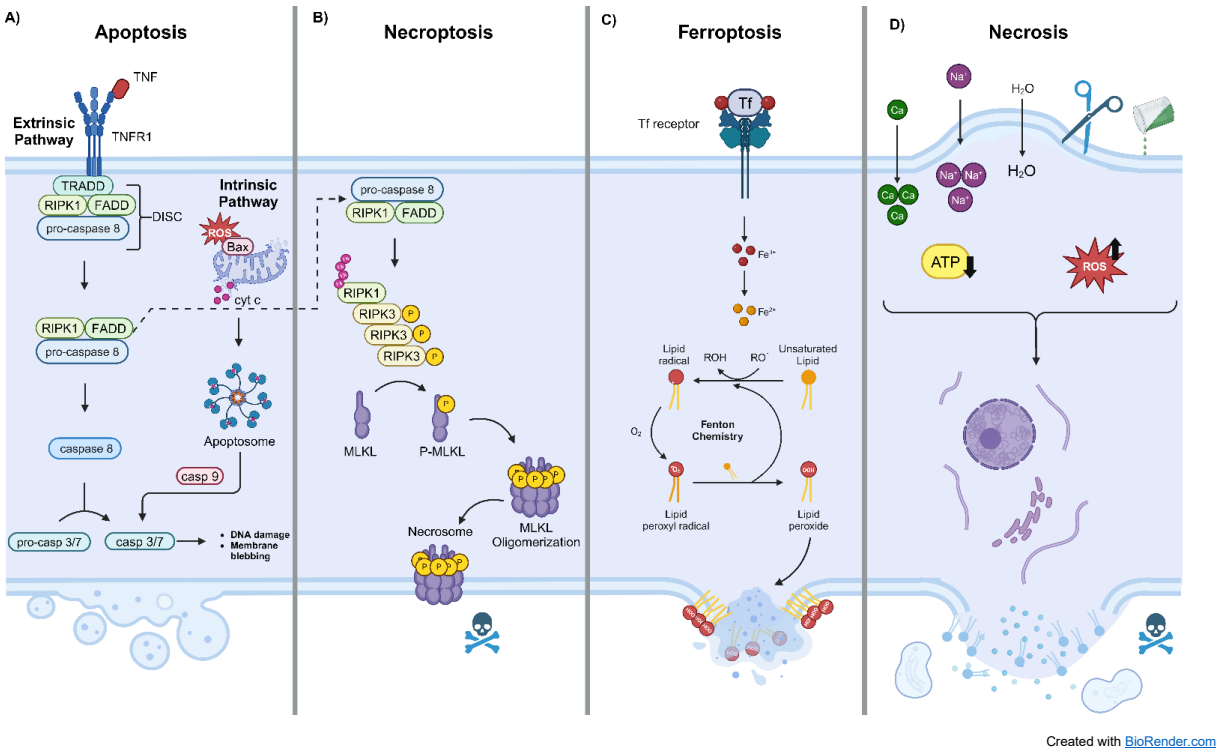

Figure 5: General overview of cell death pathways.

A) The extrinsic apoptosis pathway can be initiated through various death receptors, such as TNFR1, binding to TNF. This recruits proteins such as TRADD, RIPK1, FADD, and pro-caspase 8 forming the DISC complex. The DISC complex cleaves and activates caspase 8, which activates executioner caspases such as caspase 3 and 7. Active executioner caspases induce apoptosis by causing DNA damage and the formation of blebs. Alternatively, various intracellular stimuli, such as oxidative damage, can activate the Bcl-2 family of proteins such as Bax. The activation of Bax permeabilizes the mitochondria, releasing cytochrome c. The release of cytochrome c activates the apoptosome and cleaves caspase 9. Caspase 9 activates the executioner caspase 3, leading to apoptosis. B) Necroptosis is an alternative cell death pathway that is activated in case caspases are inhibited and are unable to induce the apoptosis pathways. The RIPK1 activated from the initial apoptosis signal can become part of the necroptosis pathway by recruiting and phosphorylating RIPK3. This activation of RIPK3 is responsible for the phosphorylation of MLKL, which leads it to oligomerize and form necrosomes and necroptotic cell death. C) Ferroptosis is an iron-dependent form of cell death that can be triggered by the accumulation of intracellular iron. Iron enters the cell bound to transferin, where it is endocytosed through the transferrin receptor. Ferric iron is reduced into ferrous iron, which can catalyze Fenton reactions in the cell. Fenton reactions lead to the autoxidation of phospholipids, forming lipid peroxides that permeabilize the plasma membrane and induce ferroptotic cell death. D) Necrosis is an unregulated inflammatory type of accidental cell death characterized by swelling and rupture, releasing intracellular content. Necrosis can be initiated by a multitude of factors including mechanical or chemical damage to the plasma membrane. Increases in ROS causing higher permeability lead to an increase in intracellular water and rupture. A decrease in ATP production leads to an inability to maintain an ion gradient, leading to an influx of calcium or sodium ions, causing water build-up and cell rupture.

Various enzymes could affect the structure of lipids in the membrane, potentially allowing pathogens to utilize this vulnerability to induce necrosis and cell rupture, leading to high levels of cytotoxicity.

1.2.6 Overview of Phosphatidylinositol 4,5-bisphosphate (PI(4,5)P2)

PI(4,5)P2 is highly involved in many biological roles, including signaling, transport, and structural roles [186]. PI(4,5)P2 is mainly located on the inner leaflet of the plasma membrane [186]. Focal adhesions are a group of proteins, including integrins, paxillin, focal adhesion kinase (FAK), talin, vinculin, and α-actinin connected to actin filaments [187–189]. PI(4,5)P2 is involved in activating and stabilizing some of these proteins, making it crucial to the formation of a functional cytoskeleton [190–192]. Many studies have shown that loss of PI(4,5)P2 leads to detachment of the actin cytoskeleton, leading to a disruption in the plasma membrane [193,194]. Some bacterial proteins can affect PI(4,5)P2, leading to membrane disruption and might lead to cell death (necrosis) [89,193].

1.3 Innate immunity

1.3.1 Macrophage and epithelial cells in the innate immune system

Macrophages and epithelial cells are a crucial part of the innate immune system, forming the first line of defense against pathogens. Macrophages play a role in initiating and resolving inflammation through the variety of cytokines, chemokines, and DAMPS that they release in response to infection [195,196]. In the presence of bacterial pathogens, macrophages aid in bacterial clearance through phagocytosis and signaling for immune recruitment by releasing various proinflammatory cytokines, including IL-6, TNF, and the IL-1 family [197,198]. Macrophage response aids in the recruitment of neutrophils by releasing cell adhesion molecules (CAMs) and vascular endothelial growth factor (VEGF) to the site of infection [199]. Initial responses to

bacterial infections in the lungs by resident alveolar macrophages make them crucial in the fight against bacteria such as the ExoU expressing *P. aeruginosa*, as they provide a crucial immune response needed to clear the infection before they are killed by the bacteria [200]. Similarly, epithelial cells are able to recognize the infection and release proinflammatory cytokines and chemokines [201]. Lung epithelial cells can aid in defense against bacteria through mucociliary clearance [202]. However, excessive mucosal buildup in the lungs can be detrimental to lung function as it can promote bacterial infection, such as the case of cystic fibrosis, which is prone to *P. aeruginosa* [10,203,204].

1.3.2 Role of immune mechanisms in response to bacterial infection

During an infection, various pattern-recognition receptors (PRRs) contribute to recognizing various bacterial agents [205]. PRRs can detect pathogen-related components called pathogen-associated molecular patterns (PAMPs), including T3SS components and flagellin through the Toll-like receptor (TLR) family and the intracellular leucine-rich repeat-containing proteins of the Nod-like receptor family (**Figure 6**) [206,207]. PRRs can also detect damage-associated molecular patterns (DAMPs) that are endogenous molecules linked to cellular damage or stress[208]. PRR activation forms signaling cascades that lead to the transcription of multimeric complexes that form the inflammasome[205,208,209]. The NLRP3 is an inflammasome that can cleave caspase-1 and activate it (**Figure 6**) [210]. Caspase-1 is important for interleukin 1 (IL-1) family maturation, which are pro-inflammatory cytokines that are important for host defense mechanism[211]. Caspase-1 is also important for cleaving gasdermin D (GSDMD), which complexes and relocates to the plasma membrane to form pores, which contribute to cell death and IL-1ß secretion (**Figure 6**) [212,213]. The NLRC4 inflammasome is also responsible for caspase-1 activation and IL-1ß maturation and can identify PAMPs which is especially important

in sensing gram-negative bacteria[214]. Previous studies reported the pro-inflammatory response induced by the *P. aeruginosa* effector protein ExoU [64,74,86]. This suggests an involvement of the inflammasome in the ExoU mechanism, which remains to be explored. However, it is unclear how ExoU-induced cell death might contribute to the inflammatory response. ExoU functions similarly to PLA_2. Therefore, lipids released by ExoU might contribute to organelle stress and indirectly lead to the formation of the NLRP3 inflammasome and the release of IL-1ß (**Figure 6**) [215]. Investigating how lipids might directly or indirectly activate the NLRP3 or NLRC4 inflammasomes, resulting in the release of IL-1ß, will lead to a better understanding of the mechanism of ExoU[216,217].

1.3.3 IL-1ß and immune response to bacterial infection

Cytokines are signaling molecules that take part in intercellular communication contributing to immune regulation [218]. Different cytokines can be either pro-inflammatory or anti-inflammatory and can be released by many immune cells, including macrophages [219]. Proinflammatory cytokines include IL-6, IL-1ß, and TNF-α; while anti inflammatory cytokines include IL-4, IL-10, IL-11, and IL-13 [219]. The pro-inflammatory cytokine IL-1ß has shown a protective role against bacterial infection, including gram-negative bacteria such as *P. aeruginosa* [220]. IL-1ß drives inflammation in many organs around the body and excessive levels can be linked to autoimmune diseases, metabolic syndrome, and aggressive cancer [221]. Excessive proinflammatory responses can ultimately harm the host if left unregulated, as IL-1ß may negatively impact bacterial clearance, highlighting its importance in managing chronic infections[222]. Chronic P. aeruginosa infections are prevalent among cystic fibrosis patients, who exhibit increased levels of IL-1ß production in the lung environment [223]. As ExoU expressing *P. aeruginosa* leads to more severe infections in patients, the role of IL-1ß in the inflammatory response becomes an important factor for investigation.

1.4 Phospholipid metabolism

1.4.1 Glycerophosphocholine (GPC) synthesis pathways

Glycerophosphocholines (GPCs) are the most abundant phospholipids in the plasma membrane [224]. GPCs can be synthesized *de novo* within a cell through a well-studied cytidine diphosphate (CDP)-choline pathway called the Kennedy pathway (**Figure 7**) [225]. The synthesis starts with the choline transport into the cell through the various choline transporters such as the choline transporter 1 (CHT1) and others [226]. Following entry, choline is phosphorylated using the choline kinase (CK), utilizing ATP and releasing an adenosine diphosphate (ADP) and a phosphocholine (PC) (**Figure 7**)[227]. Afterward, cytidine triphosphate (CTP) reacts with the generated PC to form CDP-choline, catalyzed by the CTP: phosphocholine cytidylyltransferase (CT) (**Figure 7**)[228]. The CT-controlled step is the rate-limiting step in GPC synthesis, with many CT isoforms present in the body, making it crucial for cell survival [228]. The last step in the pathway is the binding of diacylglycerol to CDP-choline by CDP-choline:1,2-diacylglycerol choline phosphotransferase (CPT), as well as CDP-choline:1,2-diacylglycerol choline/ethanolamine phosphotransferase (CEPT), leading to the release of cytidine monophosphate (CMP) and a PC (**Figure 7**)[229,230]. CEPT can catalyze the transfer of both CDP-choline as well as CDP-ethanolamine [229]. Because of the crucial function of PCs to survival, the body possesses an alternative PC synthesis pathway that is only localized in the liver.

Hepatocytes highly express the enzyme phosphatidylethanolamine N-methyltransferase (PEMT), which catalyzes the methylation of GPEs using S-adenosylmethionine (AdoMet) as a methyl group donor to form a GPC (**Figure 7**) [231,232]. Studies have shown that mice lacking the PEMT gene eating a choline-deficient diet developed liver damage, establishing the importance of the liver's role in the alternative GPC synthesis pathway [233,234].

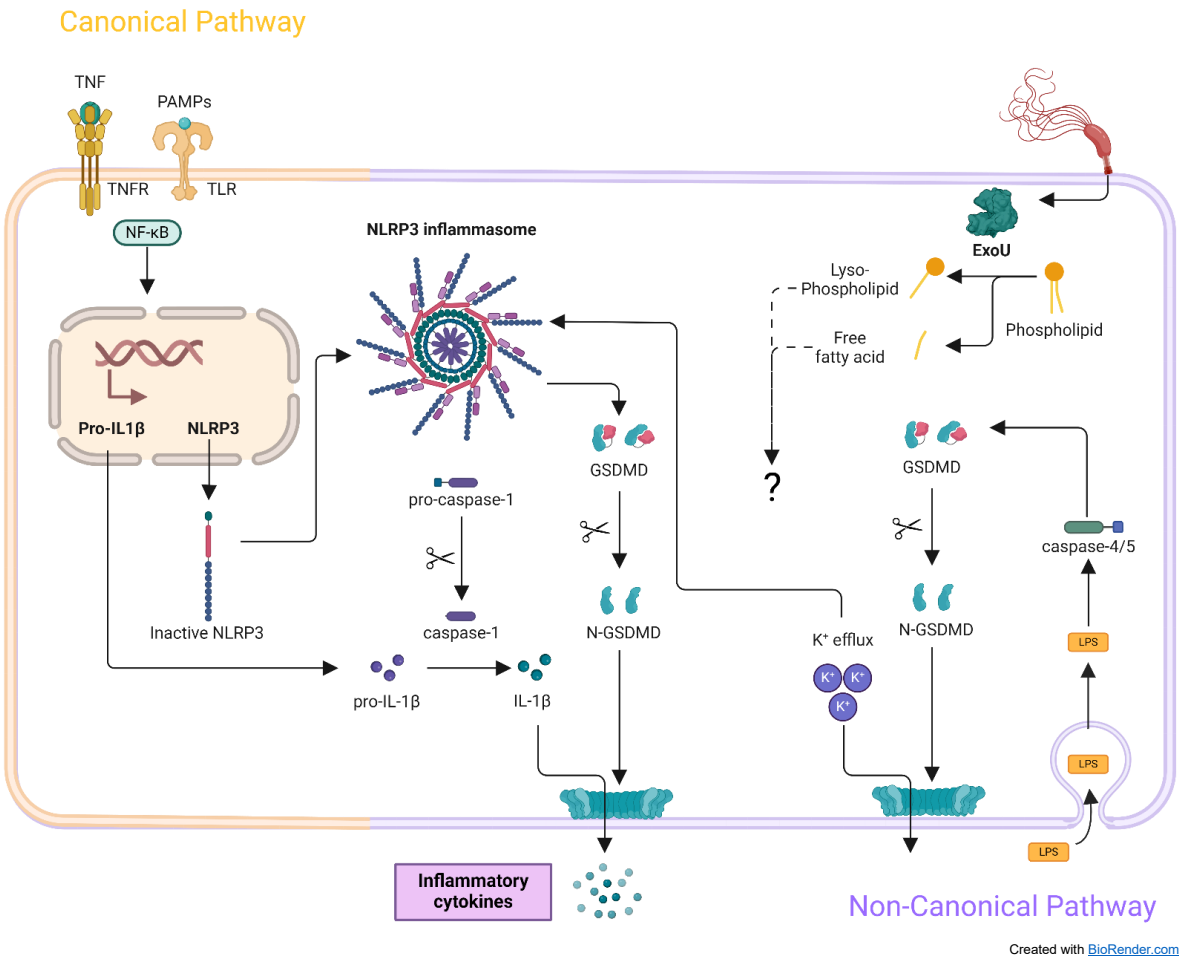

Figure 6. Canonical and non-canonical inflammasome activation pathway.

The canonical inflammasome activation pathway is triggered by the binding of TNF or PAMPs to their respective receptors on the cell surface. The activation of the receptors leads to activation of the transcription factor NF-KB and its signaling pathway. NF-KB translocates to the nucleus and initiates the transcription of NLRP3 and pro-IL1ß. A secondary signal triggers the assembly of the NLRP3 inflammasome, recruiting multiple proteins, including pro-caspase-1. Pro-caspase-1 undergoes autoproteolytic cleavage, becoming caspase-1. Caspase-1 cleaves pro-IL-1ß, producing active IL-1ß, which is ready for secretion. Active caspase-1 also cleaves gasdermin D (GSDMD), generating N-GSDMD, which oligomerizes and forms membrane pores. The gasdermin pore allows pro-inflammatory cytokine release, including activated IL-1ß. The presence of intracellular LPS activates the non-canonical pathway. LPS directly interacts and activates caspase-4/5 (in humans), leading to the cleavage of GSDMD. Gasdermin pores cause the efflux of potassium ions, which activates the NLRP3 inflammasome. ExoU catalyzes phospholipids, releasing fatty acids and lysophospholipids into the intracellular environment. Products formed by ExoU may contribute to the activation of the inflammasome pathway.

As the most abundant lipid in the plasma membrane, GPCs play major roles in maintaining membrane structure as well as membrane fusion, and disruption of GPCs could be detrimental to cell survival [235].

1.4.2 Phospholipid remodeling (Lands cycle)

The Lands cycle is a crucial mechanism for remodeling the fatty acyl chains on membrane phospholipids [236]. The remodeling starts with the activity of phospholipases such as PLA_2s, which release a fatty acid (deacylated) from the *sn-2* bound position (**Figure 8**) [237]. Other phospholipases, such as PLA_1, hydrolyze the other bound fatty acid at the *sn-1* position [237]. The products of these phospholipases include lysophospholipids and fatty acids [75]. Fatty acids could be saturated, monounsaturated, and polyunsaturated with varying numbers of double bonds in their structure, giving them different roles that could contribute to inflammation [238,239]. Unsaturated fatty acids are prone to oxidation and remodeling in the cytosol by several different enzymes (discussed in the next section). After the deacylation by a PLA_2, different enzymes are part of the reacylation process that starts with attaching free fatty acids to coenzyme-A (CoA) to form acyl-CoA by long-chain acyl-CoA synthetases (ACSL) (**Figure 8**) [240]. Various ACSL isoforms preferentially catalyze certain fatty acids, whereas ACSL4 prefers AA, eicosapentaenoic acid (EPA), and adrenic acid [240,241].

Acyl-CoA attached fatty acids are then reacylated and incorporated into phospholipids through lysophospholipid (lysoPL) acyltransferases (lysoPLATs) (**Figure 8**)[242]. Different isoforms of lysoPLATs are expressed differentially based on the cell type which create a varied profile of PLs depending on the cell type [243].

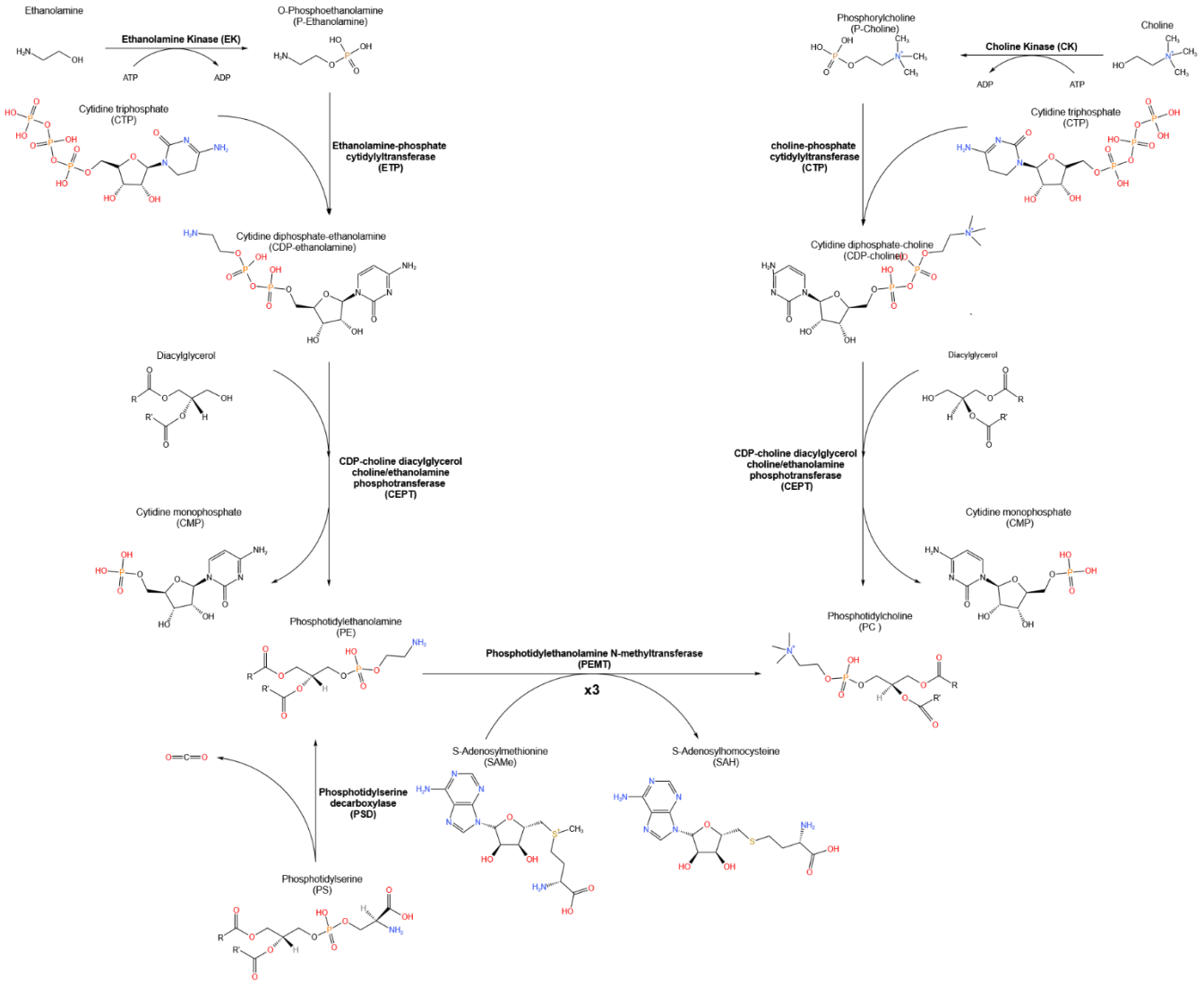

Figure 7: Phosphatidylcholine synthesis pathway.

PC synthesis is formed through de-novo synthesis as part of the Kennedy pathway and the conversion of PE to PC. The de-novo synthesis pathway is initiated with the addition of a phosphate to choline by choline kinase (CK) which generates a phosphocholine. This is followed by CDP-choline formation through the action of choline-phosphate cytidylyltransferase (CTP). Finally, cholinephosphotransferase (CEPT) catalyzes the formation of PC from CDP-choline and diacylglycerol (DAG). Similarly, GPEs undergo the same synthesis pathway with an ethanolamine converting to a PE. PC can also be synthesized through the conversion of PE to a PC as part of the phospholipid headgroup exchange pathway. Phosphatidylethanolamine (PE) is first converted to PC through a series of methylation reactions catalyzed by phosphatidylethanolamine N-methyltransferases (PEMT), where S-adenosylmethionine (SAM) acts as the methyl donor. Phosphatidyl serine (PS) could also undergo a decarboxylation to form a PE which could undergo the same methylation pathway to become a PC.

Furthermore, isoforms of lysoPLATs can preferentially reacylate different fatty acyl chains which create diverse structures in membrane PLs such as the lysophophatidylcholine acyltransferase 3 (LPCAT3) that preferentially reacylate phatidylcholines [244,245]. Acyl-CoA could also be integrated into triacylglycerides or diacylglycerides by diacylglycerol acyltransferase (DGAT) or monoacylglycerol acyltransferases (MGAT)[246]

The Lands cycle could also be damaging to the cell membrane (**Figure 8**). Because free fatty acids can be oxidized, the reacylation of peroxidized fatty acids into the phospholipids of the plasma membrane could contribute to membrane disruption and might lead to ferroptotic cell death (**Figure 8**)[243,247]. Lipid membrane remodeling proteins such as ACSL4 and LPCAT3 have been implicated in sensitizing cells to ferroptosis as part of a larger mechanism that includes peroxidation of the free fatty acids that are incorporated into the membrane leading to ferroptosis (**Figure 8**)[248,249].

1.4.3 Phospholipid oxidation and lipid peroxidation pathways

Lipid peroxidation in humans is carried out by various enzymes, including cyclooxygenases (COX), lipoxygenases (ALOX), or cytochrome p450 (CYP)[154]. Cytochrome P450 oxidoreductase (CYPOR), which plays a role in phospholipid peroxidation in ferroptosis, was suggested to be a major contributor to ExoU-mediated cytotoxicity, providing initial insight into the primary targets of ExoU[86,250]. COX is an enzyme that is known to catalyze arachidonic acid to various proinflammatory lipids, including PG E_2/D_2/F_2/I_2 [251]. The COX enzyme leads to the bis-dioxygenation of arachidonic acid to produce a hydroperoxyl endoperoxide called prostaglandin G_2 (PGG_2), which is reduced to form a hydroxy endoperoxide PGH_2, a precursor to the active COX metabolites [251]. There are two known isoforms of COX, COX-1 and COX-2,

with COX-2 being associated with inflammation as it gets activated during the inflammatory response to release and produce proinflammatory prostaglandins [252,253].

LOXs similarly can oxidize lipids, where they commonly oxygenate AA, generating a hydroperoxy eicosatetraenoic acid, which gets reduced to produce a hydroxy eicosatetraenoic acid and many pro-inflammatory bioactive lipid metabolites such as leukotrienes (LT C_4 /D_4 /E_4 /B_4) [254,255]. Various forms of LOXs can position hydroperoxide in different positions on the fatty acid chain. Macrophages express ALOX5 and ALOX15, which enhance their ability to signal inflammation [256,257]. Cytochrome P450 (CYP450) is a large family of cysteine-heme bound enzymes that is characterized by the iron in their structure [258]. CYP450 can act as monooxygenases that can insert hydroxyl or epoxy groups phospholipids. CYP450 can oxygenate arachidonic acid to become hydroxyeicosatetraenoic acids (HETE), which are potent inflammatory mediators [259–262]. Other oxidation mechanisms do not rely on enzymes and undergo autoxidation using Fenton reactions (discussed in section 1.3) (**Figure 8**) [142].

1.5 The role of lipids' in inflammasome activation

1.5.1 Effect of phospholipid saturation and oxidation on TLR4 activation

TLR4 is a pattern recognition receptor that can recognize gram-negative bacteria such as *P. aeruginosa* through the recognition of lipopolysaccharide (LPS), a component of the bacterial cell wall [263]. The activation of TLR4 has also been linked to the presence of endogenous DAMPs along with its binding proteins[264].

To recognize LPS, TLR4 binds to the LPS-binding protein (LBP) and CD14, as well as, MD-2 [265,266]. CD14 binds directly to LPS and helps in the endocytosis of TLR4 and the regulation of subsequent cytokine expression [266].

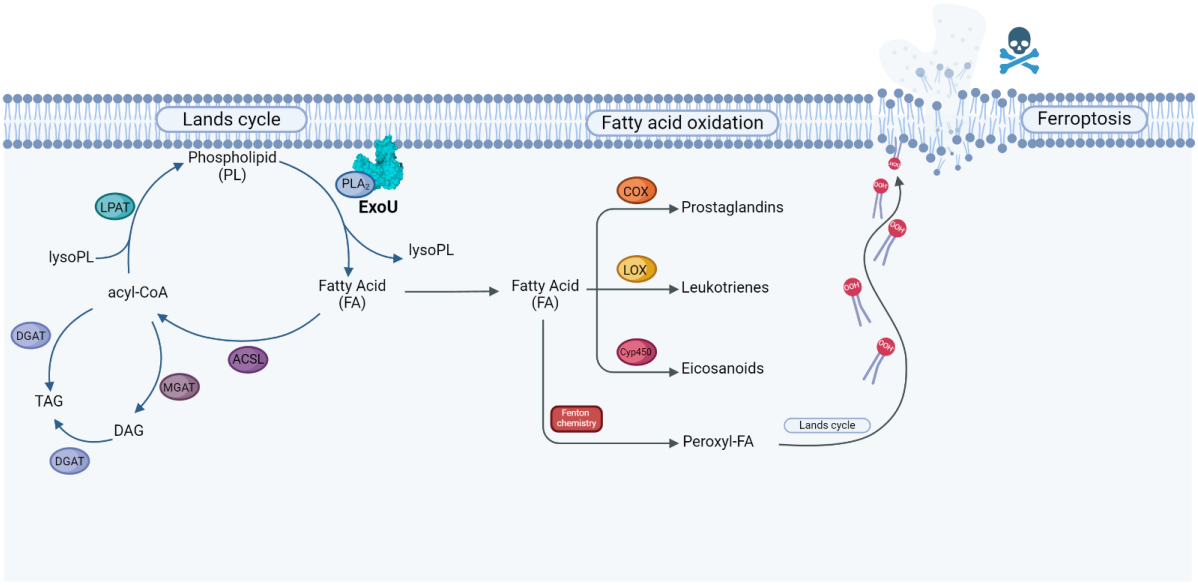

Figure 8. Phospholipid remodeling and oxidation.

The lands cycle starts with the cleavage of a phospholipid by a phospholipase such as a PLA_2 or PLA_2-like enzymes such as ExoU. A PLA_2 catalyzes the release of a fatty acid and a lysophospholipid from the *sn-2* position. The free fatty acid is converted to an acyl-CoA by long-chain acyl-CoA synthetases (ACSL) and incorporated again into a phospholipid by a lysophospholipid acyltransferase (LPAT). Acyl-CoA could also form triacylglycerides (TAGs) and diacylglycerides (DAGs) by diacylglycerol acyltransferase (DGAT) or monoacylglycerol acyltransferases (MGAT) respectively. Free fatty acids are oxidated through enzymatic or non-enzymatic reactions. Cyclooxygenases (COX) are responsible for the oxidation of polyunsaturated fatty acids and the formation of prostaglandins. Lipoxygenases (LOX) are responsible for the oxidation of polyunsaturated fatty acids forming leukotrienes. Other enzymes, such as cytochrome P450 (CYP450), form many different oxidated fatty acids or eicosanoids. Non-enzymatic fatty acid oxidation mechanisms such as Fenton reactions are mostly associated with generating peroxyl radicals and peroxidized phospholipid species. Oxidated fatty acids could be incorporated into phospholipids through the lands cycle and take part of the plasma membrane. Accumulation of oxidized phospholipid species disrupts the plasma membrane and leads to ferroptosis.

Following LPS binding, TLR4 is internalized using dynamin-dependent endocytosis[267]. TLR4 activation induces the activation of two signaling pathways, the TRAM-TRIF and the TIRAP-MyD88 complexes, leading to many downstream signaling events and cytokine production [267,268]. Internalized TLR4 is eventually degraded, which terminates the signaling cascade and inflammatory response [269]. The activation of TLR4 activates the nuclear transcription factor NF-κB, which induces the transcription of the NLRP3 inflammasome and pro-IL-1ß [270,271]. The assembly of the NLRP3 inflammasome followed by the cleavage of pro-caspase-1 to active caspase-1 allows for the processing and release of mature IL-1ß [272].

Interestingly, saturated free fatty acids have shown the ability to activate TLR4 activation and increase pro-inflammatory cytokine production and COX-2, while unsaturated fatty acids have shown no effect [273,274]. The ability of TLR4 to sense specific lipids depending on their saturation level established the diverse role of TLR4 in responding to DAMPs. TLR4-MD2 structure contains lipid binding pockets, possibly sites for saturated fatty acid binding. However, the concentration needed to activate TLR4 with fatty acids alone is much higher than the LPS needed [275,276]. This suggests that saturated fatty acids might play more of an agonist role than a ligand for TLRs [276]. Moreover, saturated fatty acids have been shown to activate TLR4 by promoting dimerization in a ligand-independent manner through the translocation into lipids rafts [277,278]. Furthermore, TLR4 dimerization and downstream signaling were inhibited by unsaturated fatty acids [278,279].

Further studies investigated whether oxidized lipids, which have been shown before to be proinflammatory, activate TLR4 or lead to a TLR4-dependent pro-inflammatory response[280]. Surprisingly, oxidized PLs showed inhibition of TLR4 in response to LPS treatment, not activation. Further investigation revealed the oxidized PLs compete with LPS for TLR4 binding,

which leads to a decrease in TLR4 activation during bacterial infections [281,282]. Moreover, this anti-inflammatory effect is concentration-dependent as increasing oxidized PLs (oxPL) concentrations showed an activation of TLR4[283]. The pro-inflammatory activation of TLR4 by oxidized PLs could also be dependent on the specific lipid species, as different PLs might induce stronger activation of TLR4 than others [284]. While low concentrations of oxPLs might be anti-inflammatory, prolonged and chronic stimulation of TLR4 with oxPLs can lead to the damage associated with oxPLs [283].

1.5.2 Lipids in non-canonical inflammasome activation and the release of IL-1ß

While TLR4 is the main PRR that senses the presence of LPS in the extracellular environment, other proposed mechanisms have been shown to allow intracellular sensing of LPS. Caspase-11 (and caspase 4/5 in humans) can sense intracellular LPS through binding, which oligomerizes caspase-11, leading to the activation of caspase-1 and the release of IL-1ß (**Figure 6**) [285,286]. Moreover, caspase-11 is not only limited to sensing LPS, as it has also been shown to be activated by oxPLs such as oxidized 1-palmitoyl-2-arachidonoyl-sn-glycero-3-phosphocholine which leads to the release of IL-1ß. The ability of oxPLs to activate caspase-11 was shown only to induce IL-1ß secretion without the induction of pyroptosis, as induced by LPS [287]. This suggests that inflammasome activation and IL-1ß release could happen independently from the induction of cell death through the non-canonical inflammasome [288].

1.6 Hypothesis and Objective

Taken together, the literature to date has identified ExoU as an effector protein with PLA2-like activity that elicits host cell death upon injection. The effect of ExoU on the host cell lipidome has not been comprehensively elucidated, nor has the mechanism of cell death triggered by this lipid metabolism been fully characterized. To address this gap in knowledge, the

overarching objective of this thesis was to elucidate the mechanism of ExoU lipid-mediated cell death and identify the metabolic changes elicited by ExoU in target cells. I hypothesized that acute infection with ExoU-expressing *P. aeruginosa* alters specific lipid metabolites in the host, which contribute to cell death and inflammation in human macrophages.

To test this hypothesis, I proposed the following aims:

Aim 1: Using a genetic loss of function approach, identify the cell death pathways through which ExoU contributes to *P. aeruginosa*-induced macrophage and human lung epithelial cell death and IL-1β secretion.

Aim 2: Identify the lipid species metabolized by ExoU in differentiated human THP-1 macrophages and, using bioinformatic approaches, map the lipidomic changes in host lipid metabolism triggered by ExoU injection.

2 MATERIALS AND METHODS

2.1 Cell culture

Human THP-1 monocytes (ATCC® TIB-202™) were cultured in R8 media, consisting of RPMI 1640 medium (Gibco, 31800089) supplemented with 8% FBS (Gibco, 12483020), 0.1% 2-ME(Gibco, 21985023), sodium bicarbonate 2 g/L (Sigma, 144-55-8), and 50 μg/mL gentamicin (Gibco, 15750060).

NuLi-1 (ATCC® CRL-4011™) human bronchial epithelial cells were cultured in BEGM (BEGM™) (Lonza, CC-3170), consisting of BEBM supplemented with the addition of SingleQuots Supplements and Growth Factors™ (Lonza, CC-4175) 0.4% BPE, 0.1% insulin, 0.1% hydrocortisone, 0.1% GA-1000, 0.1% retinoic acid, 0.1% transferrin, 0.1% triiodothyronine, 0.1% epinephrine, 0.1% hEGF, and 50 μg/mL gentamicin.

Cell lines were grown at 37°C in a 5% CO_2 environment. To differentiate THP-1 cells into macrophages, 50 ng/ml of PMA (Sigma, P8139) was added to the cells growing in the flask. After adding PMA, cells were incubated at 37°C with 5% CO2 for 72 hours. Differentiated cells were washed with Phosphate Buffered Saline (PBS) Na_2HPO_4 0.795 g/L, NaCl 9.00 g/L, KH_2PO_4 0.144 g/L (Biobar, 311-010-CL), then incubated with TrypLE™ (Gibco, 12604-013) until detached, and seeded in a 96- (Falcon, 08-772-2C) or 6-well (Falcon, 353046) plate then maintained in R8 for 24 hours.

2.2 Bacterial culture and infection

Wild Type (WT) PA14 [289] and PA14 *exoU::tn* [289,290] were acquired from the PA14 Transposon Insertion Mutant Library. PA14 WT expresses the ExoU protein [291]. PA14 *exoU::tn* is a *P. aeruginosa* strain with a lipase deficient inactive ExoU transposon mutant. PAO1 + ExoU and PAO1 WT were obtained from Drs Gregory Priebe and Gerald Pier from Boston Children's Hospital and Brigham and Women's Hospital. PAO1 WT is a second *P. aeruginosa* reference strain that naturally lacks the expression of ExoU. WT PAO1 + ExoU is a PAO1 strain ectopically expressing the ExoU protein. To obtain the PAO1+ ExoU, the PAO1 WT bacteria were transformed with the pUCP19exoUspcU plasmid as described in their published work.[292]

Bacteria were cultured overnight in LB (Fisher, BP14262) for host cell infections, then subcultured at a 1:20 dilution in LB until the required MOI was obtained. MOI was calculated through OD, which estimated bacterial CFU/mL using the equation (Y (CFU/ml) = 2.0×10^8 X (OD600) + 4.0×10^6) for *P. aeruginosa* [293]. Bacteria were subcultured to 100 MOI (~0.45 – 0.5 OD) and then diluted further according to the experiment.

Afterward, bacteria were resuspended in cell culture media (R8 or BEGM) at 0.1, 1, and 10 MOI for THP-1 and 1, 10, and 100 MOI for NuLi cells. Cells were infected with bacteria for varying time points, including 1, 3,6, 9, and 18 hours.

2.3 Cell viability assays

THP-1 macrophages and Nuli cells were seeded in a 96-well at 100,000 cells/well or 30,000 cells/well, respectively. Cell viability was assessed using the uptake of Neutral Red (NR) (Sigma, N2889) as described by the manufacturer. Briefly, NR (0.33%) was diluted 1:20 with culture media and then added to cells for 15 mins in the incubator. After dye uptake, the cells were washed with PBS and solubilized in a solution with 1:1 water; ethanol and 1% acetic acid were added. The absorbance of the NR dye was measured at 570-650 nm using a FilterMax F5 plate reader (Molecular Devices). Cell viability was also measured by Trypan-Blue exclusion (Thermo Fisher, 15-250-061). THP-1 macrophages seeded at a density of 1.2 X 106 per well in a 6-well plate were counted post-treatment or infection. TrypLE™ was used to detach the cells from the plate, followed by gentle trituration. Cells were resuspended in R8; then an aliquot was taken and diluted 1:1 with Trypan-Blue. Stained cells were counted with a hemocytometer.

2.4 IL-1β ELISA

Supernatant collected post-infection or treatment was stored at -80°C. Human IL-1β from THP-1 and NuLi cells was measured using the BD OptEIA™ Human IL-1β ELISA Set II kit (BD Biosciences, 557953) according to the manufacturer's instructions. The OD was measured at 450 - 570 nm using a FilterMax F5 plate reader (Molecular Device).

2.5 Cell inhibitor treatment

Inhibitors are presented in **Table 1**All inhibitors were dissolved in DMSO except for CuOOH, which was dissolved in ethanol. For treatments with Fer-1, CuOOH, Quer, and iFSP-1, THP-1 or Nuli seeded in 96-well plates were pre-incubated with the different inhibitors for 30 minutes before infection and for 1 or 3 hours over the duration of the infection.

All experiments that used DMSO as a solvent at a 0.1% concentration in R8 or BEGM contained a DMSO vehicle control.

2.6 CFU counting

Supernatants collected after infection of THP-1 cells were serially diluted in R8. Afterwards,100 µL of each dilution was plated on LB agar (Fisher, DF0140-01-0) plates and evenly coated with an L-shaped Cell Spreader (Fisher, 14-665-230). Agar plates were incubated at 37 °C for 24 hours. CFU was counted using DotDotGoose 1.7.0 image analysis software (American Museum of Natural History, New York, NY).

2.7 Lipid extraction and collection

Samples for lipid extraction were collected from THP-1 infected cells in a 6-well plate with PA14 WT or PA14 *exoU::tn* for 1 hour at 1 MOI as described above. Samples of PA14 WT infected cells were collected from 6 wells of a 6-well plate, two wells of PA14 *exoU::tn* infected cells, and one well of CTRL THP-1 cells to ensure a sufficient number of cells (>500,000 macrophages) required for MS analysis is collected. Afterward, cells were pelleted and then counted with a hemocytometer after Trypan-Blue staining. Both supernatant and pellets were stored at -80ºC. A list of CTRLs are listed in **Table 2** used for analysis. Before lipid extraction, collected supernatants, and media were freeze-dried using a lyophilizer (Labconco, 720401000).

Table 1: Inhibitors and inducers used in cell treatment experiments

Inhibitor	Source and Catalog #	Notes	Vehicle
Ferrostatin-1	Sigma, SML0583	Lipid hydroperoxyl radical scavenger[294]	DMSO
Quercetin	Thermo Fisher, 174070100	DNAJC5 inhibitor[63]	DMSO
CuOOH	Sigma, 247502	Inducer of lipid peroxidation[86,295]	Ethanol
Z-VAD-FMK	APExBIO, A1902	Apoptosis inhibitor[296]	DMSO
GSK872	Selleckchen, S8465	RIP3K inhibitor [297]	DMSO

Lipids were extracted from the samples using a modified Bligh and Dyer protocol described previously[298,299]. Cell pellets or supernatants were mixed with 0.1M Na acetate (J.T. Baker, LC/MS grade, 9831-03) in a Kimble 10 mL glass threaded tube (VWR, 21020-640) with black Teflon-lined cap (VWR, 60826-315) until dissolved. Acidified methanol (AcMeOH) (2% acetic acid, Fisher, A38-212; in methanol, Fisher, BP1105-4) was added to the tube and mixed. Afterward, internal lipid standards listed in **Table 3** were added to the final aqueous mixture. After the completion of the aqueous mixture, lipids were extracted by adding chloroform to form the organic layer. The organic phase was collected using a Fisherbrand 9" disposable Pasteur pipettes (Fisher, 13-678-20C), followed by three back-extractions using chloroform (Fisher, C298-500). The chloroform in the pooled organic phase was evaporated using a constant stream of nitrogen gas. Lipids were dissolved in 300 µL ethanol (Commercial Alcohols, P016EAAN) flushed with nitrogen gas and stored in 100 µL aliquots Amber 2 mL HPLC glass vials with Teflon-lined caps (Chromatographic Specialties, C779100AW (vials); C779200BB (caps)). All lipid extracts are stored at -80^{o}C until use.

Lipid extraction was performed on six biological replicates.

2.8 LC-ESI-MS/MS

GPCs were quantified with a nanobore high performance liquid chromatography-electrospray ionization, tandem mass spectrometry (nLC-ESI-MS/MS) using an Agilent 1290 Infinity II LC and a triple quadrupole-linear ion trap mass spectrometer QTRAP 5500 (AB SCIEX, Concord, Canada). Nitrogen gas was used as an inert gas in the ion source, collision gas in q2 of the mass spectrometer fragmenting the lipids, and curtain gas between the curtain plate and the orifice of the mass spectrometer.

Samples were run through the LC and maintained at 4°C in the autosampler before loading. 5 µL of each sample were dissolved in 13.5 µL of solvent A containing 0.1% formic acid (Sigma-Aldrich, 56302) and 10 mM ammonium acetate (NH_4AC) (Millipore, 2145-OP) in MS-grade water (J.T. Baker, Avantor, 9831-03).

After the samples are dissolved in solvent A, 2.5 µL each of the spike-in standards mixtures, SPLASH™, and d4, are added into the solution **Table 4**. Loaded samples were run through a 100 mm x 250 µm HPLC column packed with 3 µm C18 beads (Canadian Life Science, ReproSil-Gold 200 C18 3 µm 1g) with solvents pumped at a flow rate of 10 µL/min and a sample injection volume of 3 µL. The elution gradient for the HPLC consisted of a binary solvent gradient of solvent A (mentioned before) and solvent B containing 0.1% formic acid (Sigma-Aldrich, 56302), 10mM (NH_4AC) in 5:2 acetonitrile (ACN, J.T. Baker, Avantor, 9839-03) to isopropanol (Fisher Scientific, A416-4). The gradient strategy started with 70% solvent A and 30% solvent B for the first 8 minutes. The gradient then ramps up to 100% solvent B at 45 minutes and then holds that ratio for 1 minute. The gradient returns to 70% solvent A and 30% solvent B gradually till the end of the run at 60 minutes. Following each sample, a blank run was added to eliminate any carryover between two consecutive samples. After separation in the HPLC, the samples were ionized with an ion spray voltage at 2500 V using ESI in positive ion mode before they entered the mass spectrometer.

The analytes were detected using multiple reaction monitoring (MRM). The MRM method scanning of mass ranges between m/z 450 and 960, filtering for the lipid precursor. Collision gas was set to 10 µL/min with an entrance potential of 10 eV, a declustering potential of 100 eV, and a collision cell exit potential of 9 eV. The collision energy for fragmentation was 47 eV.

Table 2: Mass spectrometry experimental controls

Samples	Volume	Pellet (P)/ Supernatant (S)
R8 media	12,4,2 mL	S
LB media	3, 0.646 mL	S
PA14 WT	~3 mL	P, S
PA14 *exoU::tn*	~0.646 mL	P, S
THP-1	~2 mL	P, S
THP-1 + PA14 WT	~12 mL	P, S
THP-1 + PA14 *exoU::tn*	~4 mL	P, S

Table 3: Mass spectrometry lipid internal standards

Internal Standards	Catalog #
LPC(13:0/0:0)	Avanti, LM1600
PC(12:0/13:0)	Avanti, LM1000
PS(12:0/13:0)	Avanti, LM1300
PE(12:0/13:0)	Avanti, LM1100
C8 Glucosyl(ß) Ceramide (d18:1/8:0)	Avanti, 860540
C8 Galactosyl(ß) Ceramide (d18:1/8:0)	Avanti, 860538
Ceramide C16-D31	Avanti, 868516
SM(d18:1/18:1-D9)	Avanti, 860740
GM3(d18:1/18:0-D5)	Avanti, 860073W
dSPH m18:0/6:0	Cayman, 25494
dSPH m18:1(14Z)/6:0	Cayman, 25493
dSPH d3-(m18:0)	Avanti, 860474P

The diagnostic ion for GPC monitoring was set at 184.1 m/z. The compensation voltage (COV) values were optimized for each lipid class, and the optimal COV values for GPC were -4.5 V. GPCs were quantified using the Multiquant software (version 3.0.3, AB Sciex). Extraction efficiency was accounted for using lipid standards of known concentrations added at the time of extraction. Raw peak areas were corrected for instrument response, and normalization to longitudinal QC samples was measured in each run. Followed by annotation using an in-house algorithm Bayesian Annotations for Targeted Lipidomics (BATL), an R package that allows for the accurate annotation of targeted lipidomics data using a Bayesian model. BATL utilizes multiple peak features such as retention time, relative retention time (RT), subtracted RT, relative area, relative height, full width at half maximum height, asymmetry factor, and tailing factor to provide accurate targeted lipidomics annotation [300].

2.9 Statistical Analysis

Statistical analysis of the data was conducted using GraphPad Prism 10.2.0 (GraphPad Software, San Diego CA). Data with an alpha value of $p \leq 0.05$ were specified to be significant. Data were presented as the mean ± standard error of the mean (SEM). A two-way ANOVA was used to determine significant changes between two independent variables, followed by a Holm-Šídák post-hoc test for multiple comparisons as indicated in figure captions. A one-way ANOVA was used to determine significant changes between a single independent variable, followed by a Holm-Šídák post-hoc test for multiple comparisons as indicated in figure captions.

Table 4: Spike in LC/MS standards

Standard Mix Name	Internal Standards	Catalog #
d4	PC(*O*-16:0/0:0)	Cayman, 360906
	PC(*O*-18:0/0:0)	Cayman, 10010228
	PC(*O*-16:0/2:0)	Cayman, 360900
	PC(*O*-18:0/2:0)	Cayman, 10010229
SPLASH-5	PC(15:0/18:1-D7)	Avanti, 791637
	LPC(18:1-D7)	Avanti, 791643
	PE(15:0/18:1-D7)	Avanti, 791638
	LPE(18:1-D7)	Avanti, 791644
	PS(15:0/18:1-D7)	Avanti, 791639

3 RESULTS

3.1 Expression of ExoU enhances *P. aeruginosa* cytotoxicity in human THP-1 macrophages and NuLi epithelial cells

I used a genetic loss of function approach to assess the impact of *P. aeruginosa*-expressing ExoU on the viability of human macrophages. THP-1 monocytes were differentiated to macrophages followed by exposure to either ExoU-expressing *P. aeruginosa* reference strain PA14, originally isolated from burn patients[301,302] or PA14 *exoU::tn,* expressing an inactive ExoU mutant generated on the same strain. THP-1 cells were infected at a multiplicity of infection of 1 (1 MOI). Cell viability was assessed using neutral red, a cationic dye that is incorporated in lysosomes of living cells [303]. Cell viability was significantly reduced in THP-1 macrophages after 1, 2, 3, and 6 h infection with ExoU-expressing PA14 WT bacteria (**Figure 9A**). Viability of THP-1 macrophages exposed to the inactive ExoU strain PA14 *exoU::tn* was compromised after 2, 3, and 6 h of infection with cell survival significantly enhanced compared to PA14 WT bacteria at all time points (**Figure 9A**). Because THP-1 cells undergo lysosomal biogenesis in response to bacterial infection [304] which could artifactually lead to an increase in neutral red absorbance; we verified cell loss by direct counts of Trypan Blue excluding cells. Infection with both PA14 WT and PA14 *exoU::tn* triggered progressive cell death in the first three hours following infection, but PA14 *exoU::tn* was significantly less toxic (**Figure 9B**). Three percent of THP-1 macrophages survived 18 h of infection with PA14 WT. By contrast, 21% of THP-1 macrophages infected with the ExoU-deficient mutant strain survived 18 hours of infection (**Figure 9B**). ExoU expression by PA14 WT enhanced cytotoxicity across 0.1-10 MOI in the first three hours of infection (**Figure 9C**). Cell viability was significantly enhanced in PA14 *exoU::tn*-infected cells at each time point (**Figure 9C**).

To address host cell specificity, I infected NuLi human lung epithelial cells as another target of *P. aeruginosa* toxicity. Cell viability was significantly compromised in NuLi cells infected with PA14 WT at 1, 10, and 100 MOI for six hours but not PA14 *exoU::tn* until an MOI of 100 (**Figure 10**).

A series of reciprocal genetic rescue experiments were performed to provide direct evidence that ExoU was responsible for the enhanced cytotoxicity observed over the first three hours of bacterial infection and that cell survival was not the result of off-target effects of the transposon-mediated deletion in PA14 *exoU::tn*. As expected, the viability of THP-1 macrophages infected with PA14 WT was significantly reduced at one hour (**Figure 11A**) and three hours (**Figure 11B**) while host cell viability was significantly higher when cells were infected with PA14 *exoU::tn* (**Figure 11A,B**). Host cell cytotoxicity was also attenuated when THP-1 macrophages were infected with POA1, a reference strain that endogenously lacks the ExoU gene (**Figure 11A,B**). The enhanced cell viability was the result of ExoU deficiency, given that ectopic expression of POA1 with ExoU restored the cytotoxic phenotype (**Figure 11A,B**).

3.2 Quercetin treatment does not increase THP-1 macrophage viability

ExoU is injected via the T3SS as a complex with SpcU into the host cell cytoplasm[52]. ExoU dissociates from SpcU before docking to DNAJC5-positive endosomes that are uniquely anterogradely trafficked to the plasma membrane[63]. In A549 lung epithelial cells, ExoU-mediated necrosis requires DNAJC5-mediated translocation to the plasma membrane to elicit necrosis[63]. To determine whether this same trafficking is required for ExoU to trigger cell death in THP-1 macrophages, I treated THP-1 cells with the reported DNAJC5-mediated endosomal translocation inhibitor quercetin. Quercetin (25-100 μM) did not affect THP-1 macrophage viability and had no impact on cell survival following PA14 *exoU::tn* infection (**Figure 12**).

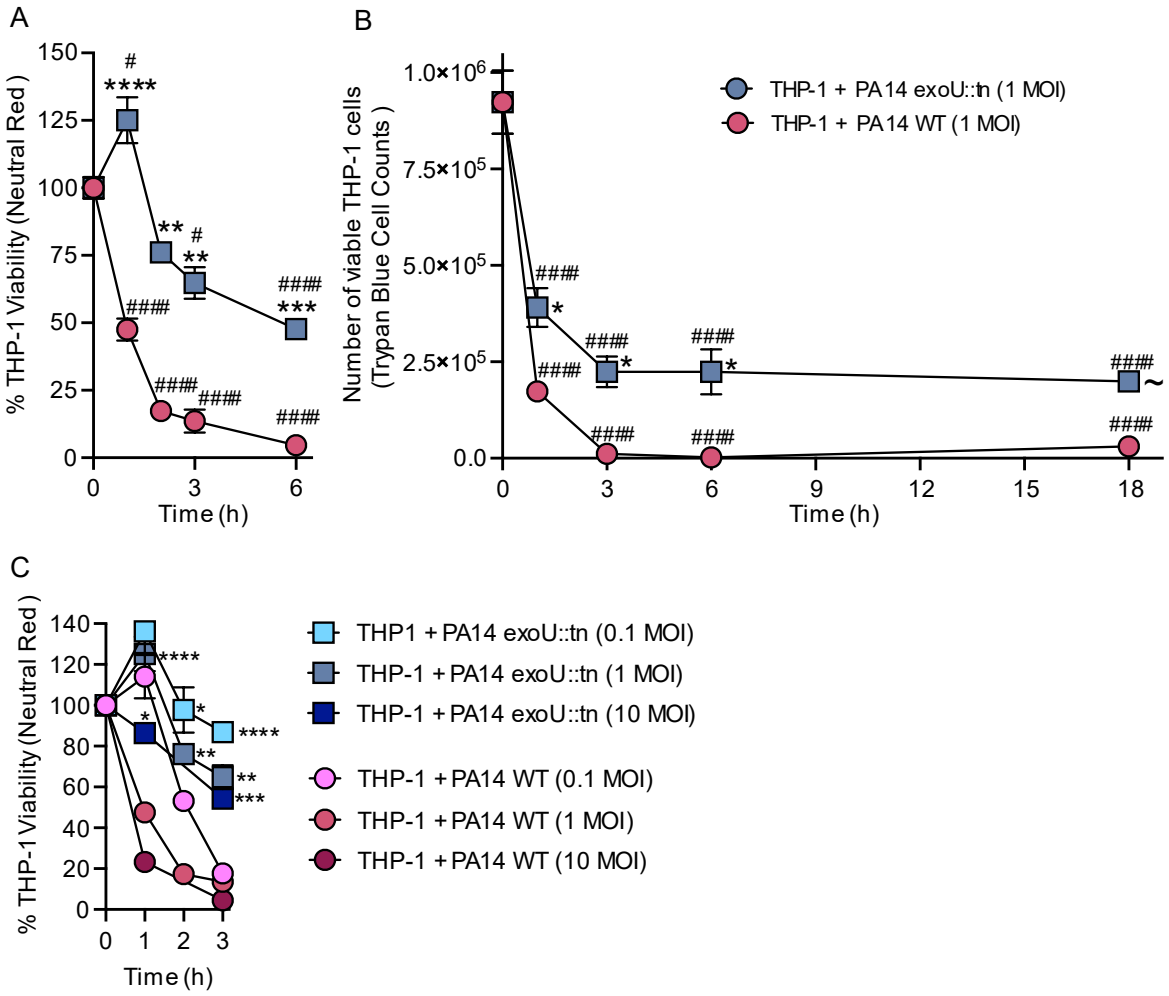

Figure 9: Loss of ExoU function increases THP-1 survival when exposed to *P. aeruginosa*.

A) Neutral red cell viability assay measuring THP-1 cells infected with *P. aeruginosa* WT or *exoU::tn* at 1 MOI for 1, 2, 3, and 6 hours. B) Trypan Blue staining of viable THP-1 cells infected with *P. aeruginosa* WT or *exoU::tn* at 1 MOI for 1, 3, 6, and 18 hours. C) Neutral red cell viability assay measuring THP-1 cells infected with *P. aeruginosa* WT or *exoU::tn* at 0.1, 1, and 10 MOI for 1, 2, and 3 hours. Data show mean ± SEM. N = 3 – 81 wells conducted over 11 independent experiments. Statistics were two-way ANOVA followed by *post hoc* Holm Sidak correction for multiple pairwise comparisons. * $p<0.05$, ** $p<0.01$,***$p<001$, **** $p<0.0001$ THP-1 + PA14 WT vs THP-1 + PA14 *exoU::tn*. # $p<0.05$, #### $p<0.0001$ Compared to uninfected (0 h) control.

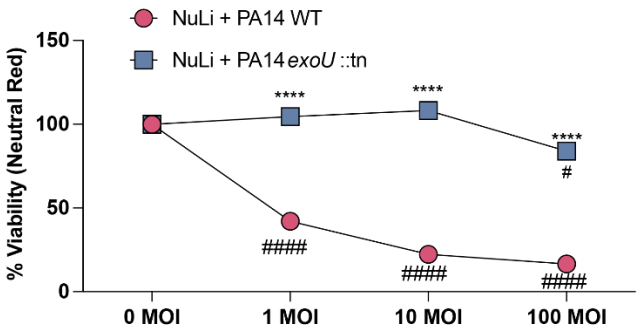

Figure 10: Loss of ExoU function increases NuLi survival when exposed to *P. aeruginosa*.

Neutral red cell viability assay measuring NuLi infected with *P. aeruginosa* WT or exoU::tn at 1, 10, and 100 MOI for 6 hours. Data show mean ± SEM. N = 9 – 27 wells conducted over 3 independent experiments. Statistics were two-way ANOVA followed by *post hoc* Holm Sidak correction for multiple pairwise comparisons. **** $p<0.0001$ NuLi + PA14 WT vs NuLi + PA14 *exoU::tn*. #### $p<0.0001$ Compared to uninfected (0 MOI) control.

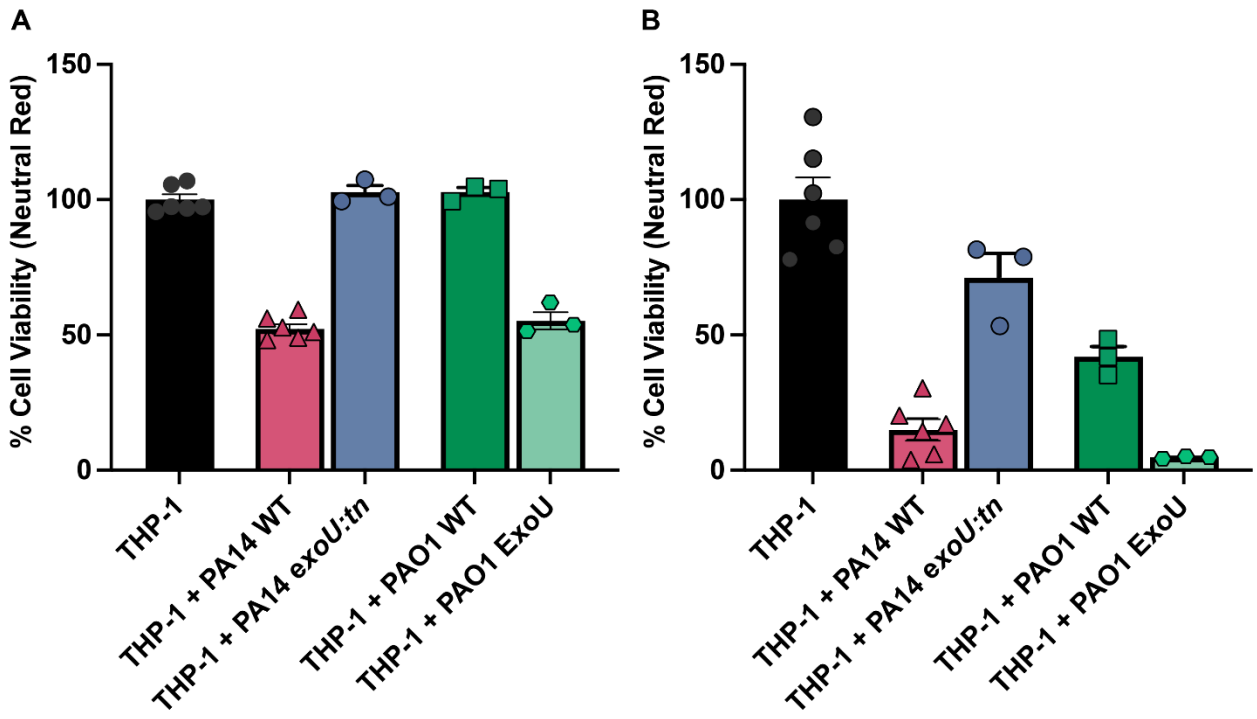

Figure 11: Ectopic expression of ExoU in the P. aeruginosa strain decreases THP-1 viability than the non-expressing *P. aeruginosa* strain.

A) Neutral red cell viability assay measuring THP-1 cells infected with PA14 WT or *exoU::tn* and PAO1 WT or PAO1 + ExoU strains at 1 MOI for 1 hour. B) Neutral red cell viability assay measuring THP-1 cells infected with *P. aeruginosa* WT or *exoU::tn* and PAO1 WT or PAO1 + ExoU strains at 1 MOI for 3 hours. Data show mean ± SEM. N = 3 – 6 technical replicates conducted over 1 experiment.

Taken together, these data indicate that ExoU elicits acute cytotoxicity in human THP-1 macrophages; however, unlike previous reports [63], the cytotoxic effects of ExoU on THP-1 macrophages are not attenuated by quercetin treatment. This result could suggests that quercetin treatment was not enough to inhibit translocation of ExoU or that THP-1 cells respond differently to quercetin than other cell types. Further analysis is required to verify the effect of quercetin on endosome trafficking in THP-1 cells and if different endosome trafficking inhibitors are required to induce similar results to the ones reported previously.

3.3 Pan-caspase inhibition does not enhance THP-1 macrophage viability following PA14 WT infection

To address the question of how ExoU triggers cell death in THP-1 macrophages, I used a series of pharmacological inhibitors to identify the cell death pathways initiated by ExoU following PA14 WT infection. To investigate the role of apoptosis, I pretreated THP-1 cells with the pan-caspase inhibitor, Z-VAD-FMK at 6.25- 50 μM for 30 mins followed by a one h infection with PA14 WT or PA14 *exoU::tn* in the presence of Z-VAD-FMK. Blocking caspase activity mildly reduced neutral red absorbances of PA14 *exoU::*tn-treated cells compared to vehicle, likely as a result of inhibiting the caspase 3-dependent lysosomal biogenesis is associated with acute bacterial infection as has been shown previously[305], but did not enhance the viability of THP-1 macrophages infected with PA14 WT compared to vehicle treatment (**Figure 13A**)These data suggest that ExoU does not trigger apoptosis in THP-1 macrophages.

3.4 Inhibition of necroptosis does not enhance THP-1 macrophage viability following PA14 WT infection

I used GSK-872, a RIPK3 inhibitor, to block necroptosis[306]. After pre-treating cells with 2.5-20 μM of GSK-872 for 30 mins, I infected THP-1 macrophages with PA14 WT or PA14 *exoU::tn* at 1 MOI for one h in the presence of GSK-872.

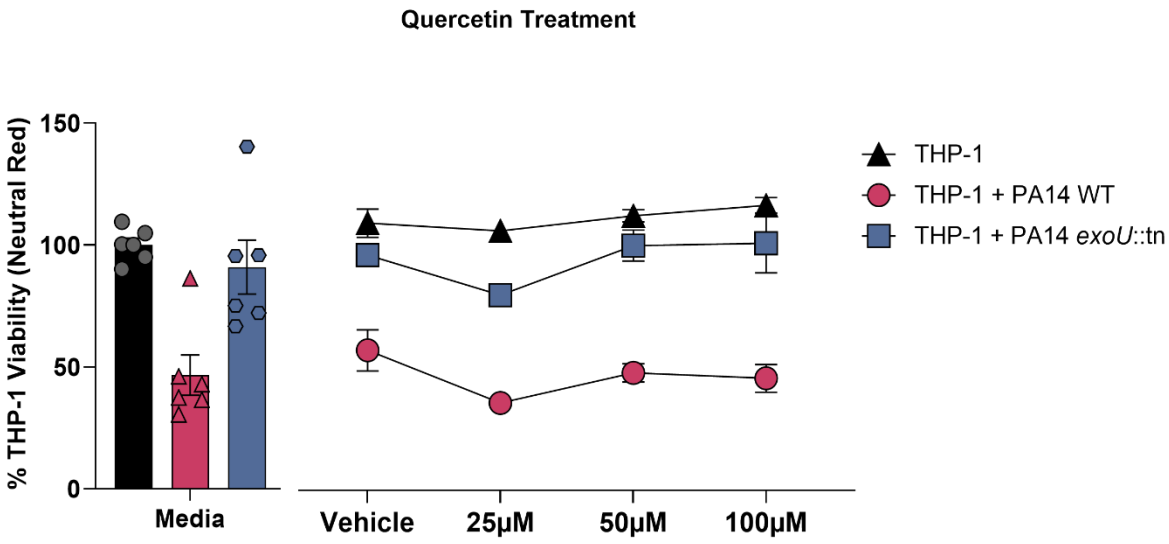

Figure 12: Quercetin treatment followed by exposure to *P. aeruginosa* does not reduce viability.

Neutral red cell viability assay measuring THP-1 cells after treatment with Quercetin at 25,50,100 µM and infected with PA14 WT or *exoU::tn* at 1 MOI for 1 hour. Data show mean ± SEM. N = 3 – 6 technical replicates conducted over 1 experiment.

There was no effect on the viability of PA14 WT-infected cells (**Figure 13B**). These data suggest that ExoU does not trigger necroptosis in THP-1 macrophages.

3.5 Ferrostatin-1 enhances THP-1 macrophage viability following one h but not three h of PA14 WT infection

To assess the contribution of ferroptosis to ExoU-induced cell death, THP-1 macrophages were pre-treated with 12.5-50 μM ferrostatin-1, a ferroptosis inhibitor, for one hour, followed by infection with PA14 WT or PA14 *exoU::tn* for 1 or 3 h in the presence of the inhibitor. Ferrostatin-1 did not affect THP-1 macrophage cell viability (**Figure 13C,D**). The viability of THP-1 macrophages infected with PA14 WT was significantly enhanced at the highest concentration of ferrostatin-1 tested (50 μM) after one h of infection (**Figure 13C**); however, treatment failed to improve cell viability after three h of infection with either PA14 WT or PA14 *exoU::tn* (**Figure 13D**). These data suggest that ExoU signals ferroptosis within the first hour of infection but that other ferroptosis-independent cell death pathways are activated at later time points.

3.6 ExoU is required for *P. aeruginosa*-induced host cell ferroptosis

Because ExoU is a phospholipase, we asked whether ExoU-mediated changes in the host lipidome were required to induce ferroptosis. We used cumene hydroperoxide (CuOOH12.5-200 μM) to promote cellular lipid peroxidization directly. THP-1 macrophages were treated with CuOOH and infected with PA14 WT or PA14 *exoU::tn* for one h. Lipid peroxidation did not elicit ferroptosis in THP-1 macrophages (**Figure 13E**). CuOOH did not reduce cell viability in THP-1 macrophages infected with PA14 exoU::tn or PA14 WT (**Figure 13E**). These data suggested that peroxidation of the endogenous THP-1 macrophage lipidome is not sufficient to induce ferroptosis; rather, ExoU-mediated lipid hydrolysis is required to render the THP-1 cell susceptible to ferroptosis.

3.7 Inhibiting ExoU-induced ferroptosis enhances inflammasome-linked IL-1β release

Inflammasome activation was assessed by measuring IL-1β secretion. Little to no IL-1β was secreted by THP-1 macrophages in the absence of bacteria (**Figure 14A**). Exposure of THP-1 macrophages to PA14 WT resulted in significant IL-1β secretion at 1 and 3 h post-infection (**Figure 14A**). Inflammasome activation was delayed in THP-1 exposed to PA14 *exoU::tn* with significant secretion observed after three but not one h of infection (**Figure 14A**). Treatment with ferrostatin had no impact on IL-1β secretion in THP-1 macrophages or in cells exposed to PA14 *exoU::tn* (**Figure 14B**). By contrast, inhibiting ferroptosis in THP-1 macrophages exposed to PA14 WT significantly increased IL-1β secretion after three h of infection (**Figure 14B**). These data suggested that inflammasome activation further contributes to THP-1 macrophage toxicity induced by ExoU.

3.8 ExoU alters the THP-1 macrophage lipidome.

Taken together, this data provide evidence that the bacterial toxin ExoU induces ferroptosis and activates the inflammasome leading to IL-1β release. It has yet to be established how ExoU signals these events. Because ExoU is thought to be a PLA_2-like enzyme, these changes are likely mediated by the changes in membrane phospholipid homeostasis. To address this, we profiled GPCs in THP-1 macrophages to investigate the effect of ExoU on the lipidome. Following exposure to PA14 WT or PA14 *exoU::tn* for one h at an MOI of 1, we performed LC-MS/MS analysis of specific GPC species of interest.

Our panel of GPCs included lyso-PCs (LPC) and PCs with various chain lengths, saturated, monounsaturated, and polyunsaturated fatty acids (**Figure 15**). We also included different fatty acid linkages, including vinyl ether-linked plasmalogen P (PC-P), ether-linked PC (PC-O), and ester-linked diacyl PC (PC) (**Figure 15**).

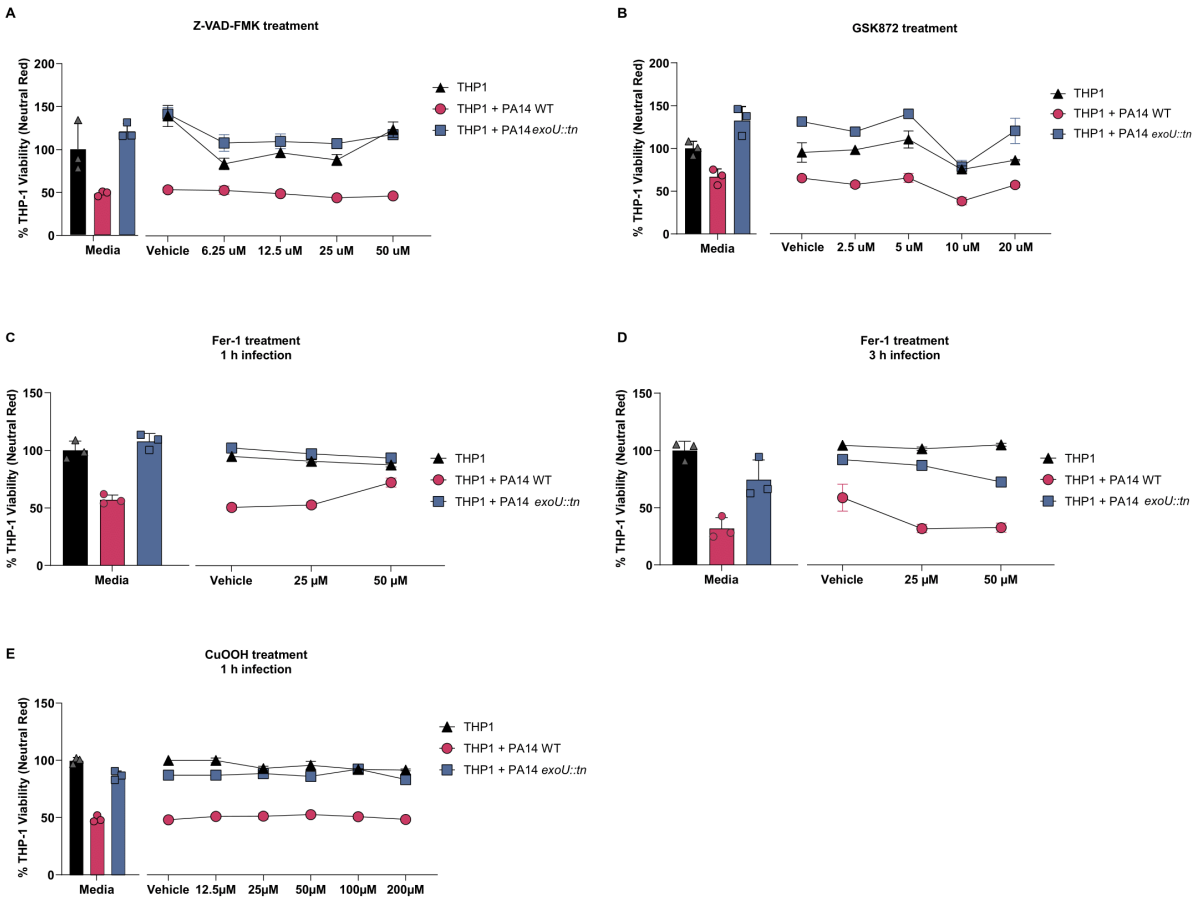

Figure 13: Inhibiting various cell death mechanisms only increases viability when inhibiting ferroptosis at one h in THP-1 cells following exposure to *P. aeruginosa*.

A) Neutral red cell viability assay measuring THP-1 cells treated with 6.25, 12.5, 25, and 50 µM zVAD and infected with *P. aeruginosa* WT or *exoU::tn* at 1 MOI for 1 hour. B) Neutral red cell viability assay measuring THP-1 cells treated with 2.5, 5, 10, and 20 µM GSK 872 and infected with *P. aeruginosa* WT or *exoU::tn* at 1 MOI for 1 hour. C) Neutral red cell viability assay measuring THP-1 cells treated with 25 and 50 µM Ferrostatin-1 and infected with *P. aeruginosa* WT or *exoU::tn* at 1 MOI for 1 hour. D) Neutral red cell viability assay measuring THP-1 cells treated with 25 and 50 µM Ferrostatin-1 and infected with *P. aeruginosa* WT or *exoU::tn* at 1 MOI for 3 hours. E) Neutral red cell viability assay measuring THP-1 cells treated with 12.5, 25, 50, 100, 200 µM CuOOH and infected with *P. aeruginosa* WT or *exoU::tn* at 1 MOI for 1 hour. Data show mean ± SEM. N = 3 – 6 technical replicates conducted over 1 experiment.

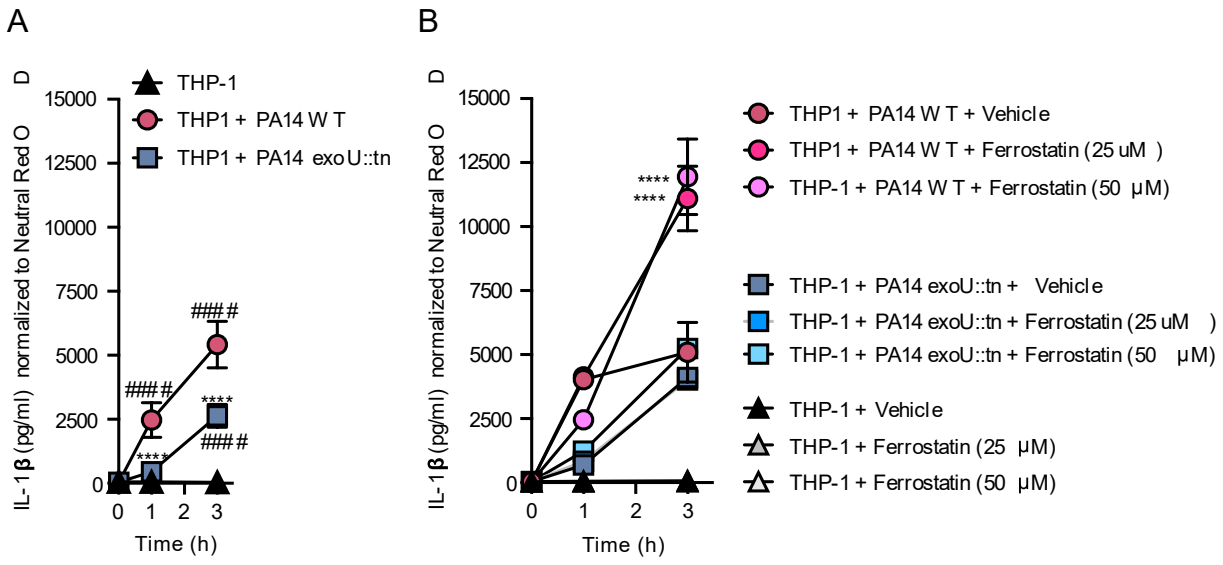

Figure 14: Inhibiting ferroptosis increases IL-1ß secretion only after long exposure to *P. aeruginosa.*

A) Sandwich ELISA measuring levels of IL-1β in THP-1 macrophage supernatant after infection with *P. aeruginosa* WT or *exoU::tn* at 1 MOI for 1 and 3 hours. B) Sandwich ELISA measuring levels of IL-1β in THP-1 macrophage supernatant treated with 25 and 50 µM Ferrostatin-1 and infected with *P. aeruginosa* WT or *exoU::tn* at 1 MOI for 1 and 3 hours. Data show mean ± SEM. For A) N = 3 – 81 wells were conducted over 11 independent experiments. For B) N = 3 – 6 wells conducted over 1 experiment. **** $p<0.0001$ THP-1 + PA14 WT vs THP-1 + PA14 *exoU::tn*. #### $p<0.0001$ Compared to THP-1 control.

Among the 80 different GPC species identified, 25 species (31.25%) were significantly altered only in PA14 WT-infected THP-1 cells, suggesting ExoU activity (**Figure 16**). While 49 (61.25%) of the measured lipids increased in both PA14 WT and PA14 *exoU::tn,* suggesting a general effect caused by the bacteria and not specific to the presence of ExoU (**Figure 16**). Only 6 (7.5%) of the GPC species were unaffected by the bacterial infection (**Figure 16**). Looking more closely at the lipids altered by ExoU, 90% of LPC species identified were significantly altered in PA14 WT-infected THP-1 cells (**Figure 16**). While only 9% of the identified PC species were altered in PA14 WT-infected THP-1 cells (**Figure 16**). Among ExoU-altered LPC species, ExoU showed no apparent preference for saturated or unsaturated fatty acid chains at the *sn-1* position (**Figure 17**). PA14 WT-infected cells also showed a significant increase in LPCs with PC-P, PC-O, and diacyl-linked fatty acid chains (**Figure 17**). PCs altered specifically by ExoU were few; however, these they only had saturated fatty acids at the *sn-2* position (**Figure 17**). On the other hand, the group of GPC species affected by the presence of bacteria did not show any apparent preference for any specific fatty acid linkage or saturation; however, it did show an increase in some predicted oxidized species (**Figure 18**). These oxidized species were not significantly different between PA14 WT or PA14 *exoU::tn* infected THP-1 cells; however, they were significantly higher than CTRL (**Figure 18**). The oxidized species' structure is predicted based on their m/z and is pending structural verification. A few GPC species showed no change in all conditions, which may have been caused by their low concentration or considerable variability between samples (**Figure 18)**.

4 DISCUSSION

In this thesis, I explored the relationship between the bacterial effector protein ExoU and its ability to induce inflammatory signals and cell death.

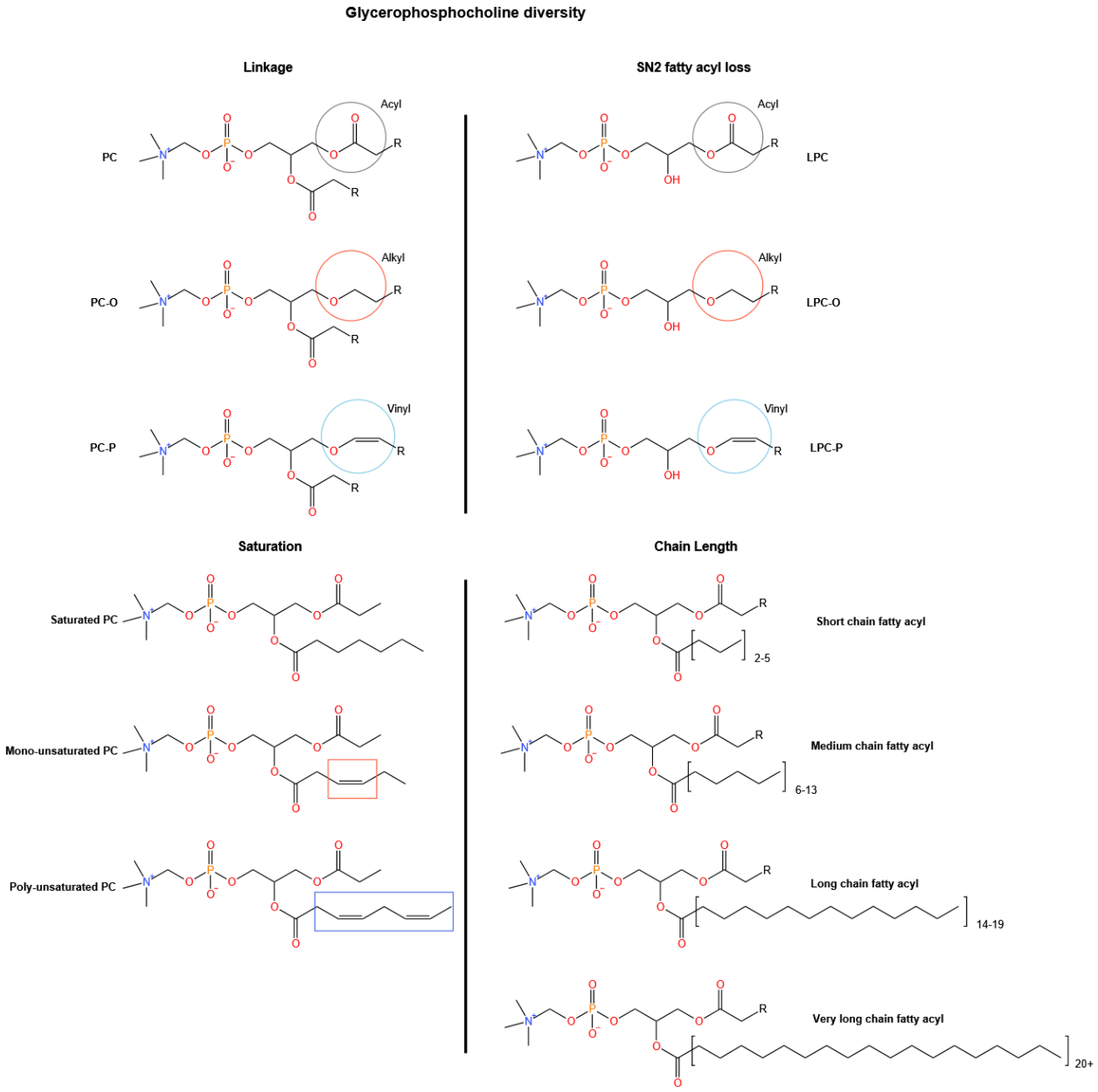

Figure 15: GPC structural variation.

GPC structural diversity shows the various structural components in the GPC panel that influence lipid structure. GPC at the *sn-1* position can have multiple linkage types including an alkyl ether linkage (PC-O), alkenyl ether linkage (PC-P), or an acyl linkage. The loss of the *sn-2* fatty acyl chain by a PLA_2 enzyme leads to the formation of a lyso-PC (LPC) with similar linkage variability depending on the substrate hydrolyzed. Fatty acid chain saturation and the double bond position create mono-unsaturated and poly-unsaturated fatty acyl chains, leading to possible oxidation sites. Lastly, various fatty acyl chain length influences polarity and create more structural variability.

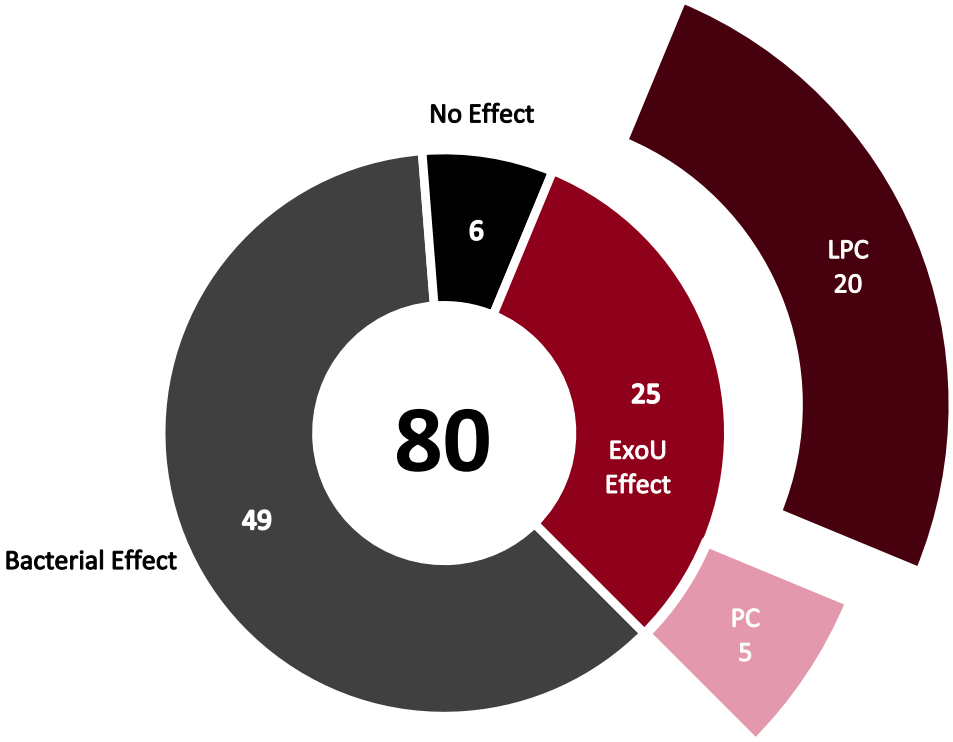

Figure 16: GPC alteration in THP-1 showing the effect of ExoU

Pie chart showing the distribution of GPC species affected by ExoU, general bacterial effects, and those unaffected lipid species. A total of 80 GPC species were measured, with 25 influenced by ExoU, 49 altered by bacterial presence, and 6 showing no significant change. Outer pie chart showing the overlap of GPC species and ExoU-affected lipids. LPC in dark red (20 species). PC species shown in pink represent those altered by ExoU (5 species).

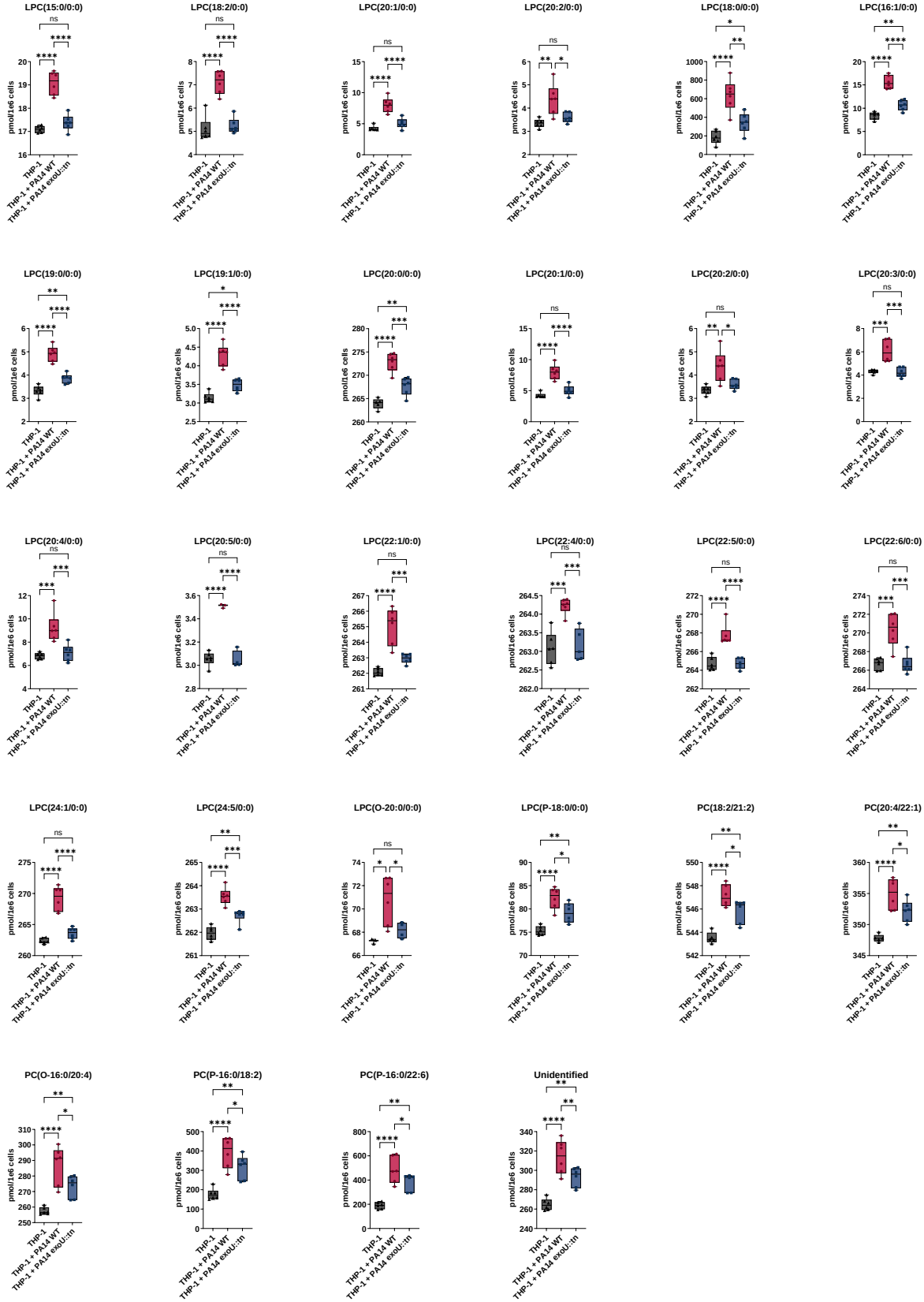
LPC(15:0/0:0)
LPC(18:2/0:0)
LPC(20:1/0:0)
LPC(20:2/0:0)
LPC(18:0/0:0)
LPC(16:1/0:0)
LPC(19:0/0:0)
LPC(19:1/0:0)
LPC(20:0/0:0)
LPC(20:1/0:0)
LPC(20:2/0:0)
LPC(20:3/0:0)
LPC(20:4/0:0)
LPC(20:5/0:0)
LPC(22:1/0:0)
LPC(22:4/0:0)
LPC(22:5/0:0)
LPC(22:6/0:0)
LPC(24:1/0:0)
LPC(24:5/0:0)
LPC(O-20:0/0:0)
LPC(P-18:0/0:0)
PC(18:2/21:2)
PC(20:4/22:1)
PC(O-16:0/20:4)
PC(P-16:0/18:2)
PC(P-16:0/22:6)
Unidentified
pmol/1e6 cells
THP-1
THP-1 + PA14 WT
THP-1 + PA14 exoU::tn
ns

Figure 17: PA14 WT increases levels of lyso-phosphocholines and other GPCs in THP-1 cells.

LC-MS/MS quantification of significantly altered GPC species in THP-1 macrophage after infection with PA14 WT or *exoU::tn* at 1 MOI for 1 hour. This graph shows GPCs significantly increased after PA14 WT only, suggesting an ExoU effect. GPC species in pmol are normalized per $1x10^6$ cells. GPC subclasses measured include LPC and PC, processing acyl, ether, and vinyl fatty acid linkages, as well as various saturated and unsaturated chains. Unidentified species are detected with unknown but predicted molecular identity belonging to GPCs, pending further structural characterization. Data show mean ± SEM. N = 6 conducted over independent experiments. Data was analyzed using one-way ANOVA and a Holm-Šídák post-hoc test for multiple comparisons. * $p<0.05$, ** $p<0.01$,***$p<001$, **** $p<0.0001$ THP-1 + PA14 WT vs THP-1 + PA14 *exoU::tn,* THP-1 + PA14 WT vs THP-1 control, THP-1 + PA14 *exoU::tn* vs THP-1 CTRL.

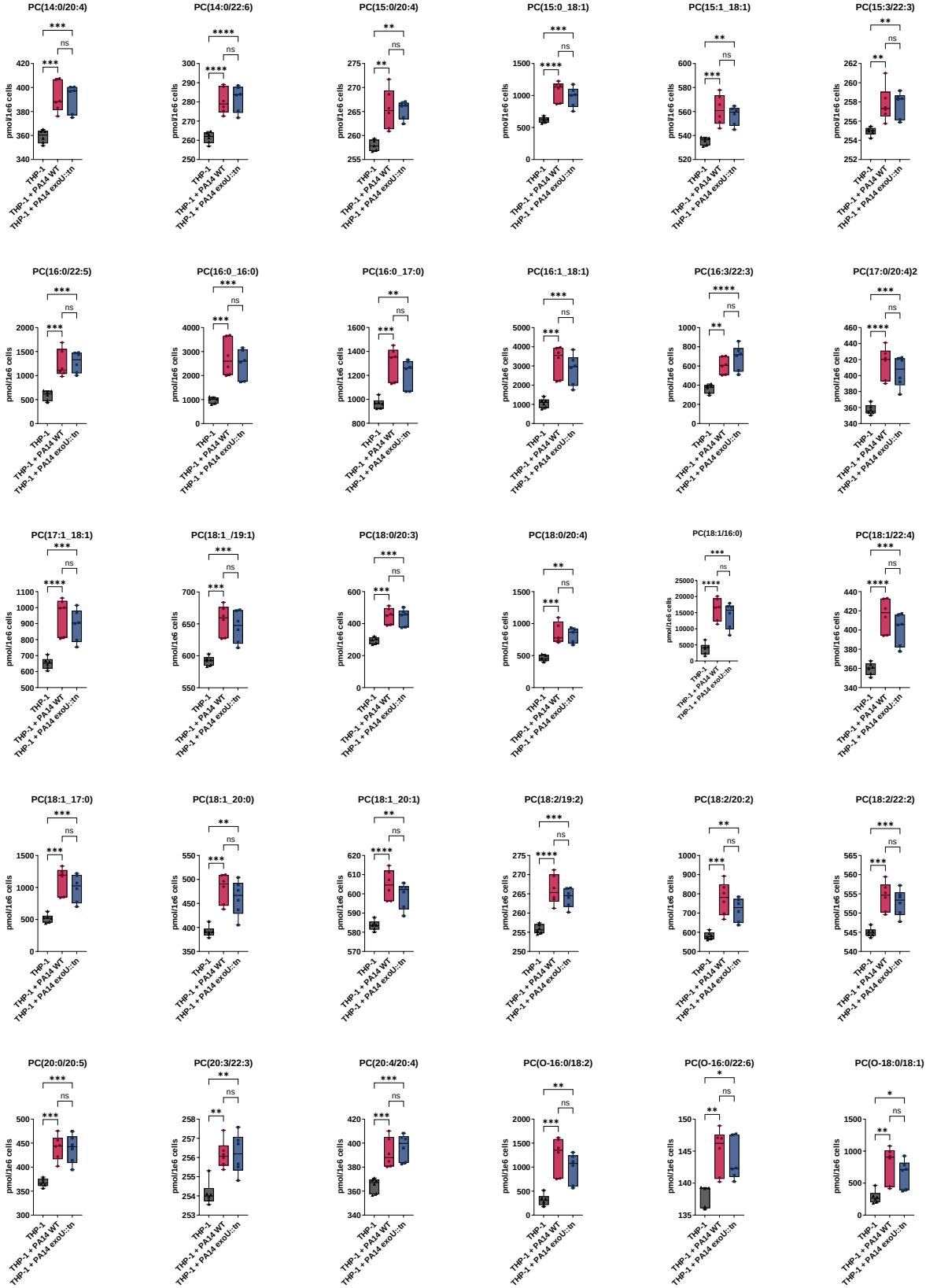
PC(14:0/20:4)
PC(14:0/22:6)
PC(15:0/20:4)
PC(15:0_18:1)
PC(15:1_18:1)
PC(15:3/22:3)
PC(16:0/22:5)
PC(16:0_16:0)
PC(16:0_17:0)
PC(16:1_18:1)
PC(16:3/22:3)
PC(17:0/20:4)2
PC(17:1_18:1)
PC(18:1_/19:1)
PC(18:0/20:3)
PC(18:0/20:4)
PC(18:1/16:0)
PC(18:1/22:4)
PC(18:1_17:0)
PC(18:1_20:0)
PC(18:1_20:1)
PC(18:2/19:2)
PC(18:2/20:2)
PC(18:2/22:2)
PC(20:0/20:5)
PC(20:3/22:3)
PC(20:4/20:4)
PC(O-16:0/18:2)
PC(O-16:0/22:6)
PC(O-18:0/18:1)
pmol/1e6 cells
THP-1
THP-1 + PA14 WT
THP-1 + PA14 exoU::tn

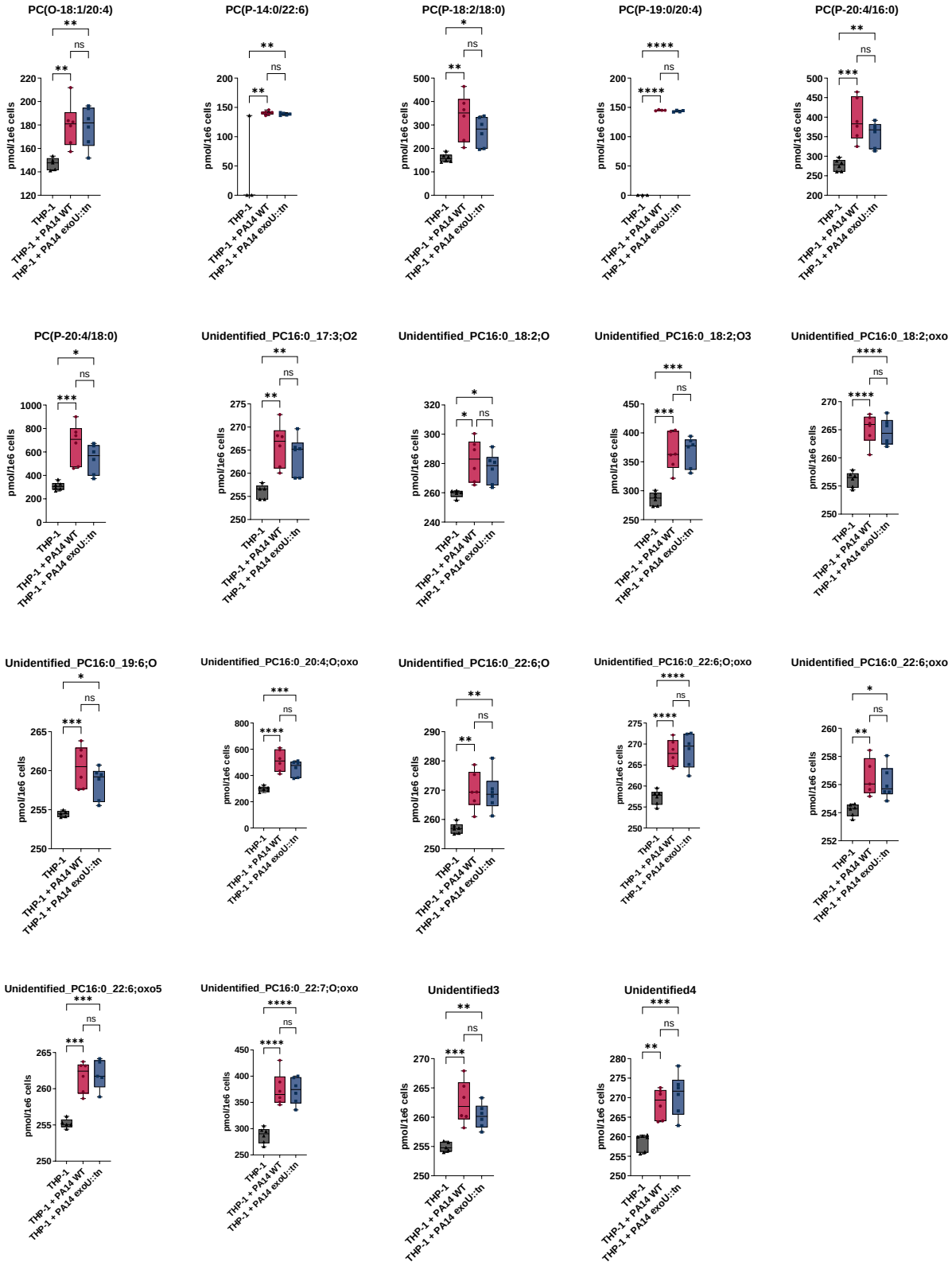
PC(O-18:1/20:4)
PC(P-14:0/22:6)
PC(P-18:2/18:0)
PC(P-19:0/20:4)
PC(P-20:4/16:0)
PC(P-20:4/18:0)
Unidentified_PC16:0_17:3;O2
Unidentified_PC16:0_18:2;O
Unidentified_PC16:0_18:2;O3
Unidentified_PC16:0_18:2;oxo
Unidentified_PC16:0_19:6;O
Unidentified_PC16:0_20:4;O;oxo
Unidentified_PC16:0_22:6;O
Unidentified_PC16:0_22:6;O;oxo
Unidentified_PC16:0_22:6;oxo
Unidentified_PC16:0_22:6;oxo5
Unidentified_PC16:0_22:7;O;oxo
Unidentified3
Unidentified4
pmol/1e6 cells
THP-1
THP-1 + PA14 WT
THP-1 + PA14 exoU::tn

Figure 18: PA14 WT and PA14 *exoU::tn* increases levels of various GPCs in THP-1 cells.

LC-MS/MS quantification of significantly altered GPC species in THP-1 macrophage after infection with *P. aeruginosa* WT or *exoU::tn* at 1 MOI for 1 hour. This graph shows GPCs that are significantly increased after PA14 WT and PA14 *exoU::tn,* suggesting a bacterial effect. GPC species in pmol are normalised per $1x10^6$ cells. GPC subclasses measured include LPC and PC, processing acyl, ether, vinyl fatty acid linkages, and various saturated and unsaturated chains. Unidentified species are detected with unknown but predicted molecular identity belonging to GPCs, pending further structural characterization. Data show mean ± SEM. N = 6 conducted over independent experiments. Data was analyzed using two-way ANOVA, and a Holm-Šídák post-hoc test for multiple comparisons. * $p<0.05$, ** $p<0.01$,***$p<001$, **** $p<0.0001$ THP-1 + PA14 WT vs THP-1 + PA14 *exoU::tn,* THP-1 + PA14 WT vs THP-1 control, THP-1 + PA14 *exoU::tn* vs THP-1 CTRL.

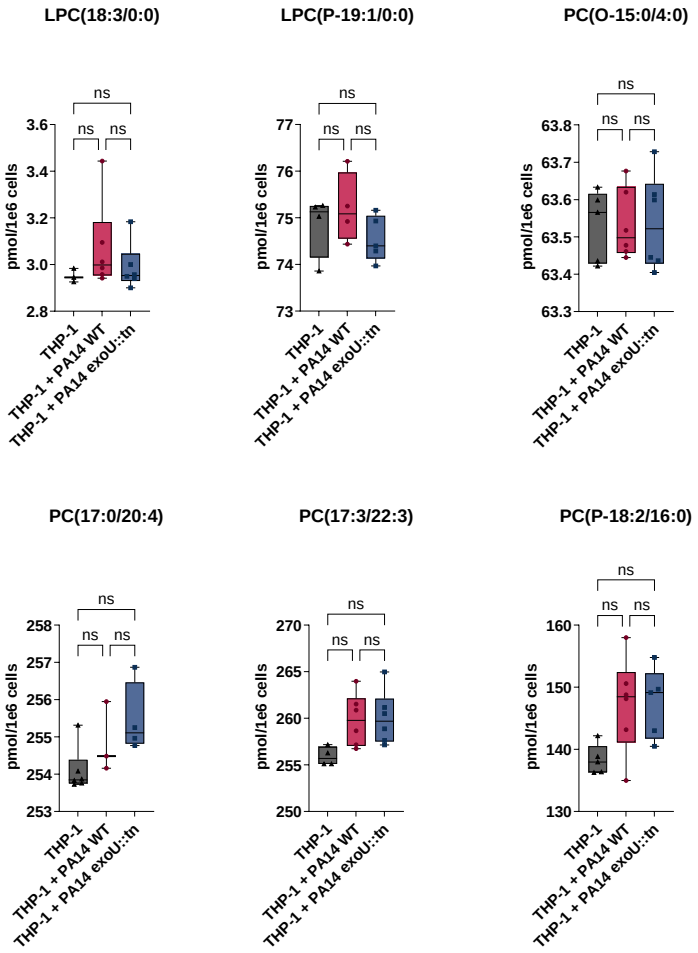

Figure 19: Unaltered GPC species after PA14 WT and PA14 *exoU::tn* infection in THP-1 cells.

LC-MS/MS quantification of significantly altered GPC species in THP-1 macrophage after infection with PA14 WT or *exoU::tn* at 1 MOI for 1 hour. This graph shows GPCs that are not significantly altered after PA14 WT or PA14 *exoU::tn*. GPC species in pmol are normalized per $1x10^6$ cells. GPC subclasses measured include LPC and PC, processing acyl, ether, vinyl fatty acid linkages, and various saturated and unsaturated chains. Data show mean ± SEM. N = 6 conducted over independent experiments. Data was analyzed using two-way ANOVA, and a Holm-Šídák post-hoc test for multiple comparisons. * $p<0.05$, ** $p<0.01$,***$p<001$, **** $p<0.0001$ THP-1 + PA14 WT vs THP-1 + PA14 *exoU::tn,* THP-1 + PA14 WT vs THP-1 control, THP-1 + PA14 *exoU::tn* vs THP-1 CTRL.

By investigating the relationship between lipid metabolism and its impact on inflammatory immune responses and cell death, this thesis offers a novel perspective on how bacteria utilize the lipidome to promote its survival, highlighting avenues for further exploration and potential applications for infectious disease treatments. I found that ExoU leads to a strong pro-inflammatory response in macrophages and an increase in cell death. In this thesis, I highlight the complex mechanism that could link ExoU to induce ferroptosis indirectly. These results tie to a dysregulated lipidome tracing to ExoU's PLA_2-like activity and dysregulation in GPC metabolism.

4.1 ExoU contributes to *P. aeruginosa* virulence

P. aeruginosa's survival in the host environment requires various defense mechanisms that P. aeruginosa employs, including but not limited to its use of effector proteins. ExoU is one of the most cytotoxic effector proteins expressed by *P. aeruginosa*, leading to severe infections [51,292]. ExoU, secreted by *P. aeruginosa*'s T3SS, possesses PLA_2-like activity relying on lipid mediators to induce its cytotoxic effects [48]. ExoU's lipid-mediated activity causes an increase in inflammatory response and induction of cell death in host cells. The identity of the ExoU-hydrolyzed lipids and the mechanism by which they induce cytotoxicity have not been fully characterized or understood.

To characterize the effects of ExoU on host cells, I used the PA14 *exoU::tn* strain expressing a lipase deficient, inactive ExoU transposon that is compared to the PA14 WT reference strain expressing an active ExoU protein. My results, testing the effect of ExoU on THP-1 macrophages and NuLi epithelial cells, showed that ExoU expressing WT *P. aeruginosa* strain leads to higher levels of cytotoxicity (**Figure 9A, Figure 10**). My results demonstrated higher levels of cytotoxicity across various time points, and MOIs were confirmed with a neutral red

cell viability assay and trypan blue staining (**Figure 9B,C**). The earliest timepoint tested at 1 hr postinfection led to significant differences between the active ExoU expressing PA14 WT strain and the inactive ExoU expressing PA14 *exoU::tn* in THP-1 cells (**Figure 9A**). Early cytotoxicity corresponds to evidence of ExoU localization at the plasma membrane postinfection at the 1 hr timepoint [307].

Although ExoU leads to high levels of cell death, the expression of ExoU is not necessary for cell death, as PA14 *exoU::tn* elicits significant levels of cell death without an active ExoU protein; however, ExoU is sufficient in causing higher levels of cell death than PA14 *exoU::tn* (**Figure 9, Figure 10**). To address any concern on whether the PA14 *exoU::tn* displays lower levels of cell death because the alteration of the ExoU protein might have caused a decrease in fitness of the *P. aeruginosa* strain, the PAO1 WT reference strain, which does not express the ExoU protein, was tested. PAO1 WT infections of THP-1 cells yielded similar results to PA14 *exoU::tn* in THP-1 viability than to WT PA14 (**Figure 11A,B**). Another strain of PAO1 with an ectopically expressed ExoU protein was able to achieve similar levels of cell death as naturally ExoU-expressing PA14 WT (**Figure 11A,B**). The presence of ExoU, therefore, accounts for the significant levels of induced cell death in infected THP-1 and NuLi. The expression of ExoU by P. aeruginosa strains provides an enhanced survival defense mechanism that allows it to survive despite the recruitment of immune cells to the site of infection. The potency of ExoU in eliminating macrophages allows the bacteria to evade immune surveillance and persist within the host.

4.2 Mechanism of ExoU-induced cell death may differ in macrophages

ExoU translocation to the inner plasma membrane is a critical step for inducing cell death, as ExoU relies on host coactivators such as $PI(4,5)P_2$ for its activity [63,71]. Previous work has shown

that affecting late endosome transport by dimerizing DNAJC5 using quercetin reduces ExoU-induced cell death in A549 epithelial cells[63]. However, treating THP-1 macrophages with quercetin at multiple concentrations followed by infection with an active ExoU-expressing strain, PA14 WT was unable to affect cell viability in a dose-dependent manner (**Figure 12**). This might suggest that the mechanism by which ExoU elicits cell death in THP-1 macrophages might not strictly depend on DNAJC5-dependent late endosome translocation to the plasma membrane. Even though most ExoU localization occurs at the plasma membrane, there is evidence of ExoU localization internally in a cytosol compartment[307]. ExoU has been shown to decrease the content of lipid bodies, which might suggest a possible interaction between ExoU and lipid bodies[64]. Further studies indicate that ExoU is detected in mitochondrial membrane-associated ER membranes (mito-MAM) fractions, suggesting that ExoU might localize at the mitochondria or only on mito-MAM sites[74]These findings could point to differences in cell types' responses to ExoU that depend on the localization site and the available lipid substrates in the vicinity of ExoU.

4.3 Ferroptosis is induced in ExoU-infected cells

P. aeruginosa induces multiple types of cell death, including apoptosis, pyroptosis, ferroptosis, and necroptosis[308–311]Because multiple mechanisms of cell death could be induced, determining the mechanism by which ExoU induces cell death becomes complicated, as many types of cell death might engage simultaneously. Representing ExoU-induced cell death as a singular type may not fully capture the complexity of the cell death mechanism, especially with the vast array of lipid mediators that could be affected by ExoU's PLA_2-like activity.

Previous studies investigating the mechanism of ExoU-induced cell death suggested necrosis as the primary form of death, as ExoU-infected cells displayed a necrotic morphology [312]. ExoU-

infected cells displayed a disruption in cytoskeleton morphology, including actin and microtubules, followed by rounding and blebbing of the host cell[89]. $PI(4,5)P_2$, a membrane phospholipid that plays a significant role in the stability of focal adhesions, helps localize the ExoU protein to the inner plasma membrane[54,72,73,189]. ExoU hydrolyzes $PI(4,5)P_2$, leading to a disruption in focal adhesions and collapse of cytoskeletal structures followed by cell lysis[89]. This provides a clear cell death modality that takes into account $PI(4,5)P_2$ as a lipid substrate of ExoU leading to cell death; however, ExoU appears to have the ability to induce cell death independently of $PI(4,5)P_2$ [89].

Apoptosis is a programmed form of cell death characterized by nuclear shrinkage and membrane blebbing[313]. Previous studies looking into the morphological characteristics of a cell infected with *P. aeruginosa* expressing ExoU noted bleb formation, suggesting possible apoptosis involvement; however, further analysis showed that the blebs had varying sizes and plasma membrane tubules, which is not a characteristic of apoptosis [89]. Further investigation using Annexin V, which binds to apoptotic cells, did not show binging, leading to the conclusion that ExoU does not drive apoptosis induction[89]. Confirming these results, treatment with zVAD, a pan caspase inhibitor known to inhibit apoptotic cell death, led to no changes in cell viability in response to ExoU expressing PA14 WT (**Figure 13A**). Although apoptosis might not be the main driver of cell death, dysregulated lipids could be inducing multiple pathways, with certain mechanisms dominating over the others depending the kinetics that control cell viability [314].

Necroptotic cell death is a regulated form of cell death that depends on mixed lineage kinase domain-like pseudokinase (MLKL), and Receptor-interacting serine-threonine protein kinase 1/3 (RIPK1/ RIPK3) for its mechanism[315]. MLKL is a pore-forming protein that binds to the plasma membrane to induce cell death by acting like a cation channel, leading to the buildup of osmotic

pressure and rupture[316,317]. Phospholipids, and especially $PI(4,5)P_2$, play a role in MLKL binding to the plasma membrane, thus influencing its ability to induce necroptosis[318,319]. ExoU's ability to cleave $PI(4,5)P_2$ suggests that it would decrease the levels of $PI(4,5)P_2$ available at the plasma membrane, which could inhibit the binding of the necrosome and the induction of necroptosis. My data showed that inhibiting necroptosis with GSK872, a RIPK3 inhibitor, did not affect cell viability when infected with ExoU expressing PA14 WT (**Figure 13B**). The ability of ExoU to cleave $PI(4,5)P_2$ possibly played a role in preventing MLKL binding, which could inhibit necroptosis in *P. aeruginosa*-infected cells.

Ferroptosis is an iron-dependent form of cell death that is mediated by lipid peroxidation and Reactive Oxygen Species (ROS) [131]. Ferrostatin-1 (fer-1) has been identified as one of the most potent synthetic ferroptosis inhibitors, acting as a radical trapping agent (RTA) and eliminating lipid peroxides from damaging the plasma membrane[320]. Decreasing the levels of lipid peroxidation using RTAs such as fer-1 has been shown to inhibit ferroptosis[321]. The ability of ExoU to act as a PLA_2 suggested a significant involvement of lipids in its ability to induce cell death [48]. Fatty acids and lysophospholipids are products of PLA_2 hydrolysis that could play a role in cell death [59]. Lipids on the membrane or free fatty acids in the cytosol can get oxidated, forming lipid peroxides or aldehydes that damage the plasma membrane and induce ferroptosis [322]. My data demonstrate that inhibiting lipid peroxidation using fer-1 treatment for 1 hr but not 3 hr leads to increased THP-1 viability after infection with ExoU expressing PA14 WT bacteria (**Figure 13C,D**). This suggests that ferroptosis might contribute to the initial stages of cell death that THP-1 cells undergo. Other types of cell death, such as the $PI(4,5)P_2$-dependent necrosis, could be the most dominant form of cell death at 3 hours and beyond [89]. ExoU products contributing to the ferroptotic cell death at 1 hr are most likely different from those associated with later time points as the mechanism of cell death is different. As ExoU catalyzes other

phospholipid classes, cellular response and the mechanism of cell death might be altered. Another possibility is that PI(4,5)P_2-induced necrosis has slower cell death kinetics for focal adhesion disruption than ferroptosis-associated substrates. Therefore, it is plausible that the inability of fer-1 to decrease cell death after 3 hours of infection is not its lack of activity but that lipid peroxidation is not implicated in driving cell death after 1 hr.

Further investigation attempted to induce ferroptosis by increasing lipid peroxidation levels through treatment with CuOOH, a peroxidizing agent. Unlike the inhibition of ferroptosis seen at 1 hr with fer-1, CuOOH treatment had no significant effect on THP-1 viability after infection with ExoU expressing PA14 WT (**Figure 13E**). This surprising finding might suggest that non-specific cellular peroxidation might not be enough to induce ferroptosis but might only sensitize the cells to ferroptotic cell death. Lipid peroxidation of specific lipid species could be more crucial to the induction of ferroptosis, such as those hydrolyzed by ExoU. Lipid peroxidation at the plasma membrane is thought to be a significant component in the induction of ferroptosis [322]. Previous studies have reported that PLA_2s, with the ability to cleave phospholipids, can protect against ferroptosis [323,324]. This might be attributed to the ability of PLA_2s to release PUFA, which might be peroxidized into the cytosol, which could prevent the induction of ferroptosis. This introduces a paradoxical contradiction as ExoU is known to act in a PLA2-like manner but has been shown to induce ferroptosis at 1 hr (**Figure 13C**). If PLA2 activity results in a decrease in ferroptosis, then the viability of cells treated with the peroxidizing agent CuOOH would increase, which is not observed (**Figure 13E**). This observation in ExoU activity compared to endogenous PLA_2s might suggest that ExoU targets different lipid substrates preferentially compared to other known PLA_2 enzymes. A possible explanation could revolve around a preference of ExoU to certain lipids. The preferential release of PUFAs by a PLA_2-like enzyme into the cytoplasm might allow for increased peroxidation as described before. The generation of

newly peroxidized lipids and their incorporation into the plasma membrane through the Land's cycle, utilizing enzymes such as ACSL4 and LPCATs, might disrupt the membrane enough to induce ferroptosis. The disruption of the plasma membrane requires a threshold of lipid peroxides to be present which might not be easily achieved in the presence of all the anti-ferroptotic mechanisms. Previous molecular dynamic simulations revealed the possible formation of lipid micro-domains that might have high enough concentrations to induce pore formation or permeabilization [325]. Therefore, ExoU's ability to induce ferroptosis might be dependent on the generation of certain membrane-disrupting phospholipids in concentrated micro-domains that allow for their peroxidation and membrane disruption. The success of anti-peroxidation treatments might be explained by the formation of micro-domains of ExoU-generated products with high-peroxidation fatty acyl chains. These concentrated and centralized peroxidized micro-domains might have been disrupted by fer-1, which removes the peroxides but cannot be induced by general peroxidation agents like CuOOH that do not target these specific sites.

4.4 ExoU increases levels of IL-1ß secretion

The impact of ExoU is not only limited to its cytotoxicity. ExoU has been shown to release various proinflammatory cytokines including IL-1α, IL-33, and IL-36γ, as well as proinflammatory lipids such as AA, PGE2, and LTB4 [84,86]. The prolonged release of inflammatory mediators contributes to chronic inflammation and long-term damage in patients [326]. My data demonstrates that ExoU-expressing *P. aeruginosa* strains lead to higher levels of the proinflammatory cytokine IL-1ß compared to the strain lacking a functional ExoU protein (**Figure 14A**). In the case of CF patients with a *P. aeruginosa* infection, higher levels of IL-1ß may lead to an increase in pulmonary injury that might be driven by ExoU expression in the lungs of infected patients [327].

As ExoU activity could be mediated by ferroptosis, especially at early infections, we investigated how inhibiting ferroptosis might affect IL-1ß secretion. Surprisingly, the levels of IL-1ß secretion in THP-1 cells increase after inhibiting ferroptosis with fer-1 after infection with ExoU expressing PA14 WT compared to the inactive ExoU strain (**Figure 14B**). IL-1ß is expressed in its inactive state as pro-IL-1ß, relying on the activation of the inflammasome and the cleavage by active caspase-1 to be converted into its active form [328]. IL-1ß is then secreted through the gasdermin D pore to induce its inflammatory activity [329]. This maturation step creates a delay between the expression of the protein and its secretion, making it crucial to prevent rampant inflammatory responses that could cause damage [330]Because ferroptosis occurs at the early stages of infection, faster cell death kinetics might provide a longer time for IL-1ß maturation. Thus, increased IL-1ß secretion from fer-1 treatment enhances a pro-inflammatory signal, and macrophages may benefit from this response, as IL-1ß serves a protective role in fighting *P. aeruginosa* infections.

4.5 ExoU alters macrophage lipidome

Elucidating the products and substrates that mediate ExoU's activity is pivotal to understanding its mechanism. The diversity in ExoU substrates is most likely the inducer of many different mechanisms, including ferroptosis, necrosis, and inflammasome activation. Mass spectrometry allows for accurate identification of phospholipid identity, producing highly accurate quantification of lipids disrupted by ExoU activity and identification of their structure.

Asymmetries between lipids of the inner and outer leaflet composition of eukaryotic plasma membranes are not only limited to differences in lipid headgroups but also include differences in acyl chains, backbone linkages, and saturation [331–333]. The cytoplasmic inner leaflet's phospholipids have been shown to have higher levels of unsaturation compared to the outer

membrane [333]. Unsaturated fatty acids are major drivers of ferroptosis as they become peroxidized and disrupt membrane integrity, making the inner leaflet of the plasma membrane an integral part of regulating the induction of ferroptosis [146,244]. In macrophages, ExoU induced an increase in specific PC species, which had a polyunsaturated fatty acyl chain at the *sn-2* position (**Figure 17**). Among the ExoU-affected GPCs, two PC species had two unsaturated fatty acyl chains (**Figure 17**). Phospholipids with diacyl PUFAs (PL-$PUFA_2$) carry PUFAs at the *sn-1* and *sn-2* positions. PL-$PUFA_2$ and specifically PC-$PUFA_2$ have been implicated to be a potent ferroptosis inducer [334]. PL-$PUFA_2$ are suggested as potential ferroptosis biomarkers because of their correlation to ferroptosis sensitivity in cell lines and their association with ferroptosis-related diseases [334]. It is unclear whether an increase in a small number of PC-$PUFA_2$ species is sufficient to provide enough sensitivity to ferroptosis; however, further analysis of other phospholipids could provide a better understanding of the dysregulation.

The localization of ExoU at the inner leaflet of the plasma membrane allows for the cleavage of more unsaturated fatty acids which could sensitize the cells for ferroptosis [307]. More interestingly, while PUFAs make a cell more susceptible to ferroptosis, increases in MUFAs make cells more resistant to ferroptosis [335,336]. However, there was no observation of any GPCs with a MUFA that was dysregulated specifically by ExoU.

A multitude of GPC species measured were increased by the presence of bacteria regardless of ExoU expression (**Figure 18**). This suggests a broader lipidome remodeling response in host cells than was hypothesized without a lipolytic enzyme like ExoU. The increase of these GPC species could be due to bacterial-induced inflammation or an altered metabolism. Understanding these broader lipidomic shifts could provide insights into potential metabolic vulnerabilities that, by themselves, do not lead to cell death but prime the cells to an inflammatory response. The

effects of ExoU on the plasma membrane are not limited to the induction of ferroptosis, especially as it was limited to the 1 hr timepoint in THP-1 cells (**Figure 13C).**

Among the dysregulated lipid species impacted by ExoU, most were LPCs (**Figure 16B**). This result confirmed ExoU's lipolytic activity as a PLA_2. As membrane integrity is essential for the survival of a cell, cells maintain homeostasis by continual remodeling of phospholipids to prevent dysregulation that could lead to changes in membrane structure and rupture [337–339]. ExoU disrupts membrane integrity by increasing the level of LPCs (**Figure 17**). The mechanism by which LPCs could contribute to ExoU-mediated cell death. LPC is known to induce oxidative stress in cells, independently from its membrane permeabilization [340]. The increase in oxidation inside the cell could contribute to the induction of ferroptosis inside the THP-1 cells we observed.

LPCs are also known to cause membrane permeabilization and cell rounding, which by themselves at physiological concentrations may not be enough to induce cell lysis [340]. Nonetheless, the ability of LPC to increase membrane curvature might enhance the blebbing caused by the cytoskeletal disruption from PI(4,5)P2 cleavage by ExoU, leading to necrosis [89,183].

The inflammatory response seen in THP-1 cells caused by ExoU might also be linked to increased LPCs. LPC is linked to the release of DAMPs through membrane permeabilization. LPCs are known to increase the release of ATP from cells, increase Ca^{2+} influx, and increase K^+ efflux [341,342]. The release of ATP through the Pannexin-1 channel by higher levels of LPC leads to the activation of the NLP3 and the processing of IL-1β by caspase-1 [342]. Afterward, LPC can activate nonselective cation channels, leading to Ca^{2+} influx and the activation of Ca^{2+}-dependent K^+ channels, causing membrane hyperpolarization[341]. Membrane hyperpolarization is required for the release of IL-1β into the extracellular environment [341]. This proposed mechanism suggests

that the increase in LPCs by ExoU activity is a driver of the processing and release of IL-1β, contributing to the pro-inflammatory responses observed in THP-1 cells (**Figure 14A**).

5 CONCLUSION

This thesis covers the function of ExoU and provides insights into its mechanism for the induction of cell death. I describe the specificity of ExoU to different cell types, THP-1 macrophages and NuLi cells, and its ability to induce cell death at multiple time points and MOIs. Then, I investigated other strains of *P. aeruginosa* to prove that ExoU is responsible for the higher levels of cell death compared to other strains. My work shows how disrupting ExoU translocation does not affect its viability in THP-1 cells, unlike previous reports, suggesting a different mechanism of action. This thesis also investigates the type of cell death induced by ExoU. Although apoptosis and necroptosis did not appear to be involved in the cell death mechanism, ferroptosis seemed to contribute at early time points infection. Induction of peroxidation, on the other hand, did not affect cell viability. This indicates a complex mechanism of cell death that occurs when cells are infected with PA14 WT bacteria, but not PA14 *exoU::tn*.

This thesis also investigates inflammatory responses induced by ExoU through the secretion of IL-1ß. ExoU appears to trigger elevated secretion of IL-1ß, suggesting an increase in inflammasome activation that could be mediated by lipids. Furthermore, inhibiting ferroptosis appears to increase the levels of inflammatory responses through IL-1ß, suggesting increased IL-1ß processing after prolonged cell survival. Finally, the identity of dysregulated GPCs was investigated and showed a significant increase in LPCs that are thought to disrupt plasma membrane structure, contribute to cell death, and lead to increased inflammatory responses.

ExoU's mechanism of cell death appears to be complex, involving many lipid substrates and mediators that induce both cytotoxicity as well as inflammation. Cell death kinetics that are

initiated by ExoU are most likely to be highly dynamic, whereas a host cell could undergo necrosis or other forms of cell death and inflammatory responses depending on the phospholipid composition in the cell membrane and the various lipid substrates in ExoU's environment. While inhibiting a single known ExoU exploited mechanism or removing a substrate could partially reduce its effects and explain how it leads to cytotoxicity, complete inhibition of ExoU activity is necessary to promote cell survival. The integration of many lipids into various essential survival mechanisms makes ExoU a potent and persistent toxin, yet a fascinating and unique protein.

6 REFERENCES

1. Lanotte, P., Mereghetti, L., Lejeune, B., Massicot, P. & Quentin, R. Pseudomonas aeruginosa and cystic fibrosis: Correlation between exoenzyme production and patient's clinical state. *Pediatric Pulmonology* **36**, 405–412 (2003).
2. Morales, E. *et al.* Hospital costs of nosocomial multi-drug resistant Pseudomonas aeruginosa acquisition. *BMC Health Services Research* **12**, 122 (2012).
3. Ratjen, F. Recent advances in cystic fibrosis. *Paediatric Respiratory Reviews* **9**, 144–148 (2008).
4. Al-Hasan, M. N., Wilson, J. W., Lahr, B. D., Eckel-Passow, J. E. & Baddour, L. M. Incidence of Pseudomonas aeruginosa Bacteremia: A Population-Based Study. *Am J Med* **121**, 702–708 (2008).
5. Kollef, M. H. *et al.* Global prospective epidemiologic and surveillance study of ventilator-associated pneumonia due to Pseudomonas aeruginosa. *Crit Care Med* **42**, 2178–2187 (2014).
6. Gonzalez, M. R. *et al.* Effect of Human Burn Wound Exudate on Pseudomonas aeruginosa Virulence. *mSphere* **1**, e00111-15 (2016).

7. Surette, M. G. The Cystic Fibrosis Lung Microbiome. *Annals of the American Thoracic Society* **11**, S61–S65 (2014).
8. Parkins, M. D., Somayaji, R. & Waters, V. J. Epidemiology, Biology, and Impact of Clonal Pseudomonas aeruginosa Infections in Cystic Fibrosis. *Clinical Microbiology Reviews* **31**, e00019-18 (2018).
9. Lu, Q. *et al.* Pseudomonas aeruginosa serotypes in nosocomial pneumonia: prevalence and clinical outcomes. *Critical Care* **18**, R17 (2014).
10. Oliver, A., Cantón, R., Campo, P., Baquero, F. & Blázquez, J. High frequency of hypermutable Pseudomonas aeruginosa in cystic fibrosis lung infection. *Science* **288**, 1251–1254 (2000).
11. Pachori, P., Gothalwal, R. & Gandhi, P. Emergence of antibiotic resistance Pseudomonas aeruginosa in intensive care unit; a critical review. *Genes Dis* **6**, 109–119 (2019).
12. Type III protein secretion is associated with poor clinical outcomes in patients with ventilator-associated pneumonia caused by Pseudomonas aeruginosa. https://oce-ovid-com.proxy.bib.uottawa.ca/article/00003246-200203000-00005/HTML.
13. Subedi, D. *et al.* Association between possession of ExoU and antibiotic resistance in Pseudomonas aeruginosa. *PLOS ONE* **13**, (2018).
14. Wu, T. *et al.* The type III secretion system facilitates systemic infections of Pseudomonas aeruginosa in the clinic. *Microbiology Spectrum* **12**, e02224-23 (2023).
15. El Solh, A. A. *et al.* Persistent Infection with Pseudomonas aeruginosa in Ventilator-associated Pneumonia. *Am J Respir Crit Care Med* **178**, 513–519 (2008).
16. Howell, H. A., Logan, L. K. & Hauser, A. R. Type III Secretion of ExoU Is Critical during Early Pseudomonas aeruginosa Pneumonia. *Mbio* **4**, (2013).

17. Galán, J. E. Common themes in the design and function of bacterial effectors. *Cell Host Microbe* **5**, 571–579 (2009).

18. Green, E. R. & Mecsas, J. Bacterial Secretion Systems: An Overview. in *Virulence Mechanisms of Bacterial Pathogens* 213–239 (John Wiley & Sons, Ltd, 2016). doi:10.1128/9781555819286.ch8.

19. Hueck, C. J. Type III protein secretion systems in bacterial pathogens of animals and plants. *Microbiol Mol Biol Rev* **62**, 379–433 (1998).

20. Marsden, A. E. *et al.* Vfr Directly Activates exsA Transcription To Regulate Expression of the Pseudomonas aeruginosa Type III Secretion System. *J Bacteriol* **198**, 1442–1450 (2016).

21. Williams McMackin, E. A., Marsden, A. E. & Yahr, T. L. H-NS Family Members MvaT and MvaU Regulate the Pseudomonas aeruginosa Type III Secretion System. *Journal of Bacteriology* **201**, 10.1128/jb.00054-19 (2019).

22. Wei, M. *et al.* Temperature-dependent expression of type III secretion system genes and its regulation in Bradyrhizobium japonicum. *Mol Plant Microbe Interact* **23**, 628–637 (2010).

23. Gophna, U., Ron, E. Z. & Graur, D. Bacterial type III secretion systems are ancient and evolved by multiple horizontal-transfer events. *Gene* **312**, 151–163 (2003).

24. Van Engelenburg, S. B. & Palmer, A. E. Imaging type-III secretion reveals dynamics and spatial segregation of Salmonella effectors. *Nat Methods* **7**, 325–330 (2010).

25. Marlovits, T. C. *et al.* Structural insights into the assembly of the type III secretion needle complex. *Science* **306**, 1040–1042 (2004).

26. Schraidt, O. & Marlovits, T. C. Three-dimensional model of Salmonella's needle complex at subnanometer resolution. *Science* **331**, 1192–1195 (2011).

27. Loquet, A. *et al.* Atomic model of the type III secretion system needle. *Nature* **486**, 276–279 (2012).

28. Lee, S. H. & Galán, J. E. Salmonella type III secretion-associated chaperones confer secretion-pathway specificity. *Mol Microbiol* **51**, 483–495 (2004).

29. Romano, F. B. *et al.* Efficient Isolation of Pseudomonas aeruginosa Type III Secretion Translocators and Assembly of Heteromeric Transmembrane Pores in Model Membranes. *Biochemistry* **50**, 7117–7131 (2011).

30. Dortet, L., Lombardi, C., Cretin, F., Dessen, A. & Filloux, A. Pore-forming activity of the Pseudomonas aeruginosa type III secretion system translocon alters the host epigenome. *Nat Microbiol* **3**, 378–386 (2018).

31. Dacheux, D., Goure, J., Chabert, J., Usson, Y. & Attree, I. Pore-forming activity of type III system-secreted proteins leads to oncosis of Pseudomonas aeruginosa-infected macrophages. *Molecular Microbiology* **40**, 76–85 (2001).

32. Edilene do Socorro Nascimento Falcão Sarges *et al.* Pseudomonas aeruginosa Type III Secretion System Virulotypes and Their Association with Clinical Features of Cystic Fibrosis Patients. *Infection and Drug Resistance* **13**, 3771–3781 (2020).

33. Horna, G. & Ruiz, J. Type 3 secretion system of Pseudomonas aeruginosa. *Microbiological Research* **246**, 126719–126719 (2021).

34. Lombardi, C. *et al.* Structural and Functional Characterization of the Type Three Secretion System (T3SS) Needle of Pseudomonas aeruginosa . *Frontiers in Microbiology* **10**, 573–573 (2019).

35. Feltman, H. *et al.* Prevalence of type III secretion genes in clinical and environmental isolates of Pseudomonas aeruginosa. *Microbiology* **147**, 2659–2669 (2001).

36. Coburn, J., Dillon, S. T., Iglewski, B. H. & Gill, D. M. Exoenzyme S of Pseudomonas aeruginosa ADP-ribosylates the intermediate filament protein vimentin. *Infection and Immunity* **57**, 996–998 (1989).

37. Fraylick, J. E., La Rocque, J. R., Vincent, T. S. & Olson, J. C. Independent and Coordinate Effects of ADP-Ribosyltransferase and GTPase-Activating Activities of Exoenzyme S on HT-29 Epithelial Cell Function. *Infection and Immunity* **69**, 5318–5328 (2001).

38. Liu, S., Yahr, T. L., Frank, D. W. & Barbieri, J. T. Biochemical relationships between the 53-kilodalton (Exo53) and 49-kilodalton (ExoS) forms of exoenzyme S of Pseudomonas aeruginosa. *J Bacteriol* **179**, 1609–1613 (1997).

39. Winsor, G. L. *et al.* Enhanced annotations and features for comparing thousands of Pseudomonas genomes in the Pseudomonas genome database. *Nucleic Acids Research* **44**, D646–D653 (2016).

40. The Arginine Finger Domain of ExoT Contributes to Actin Cytoskeleton Disruption and Inhibition of Internalization ofPseudomonas aeruginosa by Epithelial Cells and Macrophages | Infection and Immunity. https://journals.asm.org/doi/full/10.1128/iai.68.12.7100-7113.2000.

41. Sun, J. & Barbieri, J. T. Pseudomonas aeruginosa ExoT ADP-ribosylates CT10 Regulator of Kinase (Crk) Proteins *. *Journal of Biological Chemistry* **278**, 32794–32800 (2003).

42. Morrow, K. A. *et al.* Heterogeneity of pulmonary endothelial cyclic nucleotide response to Pseudomonas aeruginosa ExoY infection. *American Journal of Physiology-Lung Cellular and Molecular Physiology* **309**, L1199–L1207 (2015).

43. Belyy, A. *et al.* Actin activates Pseudomonas aeruginosa ExoY nucleotidyl cyclase toxin and ExoY-like effector domains from MARTX toxins. *Nat Commun* **7**, 13582 (2016).

44. Morrow, K. A., Frank, D. W., Balczon, R. & Stevens, T. The Pseudomonas aeruginosa Exoenzyme Y: A Promiscuous Nucleotidyl Cyclase Edema Factor and Virulence Determinant. in *Non-canonical Cyclic Nucleotides* (ed. Seifert, R.) 67–85 (Springer International Publishing, Cham, 2017). doi:10.1007/164_2016_5003.

45. Finck-Barbançon, V. *et al.* ExoU expression by Pseudomonas aeruginosa correlates with acute cytotoxicity and epithelial injury. *Molecular Microbiology* **25**, 547–557 (1997).

46. Hauser, A. R., Kang, P. J. & Engel, J. N. PepA, a secreted protein of Pseudomonas aeruginosa, is necessary for cytotoxicity and virulence. *Molecular Microbiology* **27**, 807–818 (1998).

47. Phillips, R. M., Six, D. A., Dennis, E. A. & Ghosh, P. In vivo phospholipase activity of the Pseudomonas aeruginosa cytotoxin ExoU and protection of mammalian cells with phospholipase A2 inhibitors. *Journal of Biological Chemistry* **278**, 41326–41332 (2003).

48. Sato, H. *et al.* The mechanism of action of the Pseudomonas aeruginosa-encoded type III cytotoxin, ExoU. *The EMBO Journal* **22**, 2959–2969 (2003).

49. Tamura, M. *et al.* Lysophospholipase A activity of Pseudomonas aeruginosa type III secretory toxin ExoU. *Biochemical and Biophysical Research Communications* **316**, 323–331 (2004).

50. Morales-Espinosa, R. *et al.* Fingerprint Analysis and Identification of Strains ST309 as a Potential High Risk Clone in a Pseudomonas aeruginosa Population Isolated from Children with Bacteremia in Mexico City. *Front. Microbiol.* **8**, (2017).

51. Shaver, C. M. & Hauser, A. R. Relative Contributions of Pseudomonas aeruginosa ExoU, ExoS, and ExoT to Virulence in the Lung. *Infection and Immunity* **72**, 6969–6977 (2004).

52. Finck-Barbançon, V., Yahr, T. L. & Frank, D. W. Identification and Characterization of SpcU, a Chaperone Required for Efficient Secretion of the ExoU Cytotoxin. *Journal of Bacteriology* **180**, 6224–6231 (1998).

53. Halavaty, A. S. *et al.* Structure of the Type III Secretion Effector Protein ExoU in Complex with Its Chaperone SpcU. *PLoS One* **7**, e49388 (2012).

54. Gendrin, C. *et al.* Structural Basis of Cytotoxicity Mediated by the Type III Secretion Toxin ExoU from Pseudomonas aeruginosa. *PLOS Pathogens* **8**, 2637 (2012).

55. Tessmer, M. H. *et al.* Characterization of the ExoU activation mechanism using EPR and integrative modeling. *Sci Rep* **10**, 19700 (2020).

56. Rabin, S. D. P. & Hauser, A. R. Functional regions of the Pseudomonas aeruginosa cytotoxin ExoU. *Infection and Immunity* **73**, 573–582 (2005).

57. Six, D. A. & Dennis, E. A. The expanding superfamily of phospholipase A(2) enzymes: classification and characterization. *Biochim Biophys Acta* **1488**, 1–19 (2000).

58. Leslie, C. C. Cytosolic phospholipase A_2: physiological function and role in disease. *J Lipid Res* **56**, 1386–1402 (2015).

59. Cummings, B. S., McHowat, J. & Schnellmann, R. G. Phospholipase A(2)s in cell injury and death. *J Pharmacol Exp Ther* **294**, 793–799 (2000).

60. Bank, R. P. D. RCSB PDB - 3TU3: 1.92 Angstrom resolution crystal structure of the full-length SpcU in complex with full-length ExoU from the type III secretion system of Pseudomonas aeruginosa. https://www.rcsb.org/structure/3tu3.

61. UCSF ChimeraX Home Page. https://www.cgl.ucsf.edu/chimerax/.

62. Xu, Y. *et al.* DNAJC5 facilitates USP19-dependent unconventional secretion of misfolded cytosolic proteins. *Cell Discov* **4**, 1–18 (2018).

63. Deruelle, V. *et al.* The bacterial toxin ExoU requires a host trafficking chaperone for transportation and to induce necrosis. *Nature Communications* **12**, 4024–4024 (2021).

64. Plotkowski, M.-C. *et al.* Lipid body mobilization in the ExoU-induced release of inflammatory mediators by airway epithelial cells. *Microbial Pathogenesis* **45**, 30–37 (2008).

65. Sato, H. & Frank, D. W. ExoU is a potent intracellular phospholipase. *Molecular Microbiology* **53**, 1279–1290 (2004).

66. Hershko, A. & Ciechanover, A. The ubiquitin system. *Annu Rev Biochem* **67**, 425–479 (1998).

67. Swatek, K. N. & Komander, D. Ubiquitin modifications. *Cell Res* **26**, 399–422 (2016).

68. Anderson, D. M. *et al.* Ubiquitin and ubiquitin-modified proteins activate the Pseudomonas aeruginosa T3SS cytotoxin, ExoU. *Mol Microbiol* **82**, 1454–1467 (2011).

69. Darwin, K. H. PROKARYOTIC UBIQUITIN-LIKE PROTEIN, PROTEASOMES, AND PATHOGENESIS. *Nat Rev Microbiol* **7**, 485–491 (2009).

70. McLaughlin, S., Wang, J., Gambhir, A. & Murray, D. PIP(2) and proteins: interactions, organization, and information flow. *Annu Rev Biophys Biomol Struct* **31**, 151–175 (2002).

71. Tyson, G. H. & Hauser, A. R. Phosphatidylinositol 4,5-Bisphosphate Is a Novel Coactivator of the Pseudomonas aeruginosa Cytotoxin ExoU. *Infection and Immunity* **81**, 2873–2881 (2013).

72. Springer, T. I., Reid, T.-E., Gies, S. L. & Feix, J. B. Interactions of the effector ExoU from Pseudomonas aeruginosa with short-chain phosphatidylinositides provide insights into ExoU targeting to host membranes. *Journal of Biological Chemistry* **294**, 19012–19021 (2019).

73. Zhang, A., Veesenmeyer, J. L. & Hauser, A. R. Phosphatidylinositol 4,5-Bisphosphate-Dependent Oligomerization of the Pseudomonas aeruginosa Cytotoxin ExoU. *Infection and Immunity* **86**, (2017).

74. Hardy, K. S. *et al.* ExoU Induces Lung Endothelial Cell Damage and Activates Pro-Inflammatory Caspase-1 during Pseudomonas aeruginosa Infection. *Toxins* **14**, 152–152 (2022).

75. Burke, J. E. & Dennis, E. A. Phospholipase A2 Biochemistry. *Cardiovasc Drugs Ther* **23**, 49 (2009).

76. Cao, Y., Pearman, A. T., Zimmerman, G. A., McIntyre, T. M. & Prescott, S. M. Intracellular unesterified arachidonic acid signals apoptosis. *Proceedings of the National Academy of Sciences* **97**, 11280–11285 (2000).

77. Thakur, A., Willcox, M. D. & Stapleton, F. The proinflammatory cytokines and arachidonic acid metabolites in human overnight tears: homeostatic mechanisms. *J Clin Immunol* **18**, 61–70 (1998).

78. Lin, L. L., Lin, A. Y. & Knopf, J. L. Cytosolic phospholipase A2 is coupled to hormonally regulated release of arachidonic acid. *Proc Natl Acad Sci U S A* **89**, 6147–6151 (1992).

79. Higgins, A. J. & Lees, P. The acute inflammatory process, arachidonic acid metabolism and the mode of action of anti-inflammatory drugs. *Equine Veterinary Journal* **16**, 163–175 (1984).

80. Jang, Y., Kim, M. & Hwang, S. W. Molecular mechanisms underlying the actions of arachidonic acid-derived prostaglandins on peripheral nociception. *Journal of Neuroinflammation* **17**, 30 (2020).

81. Funk, C. D. Prostaglandins and Leukotrienes: Advances in Eicosanoid Biology. *Science* **294**, 1871–1875 (2001).

82. Li, P. *et al.* LTB4 causes macrophage–mediated inflammation and directly induces insulin resistance in obesity. *Nat Med* **21**, 239–247 (2015).

83. Park, J. Y., Pillinger, M. H. & Abramson, S. B. Prostaglandin E2 synthesis and secretion: The role of PGE2 synthases. *Clinical Immunology* **119**, 229–240 (2006).

84. Pazos, M. A. *et al.* Pseudomonas aeruginosa ExoU augments neutrophil transepithelial migration. *PLOS Pathogens* **13**, (2017).

85. Saliba, A. M. *et al.* Eicosanoid-mediated proinflammatory activity of Pseudomonas aeruginosa ExoU. *Cellular Microbiology* **7**, 1811–1822 (2005).

86. Bagayoko, S. *et al.* Host phospholipid peroxidation fuels ExoU-dependent cell necrosis and supports Pseudomonas aeruginosa-driven pathology. *PLOS Pathogens* **17**, (2021).

87. Sato, H., Feix, J. B., Hillard, C. J. & Frank, D. W. Characterization of Phospholipase Activity of the Pseudomonas aeruginosa Type III Cytotoxin, ExoU. *Journal of Bacteriology* **187**, 1192–1195 (2005).

88. Hayashi, E., Hasegawa, R. & Tomita, T. Accumulation of neutral lipids in Saccharomyces carlsbergensis by myo-inositol deficiency and its mechanism. Reciprocal regulation of yeast acetyl-CoA carboxylase by fructose bisphosphate and citrate. *Journal of Biological Chemistry* **251**, 5759–5769 (1976).

89. Sato, H. & Frank, D. W. Intoxication of Host Cells by the T3SS Phospholipase ExoU: PI(4,5)P2-Associated, Cytoskeletal Collapse and Late Phase Membrane Blebbing. *PLoS One* **9**, e103127 (2014).

90. Zakeri, Z. & Lockshin, R. A. Cell death during development. *Journal of Immunological Methods* **265**, 3–20 (2002).

91. Häcker, G. The morphology of apoptosis. *Cell Tissue Res* **301**, 5–17 (2000).

92. Kerr, J. F., Wyllie, A. H. & Currie, A. R. Apoptosis: a basic biological phenomenon with wide-ranging implications in tissue kinetics. *Br J Cancer* **26**, 239–257 (1972).

93. Gao, Y., Herndon, J. M., Zhang, H., Griffith, T. S. & Ferguson, T. A. Antiinflammatory Effects of CD95 Ligand (FasL)-induced Apoptosis. *Journal of Experimental Medicine* **188**, 887–896 (1998).

94. Chen, W., Frank, M. E., Jin, W. & Wahl, S. M. TGF-beta released by apoptotic T cells contributes to an immunosuppressive milieu. *Immunity* **14**, 715–725 (2001).

95. Ashkenazi, A. & Dixit, V. M. Death Receptors: Signaling and Modulation. *Science* **281**, 1305–1308 (1998).

96. Kale, J., Osterlund, E. J. & Andrews, D. W. BCL-2 family proteins: changing partners in the dance towards death. *Cell Death Differ* **25**, 65–80 (2018).

97. Westaby, D. *et al.* Targeting the Intrinsic Apoptosis Pathway: A Window of Opportunity for Prostate Cancer. *Cancers* **14**, 51 (2022).

98. Wajant, H. Death receptors. *Essays Biochem* **39**, 53–71 (2003).

99. Guicciardi, M. E. & Gores, G. J. Life and death by death receptors. *FASEB J* **23**, 1625–1637 (2009).

100. Hsu, H., Shu, H. B., Pan, M. G. & Goeddel, D. V. TRADD-TRAF2 and TRADD-FADD interactions define two distinct TNF receptor 1 signal transduction pathways. *Cell* **84**, 299–308 (1996).

101. Ang, R. L. & Ting, A. T. Detection of RIPK1 in the FADD-Containing Death Inducing Signaling Complex (DISC) During Necroptosis. *Methods Mol Biol* **1857**, 101–107 (2018).

102. McIlwain, D. R., Berger, T. & Mak, T. W. Caspase Functions in Cell Death and Disease. *Cold Spring Harb Perspect Biol* **5**, a008656 (2013).

103. Cohen, G. M. Caspases: the executioners of apoptosis. *Biochem J* **326 (Pt 1)**, 1–16 (1997).

104. Salvesen, G. S. & Dixit, V. M. Caspase activation: the induced-proximity model. *Proc Natl Acad Sci U S A* **96**, 10964–10967 (1999).

105. Kischkel, F. C. *et al.* Cytotoxicity-dependent APO-1 (Fas/CD95)-associated proteins form a death-inducing signaling complex (DISC) with the receptor. *EMBO J* **14**, 5579–5588 (1995).

106. Xiong, S., Mu, T., Wang, G. & Jiang, X. Mitochondria-mediated apoptosis in mammals. *Protein Cell* **5**, 737–749 (2014).

107. Roos, W. P., Thomas, A. D. & Kaina, B. DNA damage and the balance between survival and death in cancer biology. *Nat Rev Cancer* **16**, 20–33 (2016).

108. Pihán, P., Carreras-Sureda, A. & Hetz, C. BCL-2 family: integrating stress responses at the ER to control cell demise. *Cell Death Differ* **24**, 1478–1487 (2017).

109. Susnow, N., Zhang, L., Margineantu, D. & Hockenbery, D. M. Bcl-2 family proteins as regulators of oxidative stress. *Semin Cancer Biol* **19**, 42–49 (2009).

110. Lindsten, T. *et al.* The combined functions of proapoptotic Bcl-2 family members bak and bax are essential for normal development of multiple tissues. *Mol Cell* **6**, 1389–1399 (2000).

111. Peña-Blanco, A. & García-Sáez, A. J. Bax, Bak and beyond - mitochondrial performance in apoptosis. *FEBS J* **285**, 416–431 (2018).

112. Saelens, X. *et al.* Toxic proteins released from mitochondria in cell death. *Oncogene* **23**, 2861–2874 (2004).

113. Yuan, S. & Akey, C. W. Apoptosome structure, assembly, and procaspase activation. *Structure* **21**, 501–515 (2013).

114. Chinnaiyan, A. M. The apoptosome: heart and soul of the cell death machine. *Neoplasia* **1**, 5–15 (1999).

115. Igney, F. H. & Krammer, P. H. Death and anti-death: tumour resistance to apoptosis. *Nat Rev Cancer* **2**, 277–288 (2002).

116. Yang, H. C. *et al.* The expression of cytokeratin and apoptosis-related molecules in echinococcosis related liver injury. *Molecular and Biochemical Parasitology* **248**, 111455 (2022).

117. Chaitanya, G. V., Alexander, J. S. & Babu, P. P. PARP-1 cleavage fragments: signatures of cell-death proteases in neurodegeneration. *Cell Communication and Signaling* **8**, 31 (2010).

118. Sreeja, J. S., Jyothy, A. & Sengupta, S. α-Fodrin in Cytoskeletal Organization and the Activity of Certain Key Microtubule Kinesins. *Genes (Basel)* **12**, 750 (2021).

119. Lin, H.-H., Hsu, H.-L. & Yeh, N.-H. Apoptotic cleavage of NuMA at the C-terminal end is related to nuclear disruption and death amplification. *J Biomed Sci* **14**, 681–694 (2007).

120. Bratton, D. L. *et al.* Appearance of Phosphatidylserine on Apoptotic Cells Requires Calcium-mediated Nonspecific Flip-Flop and Is Enhanced by Loss of the Aminophospholipid Translocase *. *Journal of Biological Chemistry* **272**, 26159–26165 (1997).

121. Miao, B. & Degterev, A. Methods to analyze cellular necroptosis. *Methods Mol Biol* **559**, 79–93 (2009).

122. Holler, N. *et al.* Fas triggers an alternative, caspase-8-independent cell death pathway using the kinase RIP as effector molecule. *Nat Immunol* **1**, 489–495 (2000).

123. Vercammen, D. *et al.* Dual signaling of the Fas receptor: initiation of both apoptotic and necrotic cell death pathways. *J Exp Med* **188**, 919–930 (1998).

124. Upton, J. W., Kaiser, W. J. & Mocarski, E. S. DAI/ZBP1/DLM-1 complexes with RIP3 to mediate virus-induced programmed necrosis that is targeted by murine cytomegalovirus vIRA. *Cell Host Microbe* **11**, 290–297 (2012).

125. Upton, J. W., Kaiser, W. J. & Mocarski, E. S. Virus inhibition of RIP3-dependent necrosis. *Cell Host Microbe* **7**, 302–313 (2010).

126. Vandenabeele, P., Declercq, W., Van Herreweghe, F. & Vanden Berghe, T. The role of the kinases RIP1 and RIP3 in TNF-induced necrosis. *Sci Signal* **3**, re4 (2010).

127. Murphy, J. M. *et al.* The pseudokinase MLKL mediates necroptosis via a molecular switch mechanism. *Immunity* **39**, 443–453 (2013).

128. Wang, H. *et al.* Mixed lineage kinase domain-like protein MLKL causes necrotic membrane disruption upon phosphorylation by RIP3. *Mol Cell* **54**, 133–146 (2014).

129. Dondelinger, Y. *et al.* MLKL compromises plasma membrane integrity by binding to phosphatidylinositol phosphates. *Cell Rep* **7**, 971–981 (2014).

130. Vanden Berghe, T. *et al.* Determination of apoptotic and necrotic cell death in vitro and in vivo. *Methods* **61**, 117–129 (2013).

131. Čepelak, I., Dodig, S. & Dodig, D. Č. Ferroptosis: Regulated Cell Death. *Arh Hig Rada Toksikol* **71**, 99–109 (2020).

132. Wen, Q., Liu, J., Kang, R., Zhou, B. & Tang, D. The release and activity of HMGB1 in ferroptosis. *Biochem Biophys Res Commun* **510**, 278–283 (2019).

133. Dai, E. *et al.* Autophagy-dependent ferroptosis drives tumor-associated macrophage polarization via release and uptake of oncogenic KRAS protein. *Autophagy* **16**, 2069–2083 (2020).

134. Kiesel, L., Przylipiak, A., Rabe, T., Przylipiak, M. & Runnebaum, B. Arachidonic acid and its lipoxygenase metabolites stimulate prolactin release in superfused pituitary cells. *Human Reproduction* **2**, 281–285 (1987).

135. Gao, M., Monian, P., Quadri, N., Ramasamy, R. & Jiang, X. Glutaminolysis and Transferrin Regulate Ferroptosis. *Mol Cell* **59**, 298–308 (2015).

136. Ponka, P., Beaumont, C. & Richardson, D. R. Function and regulation of transferrin and ferritin. *Semin Hematol* **35**, 35–54 (1998).

137. Ohgami, R. S. *et al.* Identification of a ferrireductase required for efficient transferrin-dependent iron uptake in erythroid cells. *Nat Genet* **37**, 1264–1269 (2005).

138. Konijn, A. M. *et al.* The cellular labile iron pool and intracellular ferritin in K562 cells. *Blood* **94**, 2128–2134 (1999).

139. Richardson, D. R. *et al.* Mitochondrial iron trafficking and the integration of iron metabolism between the mitochondrion and cytosol. *Proceedings of the National Academy of Sciences* **107**, 10775–10782 (2010).

140. Kristiansen, M. *et al.* Identification of the haemoglobin scavenger receptor. *Nature* **409**, 198–201 (2001).

141. Winn, N. C., Volk, K. M. & Hasty, A. H. Regulation of tissue iron homeostasis: the macrophage “ferrostat”. *JCI Insight* **5**, (2020).

142. Winterbourn, C. C. Toxicity of iron and hydrogen peroxide: the Fenton reaction. *Toxicology Letters* **82–83**, 969–974 (1995).

143. Gaschler, M. M. & Stockwell, B. R. Lipid peroxidation in cell death. *Biochem Biophys Res Commun* **482**, 419–425 (2017).

144. Shah, R., Shchepinov, M. S. & Pratt, D. A. Resolving the Role of Lipoxygenases in the Initiation and Execution of Ferroptosis. *ACS Cent. Sci.* **4**, 387–396 (2018).

145. Kagan, V. E. *et al.* Oxidized arachidonic and adrenic PEs navigate cells to ferroptosis. *Nat Chem Biol* **13**, 81–90 (2017).

146. Yang, W. S. *et al.* Peroxidation of polyunsaturated fatty acids by lipoxygenases drives ferroptosis. *Proceedings of the National Academy of Sciences* **113**, E4966–E4975 (2016).

147. Greco, A., Minghetti, L. & Levi, G. Isoprostanes, Novel Markers of Oxidative Injury, Help Understanding the Pathogenesis of Neurodegenerative Diseases. *Neurochem Res* **25**, 1357–1364 (2000).

148. Hardy, P. *et al.* Inflammatory lipid mediators in ischemic retinopathy. *Pharmacological reports : PR* **57 Suppl**, 169–90 (2005).

149. Yang, H. *et al.* Effects of Low-level Lipid Peroxidation on the Permeability of Nitroaromatic Molecules across a Membrane: A Computational Study. *ACS Omega* **5**, 4798–4806 (2020).

150. Van der Paal, J., Neyts, E. C., Verlackt, C. C. W. & Bogaerts, A. Effect of lipid peroxidation on membrane permeability of cancer and normal cells subjected to oxidative stress †Electronic supplementary information (ESI) available. See DOI: 10.1039/c5sc02311d Click here for additional data file. *Chem Sci* **7**, 489–498 (2016).

151. Wong-ekkabut, J. *et al.* Effect of Lipid Peroxidation on the Properties of Lipid Bilayers: A Molecular Dynamics Study. *Biophysical Journal* **93**, 4225–4236 (2007).

152. Leyko, W., Ertel, D. & Bartosz, G. Effect of hyperthermia and lipid peroxidation on the erythrocyte membrane structure. *Int J Radiat Biol* **59**, 1185–1193 (1991).

153. Esterbauer, H., Eckl, P. & Ortner, A. Possible mutagens derived from lipids and lipid precursors. *Mutat Res* **238**, 223–233 (1990).

154. Ayala, A., Muñoz, M. F. & Argüelles, S. Lipid Peroxidation: Production, Metabolism, and Signaling Mechanisms of Malondialdehyde and 4-Hydroxy-2-Nonenal. *Oxid Med Cell Longev* **2014**, 360438 (2014).

155. Yang, W. S. *et al.* Regulation of ferroptotic cancer cell death by GPX4. *Cell* **156**, 317–331 (2014).

156. Ferreira, A. L. A., Machado, P. E. A. & Matsubara, L. S. Lipid peroxidation, antioxidant enzymes and glutathione levels in human erythrocytes exposed to colloidal iron hydroxide in vitro. *Braz J Med Biol Res* **32**, 689–694 (1999).

157. Lucas, J. H., Wheeler, D. G., Guan, Z., Suntres, Z. & Stokes, B. T. Effect of Glutathione Augmentation on Lipid Peroxidation after Spinal Cord Injury. *Journal of Neurotrauma* **19**, 763–775 (2002).

158. Deponte, M. Glutathione catalysis and the reaction mechanisms of glutathione-dependent enzymes. *Biochimica et Biophysica Acta (BBA) - General Subjects* **1830**, 3217–3266 (2013).

159. Forcina, G. C. & Dixon, S. J. GPX4 at the Crossroads of Lipid Homeostasis and Ferroptosis. *Proteomics* **19**, e1800311 (2019).

160. Conrad, M. & Sato, H. The oxidative stress-inducible cystine/glutamate antiporter, system xc−: cystine supplier and beyond. *Amino Acids* **42**, 231–246 (2012).

161. Bridges, R. J., Natale, N. R. & Patel, S. A. System xc- cystine/glutamate antiporter: an update on molecular pharmacology and roles within the CNS. *Br J Pharmacol* **165**, 20–34 (2012).

162. Du, Y., Zhang, H., Lu, J. & Holmgren, A. Glutathione and Glutaredoxin Act as a Backup of Human Thioredoxin Reductase 1 to Reduce Thioredoxin 1 Preventing Cell Death by Aurothioglucose. *J Biol Chem* **287**, 38210–38219 (2012).

163. Marshall, K. R. *et al.* The Human Apoptosis-inducing Protein AMID Is an Oxidoreductase with a Modified Flavin Cofactor and DNA Binding Activity *. *Journal of Biological Chemistry* **280**, 30735–30740 (2005).

164. Bersuker, K. *et al.* The CoQ oxidoreductase FSP1 acts parallel to GPX4 to inhibit ferroptosis. *Nature* **575**, 688–692 (2019).

165. Conrad, M. & Pratt, D. A. The chemical basis of ferroptosis. *Nat Chem Biol* **15**, 1137–1147 (2019).

166. More than one way to die: apoptosis, necrosis and reactive oxygen damage | Oncogene. https://www.nature.com/articles/1203249.

167. Grooten, J., Goossens, V., Vanhaesebroeck, B. & Fiers, W. Cell membrane permeabilization and cellular collapse, followed by loss of dehydrogenase activity: Early events in tumour necrosis factor-induced cytotoxicity. *Cytokine* **5**, 546–555 (1993).

168. Proskuryakov, S. Y. a, Konoplyannikov, A. G. & Gabai, V. L. Necrosis: a specific form of programmed cell death? *Experimental Cell Research* **283**, 1–16 (2003).

169. Leist, M., Single, B., Castoldi, A. F., Kühnle, S. & Nicotera, P. Intracellular Adenosine Triphosphate (ATP) Concentration: A Switch in the Decision Between Apoptosis and Necrosis. *Journal of Experimental Medicine* **185**, 1481–1486 (1997).

170. Bozym, R. A. *et al.* Calcium signals and calpain-dependent necrosis are essential for release of coxsackievirus B from polarized intestinal epithelial cells. *MBoC* **22**, 3010–3021 (2011).

171. Afriyie-Asante, A. *et al.* Mycobacterium tuberculosis Exploits Focal Adhesion Kinase to Induce Necrotic Cell Death and Inhibit Reactive Oxygen Species Production. *Front. Immunol.* **12**, (2021).

172. Festjens, N., Vanden Berghe, T. & Vandenabeele, P. Necrosis, a well-orchestrated form of cell demise: Signalling cascades, important mediators and concomitant immune response. *Biochimica et Biophysica Acta (BBA) - Bioenergetics* **1757**, 1371–1387 (2006).

173. Casares, D., Escribá, P. V. & Rosselló, C. A. Membrane Lipid Composition: Effect on Membrane and Organelle Structure, Function and Compartmentalization and Therapeutic Avenues. *Int J Mol Sci* **20**, 2167 (2019).

174. Shin, H.-W., Takatsu, H. & Nakayama, K. Mechanisms of Membrane Curvature Generation in Membrane Traffic. *Membranes (Basel)* **2**, 118–133 (2012).

175. Hankins, H. M., Baldridge, R. D., Xu, P. & Graham, T. R. Role of flippases, scramblases, and transfer proteins in phosphatidylserine subcellular distribution. *Traffic* **16**, 35–47 (2015).

176. Hirama, T. *et al.* Membrane curvature induced by proximity of anionic phospholipids can initiate endocytosis. *Nat Commun* **8**, 1393 (2017).

177. Cornell, B. A. & Separovic, F. Membrane thickness and acyl chain length. *Biochim Biophys Acta* **733**, 189–193 (1983).

178. Sankhagowit, S., Lee, E. Y., Wong, G. C. L. & Malmstadt, N. Oxidation of Membrane Curvature-Regulating Phosphatidylethanolamine Lipid Results in Formation of Bilayer and Cubic Structures. *Langmuir* **32**, 2450–2457 (2016).

179. Murakami, M., Nakatani, Y., Atsumi, G., Inoue, K. & Kudo, I. Regulatory functions of phospholipase A2. *Crit Rev Immunol* **17**, 225–283 (1997).

180. Pagnan, A. *et al.* Effects of an olive-oil-rich diet on erythrocyte membrane lipid composition and cation transport systems. *Clinical Science* **76**, 87–93 (1989).

181. Uchiyama, M., Oguri, M., Mojumdar, E. H., Gooris, G. S. & Bouwstra, J. A. Free fatty acids chain length distribution affects the permeability of skin lipid model membranes. *Biochimica et Biophysica Acta (BBA) - Biomembranes* **1858**, 2050–2059 (2016).

182. Enhancement of the Phase Transition Permeability of DPPC Liposomes by Incorporation of MPPC: A New Temperature-Sensitive Liposome for use with Mild Hyperthermia. https://www-tandfonline-com.proxy.bib.uottawa.ca/doi/epdf/10.3109/08982109909035549?needAccess=true doi:10.3109/08982109909035549.

183. Fuller, N. & Rand, R. P. The influence of lysolipids on the spontaneous curvature and bending elasticity of phospholipid membranes. *Biophys J* **81**, 243–254 (2001).

184. Høyrup, P., Davidsen, J. & Jørgensen, K. Lipid Membrane Partitioning of Lysolipids and Fatty Acids: Effects of Membrane Phase Structure and Detergent Chain Length. *J. Phys. Chem. B* **105**, 2649–2657 (2001).

185. Lipid/Detergent Interaction Thermodynamics as a Function of Molecular Shape. *ACS Publications* https://pubs-acs-org.proxy.bib.uottawa.ca/doi/full/10.1021/jp962342q.

186. Wills, R. C. & Hammond, G. R. V. PI(4,5)P2: signaling the plasma membrane. *Biochem J* **479**, 2311–2325 (2022).

187. Kanchanawong, P. *et al.* Nanoscale architecture of integrin-based cell adhesions. *Nature* **468**, 580–584 (2010).

188. Cai, X. *et al.* Spatial and temporal regulation of focal adhesion kinase activity in living cells. *Mol Cell Biol* **28**, 201–214 (2008).

189. Goñi, G. M. *et al.* Phosphatidylinositol 4,5-bisphosphate triggers activation of focal adhesion kinase by inducing clustering and conformational changes. *Proceedings of the National Academy of Sciences* **111**, E3177–E3186 (2014).

190. Fukami, K., Endo, T., Imamura, M. & Takenawa, T. alpha-Actinin and vinculin are PIP2-binding proteins involved in signaling by tyrosine kinase. *J Biol Chem* **269**, 1518–1522 (1994).

191. Gilmore, A. P. & Burridge, K. Regulation of vinculin binding to talin and actin by phosphatidyl-inositol-4-5-bisphosphate. *Nature* **381**, 531–535 (1996).

192. Chinthalapudi, K. *et al.* Lipid binding promotes oligomerization and focal adhesion activity of vinculin. *Journal of Cell Biology* **207**, 643–656 (2014).

193. Terebiznik, M. R. *et al.* Elimination of host cell PtdIns(4,5)P(2) by bacterial SigD promotes membrane fission during invasion by Salmonella. *Nat Cell Biol* **4**, 766–773 (2002).

194. Raucher, D. *et al.* Phosphatidylinositol 4,5-bisphosphate functions as a second messenger that regulates cytoskeleton-plasma membrane adhesion. *Cell* **100**, 221–228 (2000).

195. Li, M. *et al.* Signaling pathways in macrophages: molecular mechanisms and therapeutic targets. *MedComm (2020)* **4**, e349 (2023).

196. Macrophages in immunoregulation and therapeutics | Signal Transduction and Targeted Therapy. https://www.nature.com/articles/s41392-023-01452-1.

197. Hirayama, D., Iida, T. & Nakase, H. The Phagocytic Function of Macrophage-Enforcing Innate Immunity and Tissue Homeostasis. *Int J Mol Sci* **19**, 92 (2017).

198. Arango Duque, G. & Descoteaux, A. Macrophage Cytokines: Involvement in Immunity and Infectious Diseases. *Front Immunol* **5**, 491 (2014).

199. Polidoro, R. B., Hagan, R. S., de Santis Santiago, R. & Schmidt, N. W. Overview: Systemic Inflammatory Response Derived From Lung Injury Caused by SARS-CoV-2 Infection Explains Severe Outcomes in COVID-19. *Front. Immunol.* **11**, (2020).

200. Diaz, M. H. & Hauser, A. R. Pseudomonas aeruginosa Cytotoxin ExoU Is Injected into Phagocytic Cells during Acute Pneumonia. *Infection and Immunity* **78**, 1447–1456 (2010).

201. Kato, A. & Schleimer, R. P. Beyond inflammation: airway epithelial cells are at the interface of innate and adaptive immunity. *Curr Opin Immunol* **19**, 711–720 (2007).

202. Parker, D. & Prince, A. Innate Immunity in the Respiratory Epithelium. *Am J Respir Cell Mol Biol* **45**, 189–201 (2011).

203. Aaron, S. D., Ramotar, K., Ferris, W., Vandemheen, K. & al, et. Adult Cystic Fibrosis Exacerbations and New Strains of Pseudomonas aeruginosa. *American Journal of Respiratory and Critical Care Medicine* **169**, 811–5 (2004).

204. Fahy, J. V. & Dickey, B. F. Airway Mucus Function and Dysfunction. *N Engl J Med* **363**, 2233–2247 (2010).

205. Latz, E., Xiao, T. S. & Stutz, A. Activation and regulation of the inflammasomes. *Nat Rev Immunol* **13**, 397–411 (2013).

206. Coburn, B., Sekirov, I. & Finlay, B. B. Type III Secretion Systems and Disease. *Clin Microbiol Rev* **20**, 535–549 (2007).

207. Grandjean, T. *et al.* The human NAIP-NLRC4-inflammasome senses the Pseudomonas aeruginosa T3SS inner-rod protein. *Int Immunol* **29**, 377–384 (2017).

208. Kelley, N., Jeltema, D., Duan, Y. & He, Y. The NLRP3 Inflammasome: An Overview of Mechanisms of Activation and Regulation. *Int J Mol Sci* **20**, 3328 (2019).

209. Lamkanfi, M. & Dixit, V. M. Mechanisms and functions of inflammasomes. *Cell* **157**, 1013–1022 (2014).

210. Franchi, L., Eigenbrod, T., Muñoz-Planillo, R. & Nuñez, G. The inflammasome: a caspase-1-activation platform that regulates immune responses and disease pathogenesis. *Nat Immunol* **10**, 241–247 (2009).

211. Dinarello, C. A. Overview of the IL-1 family in innate inflammation and acquired immunity. *Immunol Rev* **281**, 8–27 (2018).

212. Liu, X. *et al.* Inflammasome-activated gasdermin D causes pyroptosis by forming membrane pores. *Nature* **535**, 153–158 (2016).

213. Fink, S. L. & Cookson, B. T. Caspase-1-dependent pore formation during pyroptosis leads to osmotic lysis of infected host macrophages. *Cell Microbiol* **8**, 1812–1825 (2006).

214. Sundaram, B. & Kanneganti, T.-D. Advances in Understanding Activation and Function of the NLRC4 Inflammasome. *International Journal of Molecular Sciences* **22**, 1048 (2021).

215. Liang, J. J., Fraser, I. D. C. & Bryant, C. E. Lipid regulation of NLRP3 inflammasome activity through organelle stress. *Trends Immunol* **42**, 807–823 (2021).

216. Luo, X. *et al.* Docosahexaenoic acid ameliorates palmitate-induced lipid accumulation and inflammation through repressing NLRC4 inflammasome activation in HepG2 cells. *Nutr Metab (Lond)* **9**, 34 (2012).

217. He, W. *et al.* Gasdermin D is an executor of pyroptosis and required for interleukin-1β secretion. *Cell Res* **25**, 1285–1298 (2015).

218. O'Shea, J. J., Ma, A. & Lipsky, P. Cytokines and autoimmunity. *Nat Rev Immunol* **2**, 37–45 (2002).

219. Zhang, J.-M. & An, J. Cytokines, Inflammation and Pain. *Int Anesthesiol Clin* **45**, 27–37 (2007).

220. Iannitti, R. G. *et al.* IL-1 receptor antagonist ameliorates inflammasome-dependent inflammation in murine and human cystic fibrosis. *Nat Commun* **7**, 10791 (2016).

221. Kaneko, N., Kurata, M., Yamamoto, T., Morikawa, S. & Masumoto, J. The role of interleukin-1 in general pathology. *Inflammation and Regeneration* **39**, 12 (2019).

222. Schultz, M. J. *et al.* Role of interleukin-1 in the pulmonary immune response duringPseudomonas aeruginosa pneumonia. *American Journal of Physiology-Lung Cellular and Molecular Physiology* **282**, L285–L290 (2002).

223. Chen, G. *et al.* IL-1β dominates the promucin secretory cytokine profile in cystic fibrosis. *J Clin Invest* **129**, 4433–4450 (2019).

224. van Meer, G., Voelker, D. R. & Feigenson, G. W. Membrane lipids: where they are and how they behave. *Nat Rev Mol Cell Biol* **9**, 112–124 (2008).

225. Kennedy, E. P. Metabolism of Lipides. *Annual Review of Biochemistry* **26**, 119–148 (1957).

226. Traiffort, E., O'Regan, S. & Ruat, M. The choline transporter-like family SLC44: Properties and roles in human diseases. *Molecular Aspects of Medicine* **34**, 646–654 (2013).

227. Fagone, P. & Jackowski, S. Phosphatidylcholine and the CDP–choline cycle. *Biochimica et Biophysica Acta (BBA) - Molecular and Cell Biology of Lipids* **1831**, 523–532 (2013).

228. Karim, M., Jackson, P. & Jackowski, S. Gene structure, expression and identification of a new CTP:phosphocholine cytidylyltransferase β isoform. *Biochimica et Biophysica Acta (BBA) - Molecular and Cell Biology of Lipids* **1633**, 1–12 (2003).

229. HENNEBERRY, A. L. & McMASTER, C. R. Cloning and expression of a human choline/ethanolaminephosphotransferase: synthesis of phosphatidylcholine and phosphatidylethanolamine. *Biochemical Journal* **339**, 291–298 (1999).

230. Henneberry, A. L., Wistow, G. & McMaster, C. R. Cloning, Genomic Organization, and Characterization of a Human Cholinephosphotransferase *. *Journal of Biological Chemistry* **275**, 29808–29815 (2000).

231. Vance, D. E., Walkey, C. J. & Cui, Z. Phosphatidylethanolamine *N*-methyltransferase from liver. *Biochimica et Biophysica Acta (BBA) - Lipids and Lipid Metabolism* **1348**, 142–150 (1997).

232. Vance, D. E. & Ridgway, N. D. The methylation of phosphatidylethanolamine. *Progress in Lipid Research* **27**, 61–79 (1988).

233. Waite, K. A., Cabilio, N. R. & Vance, D. E. Choline Deficiency–Induced Liver Damage Is Reversible in Pemt−/− Mice. *The Journal of Nutrition* **132**, 68–71 (2002).

234. Walkey, C. J., Yu, L., Agellon, L. B. & Vance, D. E. Biochemical and Evolutionary Significance of Phospholipid Methylation *. *Journal of Biological Chemistry* **273**, 27043–27046 (1998).

235. Shin, L. *et al.* Lysophosphatidylcholine inhibits membrane-associated SNARE complex disassembly. *J Cell Mol Med* **16**, 1701–1708 (2012).

236. Moessinger, C. *et al.* Two different pathways of phosphatidylcholine synthesis, the Kennedy Pathway and the Lands Cycle, differentially regulate cellular triacylglycerol storage. *BMC Cell Biology* **15**, 43 (2014).

237. Phospholipases. in *Encyclopedic Reference of Molecular Pharmacology* 733–739 (Springer, Berlin, Heidelberg, 2004). doi:10.1007/3-540-29832-0_1263.

238. Arisawa, K. *et al.* Saturated fatty acid in the phospholipid monolayer contributes to the formation of large lipid droplets. *Biochemical and Biophysical Research Communications* **480**, 641–647 (2016).

239. Calder, P. C. & Grimble, R. F. Polyunsaturated fatty acids, inflammation and immunity. *Eur J Clin Nutr* **56 Suppl 3**, S14-19 (2002).

240. Reeves, A. R. *et al.* Myeloid-specific deficiency of long-chain acyl CoA synthetase 4 (Acsl4) reduces inflammation in vitro and in vivo by remodeling phospholipids and reducing production of arachidonic acid-derived proinflammatory lipid mediators. *J Immunol* **207**, 2744–2753 (2021).

241. Kang, M. J. *et al.* A novel arachidonate-preferring acyl-CoA synthetase is present in steroidogenic cells of the rat adrenal, ovary, and testis. *Proc Natl Acad Sci U S A* **94**, 2880–2884 (1997).

242. Martin, S. A., Gijón, M. A., Voelker, D. R. & Murphy, R. C. Measurement of lysophospholipid acyltransferase activities using substrate competition[S]. *Journal of Lipid Research* **55**, 782–791 (2014).

243. O'Donnell, V. B. New appreciation for an old pathway: the Lands Cycle moves into new arenas in health and disease. *Biochemical Society Transactions* **50**, 1–11 (2022).

244. Lands, W. E., Inoue, M., Sugiura, Y. & Okuyama, H. Selective incorporation of polyunsaturated fatty acids into phosphatidylcholine by rat liver microsomes. *J Biol Chem* **257**, 14968–14972 (1982).

245. Okuyama, H., Yamada, K. & Ikezawa, H. Accepton concentration effect in the selectivity of acyl coenzyme A: U aclglycerylphosphorylcholine acyltransferase system in rat liver. *J Biol Chem* **250**, 1710–1713 (1975).

246. Shi, Y. & Cheng, D. Beyond triglyceride synthesis: the dynamic functional roles of MGAT and DGAT enzymes in energy metabolism. *Am J Physiol Endocrinol Metab* **297**, E10–E18 (2009).

247. Bartolacci, C. *et al.* Targeting de novo lipogenesis and the Lands cycle induces ferroptosis in KRAS-mutant lung cancer. *Nat Commun* **13**, 4327 (2022).

248. Doll, S. *et al.* ACSL4 dictates ferroptosis sensitivity by shaping cellular lipid composition. *Nat Chem Biol* **13**, 91–98 (2017).

249. Dixon, S. J. *et al.* Human Haploid Cell Genetics Reveals Roles for Lipid Metabolism Genes in Nonapoptotic Cell Death. *ACS Chem. Biol.* **10**, 1604–1609 (2015).

250. Zou, Y. *et al.* Cytochrome P450 oxidoreductase contributes to phospholipid peroxidation in ferroptosis. *Nat Chem Biol* **16**, 302–309 (2020).

251. Rouzer, C. A. & Marnett, L. J. Mechanism of Free Radical Oxygenation of Polyunsaturated Fatty Acids by Cyclooxygenases. *Chem. Rev.* **103**, 2239–2304 (2003).

252. Adelizzi, R. A. COX-1 and COX-2 in health and disease. *J Am Osteopath Assoc* **99**, S7-12 (1999).

253. Simon, L. S. Role and regulation of cyclooxygenase-2 during inflammation. *Am J Med* **106**, 37S-42S (1999).

254. Samuelsson, B. Leukotrienes: Mediators of Immediate Hypersensitivity Reactions and Inflammation. *Science* **220**, 568–575 (1983).

255. Haeggström, J. Z. & Funk, C. D. Lipoxygenase and Leukotriene Pathways: Biochemistry, Biology, and Roles in Disease. *Chem. Rev.* **111**, 5866–5898 (2011).

256. Kuhn, H., Banthiya, S. & van Leyen, K. Mammalian lipoxygenases and their biological relevance. *Biochimica et Biophysica Acta (BBA) - Molecular and Cell Biology of Lipids* **1851**, 308–330 (2015).

257. Snodgrass, R. G. & Brüne, B. Regulation and Functions of 15-Lipoxygenases in Human Macrophages. *Front Pharmacol* **10**, 719 (2019).

258. Munro, A. W., McLean, K. J., Grant, J. L. & Makris, T. M. Structure and function of the cytochrome P450 peroxygenase enzymes. *Biochem Soc Trans* **46**, 183–196 (2018).

259. Kroetz, D. L. & Zeldin, D. C. Cytochrome P450 pathways of arachidonic acid metabolism. *Curr Opin Lipidol* **13**, 273–283 (2002).

260. Bittleman, D. B. & Casale, T. B. 5-Hydroxyeicosatetraenoic acid (HETE)-induced neutrophil transcellular migration is dependent upon enantiomeric structure. *Am J Respir Cell Mol Biol* **12**, 260–267 (1995).

261. Johnson, H. G., McNee, M. L. & Sun, F. F. 15-Hydroxyeicosatetraenoic acid is a potent inflammatory mediator and agonist of canine tracheal mucus secretion. *Am Rev Respir Dis* **131**, 917–922 (1985).

262. Denisov, I. G., Makris, T. M., Sligar, S. G. & Schlichting, I. Structure and Chemistry of Cytochrome P450. *Chem. Rev.* **105**, 2253–2278 (2005).

263. Raoust, E. *et al.* Pseudomonas aeruginosa LPS or Flagellin Are Sufficient to Activate TLR-Dependent Signaling in Murine Alveolar Macrophages and Airway Epithelial Cells. *PLoS One* **4**, e7259 (2009).

264. Jang, G.-Y. *et al.* Interactions between tumor-derived proteins and Toll-like receptors. *Exp Mol Med* **52**, 1926–1935 (2020).

265. Miyake, K. *et al.* Essential role of MD-2 in B-cell responses to lipopolysaccharide and Toll-like receptor 4 distribution. *J Endotoxin Res* **8**, 449–452 (2002).

266. Zanoni, I. *et al.* CD14 controls the LPS-induced endocytosis of Toll-like Receptor 4. *Cell* **147**, 868–880 (2011).

267. Kagan, J. C. *et al.* TRAM couples endocytosis of Toll-like receptor 4 to the induction of interferon-β. *Nat Immunol* **9**, 361–368 (2008).

268. Jiang, Z. *et al.* CD14 is required for MyD88-independent LPS signaling. *Nat Immunol* **6**, 565–570 (2005).

269. Husebye, H. *et al.* Endocytic pathways regulate Toll-like receptor 4 signaling and link innate and adaptive immunity. *EMBO J* **25**, 683–692 (2006).

270. Küper, C., Beck, F.-X. & Neuhofer, W. Toll-like receptor 4 activates NF-κB and MAP kinase pathways to regulate expression of proinflammatory COX-2 in renal medullary collecting duct cells. *Am J Physiol Renal Physiol* **302**, F38-46 (2012).

271. Cogswell, J. P. *et al.* NF-kappa B regulates IL-1 beta transcription through a consensus NF-kappa B binding site and a nonconsensus CRE-like site. *J Immunol* **153**, 712–723 (1994).

272. Mao, L., Kitani, A., Strober, W. & Fuss, I. J. The Role of NLRP3 and IL-1β in the Pathogenesis of Inflammatory Bowel Disease. *Front. Immunol.* **9**, (2018).

273. Joo Y. Lee *et al.* Saturated fatty acids, but not unsaturated fatty acids, induce the expression of cyclooxygenase-2 mediated through Toll-like receptor 4. *Journal of Biological Chemistry* **276**, 16683–16689 (2001).

274. Shi, H. *et al.* TLR4 links innate immunity and fatty acid–induced insulin resistance. *J Clin Invest* **116**, 3015–3025 (2006).

275. Kang, J. Y. & Lee, J.-O. Structural Biology of the Toll-Like Receptor Family. *Annual Review of Biochemistry* **80**, 917–941 (2011).

276. Hwang, D. H., Kim, J.-A. & Lee, J. Y. Mechanisms for the activation of Toll-like receptor 2/4 by saturated fatty acids and inhibition by docosahexaenoic acid. *European Journal of Pharmacology* **785**, 24–35 (2016).

277. Rhee, S. H. & Hwang, D. Murine TOLL-like Receptor 4 Confers Lipopolysaccharide Responsiveness as Determined by Activation of NFκB and Expression of the Inducible Cyclooxygenase *. *Journal of Biological Chemistry* **275**, 34035–34040 (2000).

278. Wong, S. W. *et al.* Fatty Acids Modulate Toll-like Receptor 4 Activation through Regulation of Receptor Dimerization and Recruitment into Lipid Rafts in a Reactive Oxygen Species-dependent Manner *. *Journal of Biological Chemistry* **284**, 27384–27392 (2009).

279. GPR120 Is an Omega-3 Fatty Acid Receptor Mediating Potent Anti-inflammatory and Insulin-Sensitizing Effects: Cell. https://www.cell.com/fulltext/S0092-8674(10)00888-3.

280. Que, X. *et al.* Oxidized phospholipids are proinflammatory and proatherogenic in hypercholesterolaemic mice. *Nature* **558**, 301–306 (2018).

281. Erridge, C., Kennedy, S., Spickett, C. M. & Webb, D. J. Oxidized Phospholipid Inhibition of Toll-like Receptor (TLR) Signaling Is Restricted to TLR2 and TLR4. *J Biol Chem* **283**, 24748–24759 (2008).

282. Oskolkova, O. V. *et al.* Oxidized phospholipids are more potent antagonists of lipopolysaccharide than inducers of inflammation. *J Immunol* **185**, 7706–7712 (2010).

283. Miller, Y. I. & Shyy, J. Y.-J. Context-dependent role of oxidized lipids and lipoproteins in inflammation. *Trends Endocrinol Metab* **28**, 143–152 (2017).

284. Manček-Keber, M. *et al.* Toll-like receptor 4 senses oxidative stress mediated by the oxidation of phospholipids in extracellular vesicles. *Sci Signal* **8**, ra60 (2015).

285. Hagar, J. A., Powell, D. A., Aachoui, Y., Ernst, R. K. & Miao, E. A. Cytoplasmic LPS activates caspase-11: implications in TLR4-independent endotoxic shock. *Science* **341**, 1250–1253 (2013).

286. Py, B. F. *et al.* Caspase-11 Controls Interleukin-1β Release through Degradation of TRPC1. *Cell Rep* **6**, 1122–1128 (2014).

287. Zanoni, I. *et al.* An endogenous caspase-11 ligand elicits interleukin-1 release from living dendritic cells. *Science* **352**, 1232–1236 (2016).

288. Downs, K. P., Nguyen, H., Dorfleutner, A. & Stehlik, C. An overview of the non-canonical inflammasome. *Molecular Aspects of Medicine* **76**, 100924 (2020).

289. Liberati, N. T. *et al.* An ordered, nonredundant library of Pseudomonas aeruginosa strain PA14 transposon insertion mutants. *Proceedings of the National Academy of Sciences* **103**, 2833–2838 (2006).

290. Welcome To PA14 Transposon Insertion Mutant Library. https://pa14.mgh.harvard.edu/cgi-bin/pa14/home.cgi.

291. Fischer, S., Dethlefsen, S., Klockgether, J. & Tümmler, B. Phenotypic and Genomic Comparison of the Two Most Common ExoU-Positive Pseudomonas aeruginosa Clones, PA14 and ST235. *mSystems* **5**, e01007-20 (2020).

292. Allewelt, M., Coleman, F. T., Grout, M., Priebe, G. P. & Pier, G. B. Acquisition of expression of the Pseudomonas aeruginosa ExoU cytotoxin leads to increased bacterial virulence in a murine model of acute pneumonia and systemic spread. *Infect Immun* **68**, 3998–4004 (2000).

293. Dong-ju Kim,. Relation of microbial biomass to counting units for Pseudomonas aeruginosa. *Afr. J. Microbiol. Res.* **6**, (2012).

294. Miotto, G. *et al.* Insight into the mechanism of ferroptosis inhibition by ferrostatin-1. *Redox Biology* **28**, 101328 (2020).

295. Lovatt, M. *et al.* Peroxiredoxin-1 regulates lipid peroxidation in corneal endothelial cells. *Redox Biology* **30**, 101417 (2020).

296. Ai, Y. *et al.* Mannose antagonizes GSDME-mediated pyroptosis through AMPK activated by metabolite GlcNAc-6P. *Cell Res* **33**, 904–922 (2023).

297. Chen, J. *et al.* RIP3 dependent NLRP3 inflammasome activation is implicated in acute lung injury in mice. *Journal of Translational Medicine* **16**, 233 (2018).

298. Ghorbani, P. *et al.* Choline metabolism underpins macrophage IL-4 polarization and RELMα up-regulation in helminth infection. *PLoS Pathog* **19**, e1011658 (2023).

299. Xu, H., Valenzuela, N., Fai, S., Figeys, D. & Bennett, S. A. L. Targeted lipidomics - advances in profiling lysophosphocholine and platelet-activating factor second messengers. *FEBS J* **280**, 5652–5667 (2013).

300. Chitpin, J. G. *et al.* BATL: Bayesian annotations for targeted lipidomics. *Bioinformatics* **38**, 1593–1599 (2022).

301. Schroth, M. N., Cho, J. J., Green, S. K., Kominos, S. D. & Microbiology Society Publishing. Epidemiology of Pseudomonas aeruginosa in agricultural areas*. *Journal of Medical Microbiology* **67**, 1191–1201 (2018).

302. Rahme, L. G. *et al.* Common Virulence Factors for Bacterial Pathogenicity in Plants and Animals. *Science* **268**, 1899–1902 (1995).

303. Repetto, G., del Peso, A. & Zurita, J. L. Neutral red uptake assay for the estimation of cell viability/cytotoxicity. *Nat Protoc* **3**, 1125–1131 (2008).

304. Sachdeva, K. & Sundaramurthy, V. The Interplay of Host Lysosomes and Intracellular Pathogens. *Front Cell Infect Microbiol* **10**, 595502 (2020).

305. Leow, S. M. *et al.* Sub-lethal oxidative stress induces lysosome biogenesis via a lysosomal membrane permeabilization-cathepsin-caspase 3-transcription factor EB-dependent pathway. *Oncotarget* **8**, 16170–16189 (2017).

306. Morgan, M. J. & Kim, Y.-S. Roles of RIPK3 in necroptosis, cell signaling, and disease. *Exp Mol Med* **54**, 1695–1704 (2022).

307. Rabin, S. D. P., Veesenmeyer, J. L., Bieging, K. T. & Hauser, A. R. A C-Terminal Domain Targets the Pseudomonas aeruginosa Cytotoxin ExoU to the Plasma Membrane of Host Cells. *Infection and Immunity* **74**, 2552–2561 (2006).

308. Qi, J. *et al.* P. aeruginosa Mediated Necroptosis in Mouse Tumor Cells Induces Long-Lasting Systemic Antitumor Immunity. *Front Oncol* **10**, 610651 (2021).

309. Valente, E., Assis, M. C., Alvim, I. M. P., Pereira, G. M. B. & Plotkowski, M. C. Pseudomonas aeruginosa induces apoptosis in human endothelial cells. *Microbial Pathogenesis* **29**, 345–356 (2000).

310. Dar, H. H. *et al.* P. aeruginosa augments irradiation injury via 15-lipoxygenase-catalyzed generation of 15-HpETE-PE and induction of theft-ferroptosis. *JCI Insight* **7**, e156013 (2022).

311. Santoni, K. *et al.* Caspase-1-driven neutrophil pyroptosis and its role in host susceptibility to Pseudomonas aeruginosa. *PLOS Pathogens* **18**, e1010305 (2022).

312. Kaufman, M. R. *et al.* Pseudomonas aeruginosa mediated apoptosis requires the ADP-ribosylating activity of ExoS. *Microbiology* **146**, 2531–2541 (2000).

313. Elmore, S. Apoptosis: A Review of Programmed Cell Death. *Toxicol Pathol* **35**, 495–516 (2007).

314. Forcina, G. C., Conlon, M., Wells, A., Cao, J. Y. & Dixon, S. J. Systematic Quantification of Population Cell Death Kinetics in Mammalian Cells. *Cell Syst* **4**, 600-610.e6 (2017).

315. Sun, L. *et al.* Mixed lineage kinase domain-like protein mediates necrosis signaling downstream of RIP3 kinase. *Cell* **148**, 213–227 (2012).

316. Chen, X. *et al.* Translocation of mixed lineage kinase domain-like protein to plasma membrane leads to necrotic cell death. *Cell Res* **24**, 105–121 (2014).

317. Xia, B. *et al.* MLKL forms cation channels. *Cell Res* **26**, 517–528 (2016).

318. Quarato, G. *et al.* Sequential Engagement of Distinct MLKL Phosphatidylinositol-Binding Sites Executes Necroptosis. *Molecular Cell* **61**, 589–601 (2016).

319. Dovey, C. M. *et al.* MLKL Requires the Inositol Phosphate Code to Execute Necroptosis. *Molecular Cell* **70**, 936-948.e7 (2018).

320. Dixon, S. J. *et al.* Ferroptosis: an iron-dependent form of nonapoptotic cell death. *Cell* **149**, 1060–1072 (2012).

321. Zilka, O. *et al.* On the Mechanism of Cytoprotection by Ferrostatin-1 and Liproxstatin-1 and the Role of Lipid Peroxidation in Ferroptotic Cell Death. *ACS Cent Sci* **3**, 232–243 (2017).

322. Aldrovandi, M., Fedorova, M. & Conrad, M. Juggling with lipids, a game of Russian roulette. *Trends in Endocrinology & Metabolism* **32**, 463–473 (2021).

323. Mao, C., Lei, G., Zhuang, L. & Gan, B. Phospholipase iPLA2β acts as a guardian against ferroptosis. *Cancer Commun (Lond)* **41**, 1082–1085 (2021).

324. Oh, M. *et al.* The lipoprotein-associated phospholipase A2 inhibitor Darapladib sensitises cancer cells to ferroptosis by remodelling lipid metabolism. *Nat Commun* **14**, 5728 (2023).

325. Agmon, E., Solon, J., Bassereau, P. & Stockwell, B. R. Modeling the effects of lipid peroxidation during ferroptosis on membrane properties. *Sci Rep* **8**, 5155 (2018).

326. Chen, L. *et al.* Inflammatory responses and inflammation-associated diseases in organs. *Oncotarget* **9**, 7204 (2018).

327. Kolb, M., Margetts, P. J., Anthony, D. C., Pitossi, F. & Gauldie, J. Transient expression of IL-1β induces acute lung injury and chronic repair leading to pulmonary fibrosis. *J Clin Invest* **107**, 1529–1536 (2001).

328. Lopez-Castejon, G. & Brough, D. Understanding the mechanism of IL-1β secretion. *Cytokine Growth Factor Rev* **22**, 189–195 (2011).

329. Heilig, R. *et al.* The Gasdermin-D pore acts as a conduit for IL-1β secretion in mice. *Eur J Immunol* **48**, 584–592 (2018).

330. Hazuda, D. J., Lee, J. C. & Young, P. R. The kinetics of interleukin 1 secretion from activated monocytes. Differences between interleukin 1 alpha and interleukin 1 beta. *J Biol Chem* **263**, 8473–8479 (1988).

331. Fadeel, B. & Xue, D. The ins and outs of phospholipid asymmetry in the plasma membrane: roles in health and disease. *Crit Rev Biochem Mol Biol* **44**, 264–277 (2009).

332. Klose, C., Surma, M. A. & Simons, K. Organellar lipidomics--background and perspectives. *Curr Opin Cell Biol* **25**, 406–413 (2013).

333. Lorent, J. H. *et al.* Plasma membranes are asymmetric in lipid unsaturation, packing and protein shape. *Nat Chem Biol* **16**, 644–652 (2020).

334. Qiu, B. *et al.* Phospholipids with two polyunsaturated fatty acyl tails promote ferroptosis. *Cell* **187**, 1177-1190.e18 (2024).

335. Tesfay, L. *et al.* Steroyl-CoA Desaturase 1 (SCD1) protects ovarian cancer cells from ferroptotic cell death. *Cancer Res* **79**, 5355–5366 (2019).

336. Mortensen, M. S., Ruiz, J. & Watts, J. L. Polyunsaturated Fatty Acids Drive Lipid Peroxidation during Ferroptosis. *Cells* **12**, 804 (2023).

337. John Peter, A. T. *et al.* Rewiring phospholipid biosynthesis reveals resilience to membrane perturbations and uncovers regulators of lipid homeostasis. *EMBO J* **41**, e109998 (2022).

338. Zhang, Y., Chen, X., Gueydan, C. & Han, J. Plasma membrane changes during programmed cell deaths. *Cell Res* **28**, 9–21 (2018).

339. Li, Z. *et al.* LPCAT1-mediated membrane phospholipid remodelling promotes ferroptosis evasion and tumour growth. *Nat Cell Biol* **26**, 811–824 (2024).

340. Colles, S. M. & Chisolm, G. M. Lysophosphatidylcholine-induced cellular injury in cultured fibroblasts involves oxidative events. *J Lipid Res* **41**, 1188–1198 (2000).

341. Stock, C., Schilling, T., Schwab, A. & Eder, C. Lysophosphatidylcholine Stimulates IL-1β Release from Microglia via a P2X7 Receptor-Independent Mechanism1. *The Journal of Immunology* **177**, 8560–8568 (2006).

342. Ismaeel, S. & Qadri, A. ATP Release Drives Inflammation with Lysophosphatidylcholine. *ImmunoHorizons* **5**, 219–233 (2021).